Optimum Power Allocation for Cooperative Communications

by

Muhammad Mehboob Fareed

A thesis
presented to the University of Waterloo
in fulfillment of the
thesis requirement for the degree of
Doctor of Philosophy
in
Electrical and Computer Engineering

Waterloo, Ontario, Canada, 2009

AUTHOR'S DECLARATION

I hereby declare that I am the sole author of this thesis. This is a true copy of the thesis, including any required final revisions, as accepted by my examiners.

I understand that my thesis may be made electronically available to the public.

Abstract

Cooperative communication is a new class of wireless communication techniques in which wireless nodes help each other relay information and realize spatial diversity advantages in a distributed manner. This new transmission technique promises significant performance gains in terms of link reliability, spectral efficiency, system capacity, and transmission range. Analysis and design of cooperative communication wireless systems have been extensively studied over the last few years. The introduction and integration of cooperative communication in next generation wireless standards will lead to the design of an efficient and reliable fully-distributed wireless network. However, there are various technical challenges and open issues to be resolved before this promising concept becomes an integral part of the modern wireless communication devices.

A common assumption in the literature on cooperative communications is the equal distribution of power among the cooperating nodes. Optimum power allocation is a key technique to realize the full potentials of relay-assisted transmission promised by the recent information-theoretic results. In this dissertation, we present a comprehensive framework for power allocation problem. We investigate the error rate performance of cooperative communication systems and further devise open-loop optimum power allocation schemes to optimize the performance. By exploiting the information about the location of cooperating nodes, we are able to demonstrate significant improvements in the system performance.

In the first part of this dissertation, we consider single-relay systems with amplify-and-forward relaying. We derive upper bounds for bit error rate performance assuming various cooperation protocols and minimize them under total power constraint. In the second part, we consider a multi-relay network with decode-and-forward relaying. We propose a simple relay selection scheme for this multi-relay system to improve the throughput of the system, further optimize its performance through power allocation. Finally, we consider a multi-source multi-relay broadband cooperative network. We

derive and optimize approximate symbol error rate of this OFDMA (orthogonal frequency division multiple access) system.

Acknowledgements

I am thankful to Allah, the most merciful and most compassionate for blessing me with the strength to seek knowledge and complete this work.

I would like to express my deepest appreciation and sincere gratitude to my adviser, Professor Murat Uysal, who has provided me with an endless support, assistance, and motivation. I am grateful beyond words for his insightful suggestions, invaluable advices, and enlightening discussions.

It is my pleasure to thank my doctoral thesis committee members Dr. Amir Khandani, Dr. Liang-Liang Xie, Dr. Henry Wolkowicz, and Dr. Kemal Tepe for their valuable time and meticulous efforts.

Words cannot adequately express my heartiest thanks to my parents and other family members for their love, kindness, and prayers. Their support and encouragement was essential to achieve my endeavors.

Last, but not least, I am thankful to my colleagues with whom I enjoyed discussing problems and sharing ideas. Special thanks to Dr. Hakam Muhaidat for his insightful discussions and cooperation. I also wish to acknowledge the help of all the people who have contributed to my education and my well-being at University of Waterloo and elsewhere.

Dedication

To my parents

Table of Contents

List of Figures

List of Tables

Abbreviations

AaF	Amplify-and-forward
APS	All participant
APS	Average power scaling
AWGN	Additive white Gaussian noise
BER	Bit error rate
CP	Cyclic prefix
CRC	Cyclic redundancy check
CSI	Channel state information
DaF	Decode-and-forward
EPA	Equal power allocation
FFT	Fast Fourier Transform
IFFT	Inverse Fast Fourier Transform
i.i.d	Identical independent distribution
MIMO	Multiple-input-multiple-output
MISO	Multi-input-single-output
MRC	Maximal-ratio-combining
ML	Maximum-likelihood
OFDM	Orthogonal frequency division multiplexing
OPA	Optimum power allocation
OFDMA	Orthogonal frequency division multiple access
PEP	Pairwise error probability
RS	Relay Selection
SER	Symbol error rate

SIMO	Single-input-multi-output
SNR	Signal-to-Noise Ratio
STBC	Space-time block coding

Notations

$(.)^*$	Conjugate operation
$(.)^{\mathrm{T}}$	Transpose operation
$(.)^{\mathrm{H}}$	Conjugate transpose operation
$E_x[.]$	Expectation with respect to variable x
(k,l)	The (k,l)th entry of a matrix
(k)	The kth entry of a vector
$\lvert . \rvert$	The absolute value
$\lVert . \rVert$	Euclidean norm of a vector
I_N	The identity matrix of size N
Q	FFT matrix of size $N \times N$
$\Gamma(.)$	The gamma function
$E_i(.)$	The exponential-integral function
$Q(.)$	The Gaussian-Q function
det(.)	The determinant of a matrix
$diag(.)$	The diagonal of a matrix
$\Gamma(.,.)$	The incomplete gamma function

Chapter 1

1.1 Introduction

Dramatic increase in the flow of information has fueled intensive research efforts in wireless communications in the last decade. To meet the increasing demand of wireless multimedia and interactive internet services for future communication systems, higher-speed data transmission and improved power efficiency is required as compared to current wireless communication systems.

From a historical point of view, we observe that wireless communication systems create a new generation roughly every 10 years. Analogue wireless telecommunication systems which represent first-generation (1G) were introduced in the early 1980's, and second-generation (2G) digital systems came in the early 1990's. Third-generation (3G) systems are currently being deployed all over the world. For the definition of a future standard, intensive conceptual and research work has been already initiated.

GSM and IS-95 which were primarily designed for voice and low-rate data applications represent 2G systems. These systems were not capable to support high-rate data services. Introduction of 3G applications is intended to deal with the customer demands such as broadband data and internet access. The business model for telecommunication companies has shifted from voice services to multimedia communication and internet applications.

In the last few years, other forms of wireless technologies such as Wi-Fi, WiMax, and Bluetooth were also introduced. Due to different service types, data rates, and user requirements several wireless technologies co-exist in the current market and pose a challenge of interoperability. It is expected that the next generation systems, also known as the fourth generation (4G) systems, will accommodate and integrate all existing and future technologies in a single standard. 4G systems would have the property of "high usability" [1]; it will enable the consumer to use the system at anytime, anywhere, and with any technology. With the help of an integrated wireless terminal, users would have access to a variety of multimedia applications in a reliable environment at low cost. Next

generation wireless communication systems must support high capacity and variable rate information transmission with high bandwidth and power efficiency to conserve limited spectrum resources.

1.2 Diversity Techniques

A fundamental technical challenge for reliable and high-speed communication is to cope with the physical limitations of the wireless channel. The attenuation resulting from the destructive addition of multipath in the propagation media is a major source of impairment in wireless communications. This attenuation in signal amplitude is generally modeled by Rayleigh fading. Rayleigh fading channel suffers from a large signal-to-noise ratio (SNR) penalty as compared to the classical additive white Gaussian noise (AWGN) channel. This performance loss is due to linear dependency of bit-error probability on the SNR in Rayleigh fading in contrast to the AWGN which has exponential dependency.

Diversity is a key technique to combat fading, and hence to recover transmit-power loss, in wireless communication systems [2]. The diversity concept makes intelligent use of the fact that if multiple replicas of the same information signal are sent over independent fading channels, the probability of all the signals being faded will be less than the probability of only one being faded. Mathematically, "diversity order" is defined as

$$d = \lim_{SNR \to \infty} -\frac{\log(P_e)}{\log(SNR)} \tag{1.1}$$

where P_e is the error probability for a given communication link. Availability of independently faded versions of the transmitted signal is important for the effectiveness of all diversity techniques. A comprehensive study of diversity methods (such as time, frequency, and spatial diversity) can be found in [2], [3]. In the following, we will only discuss spatial diversity which is closely related to cooperative diversity which this dissertation focuses on.

Spatial diversity, which is also referred as antenna diversity in the literature, utilizes multiple antennas at the receiver and/or transmitter. The antenna spacing is kept wide enough with respect to the carrier wavelength to create independent fading channels. This technique does not require extra bandwidth as compared to other diversity techniques, e.g., frequency diversity. Depending on the location of multiple antennas, spatial diversity is further classified as "transmit diversity" and "receive diversity". Multiple antennas at the receive side has been already used in uplink transmission (i.e., from mobile station to base station) of the current cellular communication systems. However, due to size limitations and the expense of multiple down-conversion of RF paths, the use of multiple receive antennas at the mobile handset for the downlink transmission (i.e., from base station to mobile station) is more difficult to implement. This motivates the use of multiple transmit antennas at the transmitter. It is feasible to add hardware and additional signal processing burden to base stations rather than the mobile handsets. Due to fact that a base station serves many mobile stations, it also becomes more economical. Since the transmitter is assumed to know less about the channel than the receiver, transmit diversity has traditionally been viewed as more difficult to exploit despite its obvious advantages. However, within the last decade, transmit diversity [4]-[7] has attracted a great attention and practical solutions to realize transmit diversity advantages, such as space-time coding and spatial multiplexing, have been proposed.

1.3 Cooperative Diversity

Although transmit and receive diversity techniques offer distinct advantages, there are various scenarios where the deployment of multiple antennas is not practical due to the size, power limitations, and hardware complexity of the terminals. Examples of these scenarios include wireless sensor networks and ad-hoc networks which are gaining popularity in recent years. Cooperative diversity (also known as "cooperative communications" or "user cooperation") [8]-[14] has emerged as a powerful alternative to reap the benefits of MIMO (multiple-input multiple-output)

communications in a wireless scenario with single-antenna terminals. Cooperative communication takes advantage of the broadcast nature of wireless transmission and creates a virtual antenna array through cooperating nodes. The basic ideas behind user cooperation can be traced back to Cover and El Gamal's work on the information theoretic properties of the relay channel [8]. The recent surge of interest in cooperative communication, however, has been subsequent to the works of Sendonaris et al. [9], [10] and Laneman et al. [11], [12]. In [11], Laneman et al. consider a user cooperation scenario where the source signal is transmitted to a destination terminal through $N-1$ half-duplex relay terminals and demonstrate that the receiver achieves a diversity order of N. Their proposed user cooperation protocol is built upon a two-phase transmission scheme. In the first phase (i.e., broadcasting phase), the source broadcasts to the destination and relay terminals. In the second phase (i.e., relaying phase), the relays transmit processed version of their received signals to the destination using either orthogonal subchannels (i.e., repetition based cooperative diversity), or the same subchannel, (i.e., space-time coded cooperative diversity). The latter relies on the implementation of conventional orthogonal space-time block coding (STBC) [7] in a distributed fashion among the relay nodes.

The user cooperation protocol considered in [11], [12] effectively realizes receive diversity advantages in a distributed manner and is also known as orthogonal relaying. In [14], Nabar et al. establish a unified framework of TDMA-based cooperation protocols for single-relay wireless networks. They quantify achievable performance gains for distributed schemes in an analogy to conventional co-located multiantenna configurations. Specifically, they consider three protocols named Protocol I, Protocol II, and Protocol III. In Protocol I[1], during the first time slot, the source terminal communicates with the relay and destination. During the second time slot, both the relay and source terminals communicate with the destination terminal. Protocol II is the same cooperation protocol proposed by Laneman et al. in [12]. Protocol III is identical to Protocol I apart from the fact

[1] Protocol I is also known as non-orthogonal relaying [15].

that the destination terminal chooses not to receive the direct source-to-destination transmission during the first time slot for reasons which are possibly imposed from the upper-layer networking protocols (e.g., the destination terminal may be engaged in data transmission to another terminal during the first time slot). It can be noticed from the descriptions of protocols that the signal transmitted to both the relay and destination terminals is the same over the two time slots in Protocol II. Therefore, classical space-time code construction does not apply to Protocol II. On the other hand, Protocol I and Protocol III can transmit different signals to the relay and destination terminals. Hence, the conventional STBC can be easily applied to these protocols in a distributed fashion.

The aforementioned protocols can work either with regenerative (decode-and-forward) or non-regenerative (amplify-and-forward) relaying techniques. In amplify-and-forward (AaF) relaying, the relay terminal retransmits a scaled version of the received signal without any attempt to decode it. On the other hand, in decode-and-forward (DaF) relaying, the relay terminal decodes its received signal and then re-encodes it (possibly using a different codebook) for transmission to the destination.

1.4 Related Literature, Motivation, and Contributions

In pioneering works on cooperative communication systems, the overall transmit power is supposed to be uniformly allocated among the source and relay terminals. Some recent work has shown that the performance of cooperative communication schemes can be substantially improved by optimally distributing the power among cooperating nodes.

1.4.1 Power Allocation for AaF Relaying

In [16], Host-Madsen and Zhang derive bounds on ergodic capacity for fading relay channels and study power allocation problem to maximize channel capacity. Their proposed power allocation scheme requires the feedback of channel state information (CSI) of all communication channels to the source for each channel realization. In [17], Ahmed and Aazhang propose a power allocation method relying on partial feedback information. Jingmei et al. [18] investigate power allocation for a two-hop

relaying system assuming full CSI available at the source while the relay has either full or partial CSI. They also extended [18] in [19] for source terminal with multiple antennas. In another paper by Jingmei et al.[20], power allocation schemes are studied in a multi-cell environment.

Close-loop power allocation schemes require the availability of CSI at the transmitter side and their implementation might be problematic in some practical applications. In [21], Hasna and Alouini investigate the optimal power allocation problem for an open-loop transmission scheme (i.e., CSI information available only at the receiver side) to minimize the outage probability. Their results for AaF-relaying are, however, restricted to multi-hop systems without diversity advantages. In [22], [23] Yindi and Hassibi derive an upper bound on the pairwise error probability (PEP) for a large number of relays and minimize PEP bound to formulate optimal power allocation method. They consider a dual-hop scenario in their work. In the broadcasting phase, source sends information to all relays and then stops transmission. In the relaying phase, only the relays forward their received signals to the destination. Under this dual-hop scenario, their conclusion on the optimal power allocation method is that the source uses half the total power and the relays share the other half fairly. For single-relay case, this simply reduces to equal power allocation. It should be emphasized that this conclusion is a result of their implicit underlying assumption that relays are located halfway between source and destination terminals. In [24], Deng et al. adopt average signal-to-noise ratio (SNR) and outage performance as the optimization metrics and investigate the power allocation problem for Protocol II. Their proposed method maximizes the sum and product, respectively, of the SNRs in the direct and relaying link and results in improved outage probability performance.

In the first part of our research which has been already published by the author [25]-[27], we present a comprehensive framework for power allocation problem in a single-relay scenario taking into account the effect of relay location. In particular, we aim to answer the two fundamental questions:

Q1) How should the overall transmit power be shared between broadcasting and relaying phases?;

Q2) In the relaying phase, how much power should be allocated to relay-to-destination and source-to-destination links?

The power allocation problem is formulated to minimize a union bound on the bit error rate (BER) performance assuming AaF relaying. We consider both orthogonal and non-orthogonal cooperation protocols. Optimized protocols demonstrate significant performance gains over their original versions which assume equal sharing of overall transmit power between the source and relay terminals as well as between broadcasting and relaying phases. It is observed that optimized virtual (distributed) antenna configurations are able to demonstrate a BER performance as close as 0.4 dB within their counterpart co-located antenna configurations.

1.4.2 Power Allocation for DaF Relaying

For DaF relaying in a single-relay scenario, Sendonaris et al. [9], [10] have presented a maximum likelihood (ML) decoder and demonstrated that it is able to provide a diversity order of two, i.e., full diversity for the single-relay case. The complexity of this detector becomes unmanageable for higher order modulations. To address this complexity issue, so-called λ-MRC decoder has also been proposed in [9]. λ-MRC decoder is a variant of maximum ratio combining (MRC) and relies on source-to-relay channel state information (CSI) to construct a weighted MRC metric. In [11], [12], Laneman et al. have shown that full diversity in DaF relaying can be achieved with conventional MRC if relay node(s) only forward the correctly decoded information. The practical implementation of such an approach requires the use of error detection methods such as cyclic redundancy check (CRC) at the relay terminal. In [28], Wang et al. have presented a demodulation scheme called cooperative MRC (C-MRC) which achieves full diversity without the use of CRC. However, their proposed method needs CSI of all underlying links at destination node to construct MRC weights and requires $N+1$ time slots to complete transmission of one symbol for a cooperative network with N relays. The deployment of conventional space-time coding among relay nodes can reduce the number of time slots required for transmission, however node erasure (i.e., event that a relay node fails to

decode and remains silent) can significantly impair the performance for space-time trellis codes [5]. Orthogonal space-time block codes are immune to node erasure, however they suffer from reduction in throughput rate for more than two relay nodes [7].

In contrast to earlier works which assume the participation of all relays, relay selection has emerged as a powerful technique with a higher throughput, because fewer time slots are required to complete transmission of one block. In [29], Bletsas et al. have proposed simple relay selection criteria for a multi-relay network. Their method first searches the set of relays which are able to decode successfully, i.e., practical implementation requires error detection such as CRC (cyclic redundancy check), and then chooses the "best" relay for transmission in relaying phase. Determination of the best relay depends either on the minimum or harmonic mean of source-to-relay and relay-to-destination channel SNRs. In [30], Beres and Adve have proposed another selection criterion in which relay-to-destination link with the maximum SNR is chosen. They have presented outage analysis and demonstrated that relay selection outperforms distributed space-time coding. The practical implementation of their scheme requires error detection such as CRC at relay nodes similar to [9]. In [31], Ibrahim et al. have proposed another relay selection method based on the scaled harmonic mean of instantaneous source-to-relay and relay-to-destination channel SNRs. The source node first calculates the harmonic mean for each relaying link, and then compares the maximum one with the SNR of source-to-destination link. Based on this comparison, the source terminal decides whether it should use the whole power in the direct link or should reserve some portion of the overall power for use of the selected relay node. This close-loop scheme requires feedback of source-to-relay and relay-to-destination CSIs to the source node so that power can be adjusted before transmission. In this method, the selected relay forwards only if the information has been decoded correctly. One suggested way in [31] to implement this in practice is to impose a SNR threshold on the received signal. An error rate performance analysis is further presented in [31] which is mainly restricted for a

symmetrical case where all source-to-relay channels have same variances; in other words relay nodes are equidistant from the source.

In the second part of research, which has been already published by the author [27], [32], [33] during the course of research, we consider a multi-relay network operating in DaF mode. We propose a novel relay selection scheme and optimize power allocation for this scheme. Unlike the competing schemes, it requires neither error detection methods at relay nodes nor feedback information at the source. We derive a closed-form symbol error rate (SER) expression for multi-relay network under consideration and demonstrate that the proposed selection method is able to extract the full diversity. We formulate a power allocation strategy to minimize the SER which brings further improvements over the equal power allocation among the source and relay nodes. Extensive Monte Carlo simulations are also presented to confirm the derived SER expressions and to compare the performance of the proposed scheme with its competitors. Our proposed method outperforms competing schemes and works within 0.3 dB of the performance bound achievable by a symbol-by-symbol genie-assisted receiver.

1.4.3 Power Allocation for Multiple Source Nodes over Frequency-Selective Channels

A growing attention in the current literature focuses on the design of broadband cooperative communications [34-45]. A particular research area of practical significance is the design and analysis of cooperative OFDM (Orthogonal Frequency Division Multiplexing) systems. OFDM has been already adopted by various industry standards such as IEEE802.11 (Wi-Fi) and 802.16 (WiMax) in point-to-point links. Its integration with cooperative transmission [34-38] opens up new possibilities in system design providing improvements in spectral efficiency, link reliability, and extended coverage.

In [34], Barbarossa and Scutari have investigated the performance of the distributed implementation of Alamouti code in a single-relay DaF OFDM system over frequency-selective fading channels. Mheidat et al. [35] have considered AaF relaying in a single-relay scenario and

studied the performance of distributed space-time coded OFDM systems through the derivation of PEP. In [36], Seddik and Liu have addressed the design of distributed space-frequency codes (DSFCs) for OFDM systems with DaF and AaF relaying. In [36], Shin et al. have addressed practical implementation issues such as channel estimation, timing, and frequency synchronization OFDM cooperative diversity system. Can et al. [38] have also discussed issues related to practical implementation of OFDM based multi-hop cellular networks. Particular attentions have been given to synchronization, adaptive relaying, and resource analysis (i.e., hardware complexity and power consumption).

OFDMA (Orthogonal Frequency Division Multiple Access) is an extension of the OFDM to the multiuser environment in which disjoint sets of carriers are assigned to different users [39]. In [40], Guoqing and Hui have studied the resource allocation problem for an OFDMA cooperative network. They have formulated an optimal source/relay/subcarrier allocation problem to maximize the achievable sum rate with fairness constraint on relay nodes. In [41], Ng and Yu have considered an OFDMA cooperative cellular data network with a base station and a number of subscribers which have the ability to relay information for each other. Aiming to maximize the sum of utility function (which is a function of achievable data rate), they have presented a centralized utility maximization framework where relay selection, choice of relay strategy (i.e., DaF vs. AaF), allocation of power, bandwidth, and user traffic demands are considered as optimization parameters. In [42], Pischella and Belfiore have studied resource allocation for the downlink of an OFDMA-based single-hop system. Their scheme is also based on optimization of a utility function. In [43], Kim et al. have investigated cross-layer approaches for OFDMA multi-hop wireless networks to maximize the minimum end-to-end throughput among all the nodes under the routing and the PHY/MAC constraints. In [44], Lee et al. have addressed the problem of efficient usage of subcarriers in downlink OFDMA multi-hop cellular networks. Zhang and Lau [45] have considered the problem of dynamically adjusting the resources (subbands) allocated to the relay node in a single-relay OFDMA system.

In the final part of research, we investigate the performance of a cooperative OFDMA system with DaF relaying. Specifically, we derive a closed-form approximate SER expression and analyze the achievable diversity orders. Depending on the relay location, a diversity order up to $\left(L_{S_kD}+1\right)+\sum_{m=1}^{M}\max\left(L_{S_kR_m}+1, L_{R_mD}+1\right)$ is available, where M is the number of relays, $L_{S_kD}+1$, $L_{S_kR_m}+1$, and $L_{R_mD}+1$ are the channel lengths of source-to-destination, source-to-m^{th} relay, and m^{th} relay-to-destination links, respectively. Monte-Carlo simulation results are also presented to confirm the analytical findings. We study power allocation and relay selection schemes as potential methods for performance improvement.

Chapter 2
Power Allocation for AaF Relaying

2.1 Introduction

In this chapter, we present a framework for power allocation problem in open-loop single-relay networks considering Protocols I, II and III of [14] with AaF relaying. Considering BER as the performance metric and taking into account the effect of relay location, we attempt to answer the following fundamental questions:

Q1) How should overall transmit power be shared between broadcasting and relaying phases?

Q2) How much power should be allocated to relay-to-destination and source-to-destination links in the relaying phase?

For each considered protocol, we propose optimal power allocation methods based on the minimization of a union bound on the BER. Optimized protocols demonstrate significant performance gains over their original versions which assume equal sharing of overall transmit power between broadcasting and relay phases and equal sharing of available power in the relaying phase between relay-to-destination and source-to-destination links.

This chapter is organized as follows: In Section 2.2, we introduce the relay-assisted transmission model and describe received signal models for Protocols I, II and III. In Section 2.3, we derive Chernoff bounds on the PEP and calculate union bounds on the BER for each of the protocols. In Section 2.4, we present the power allocation methods which are optimum in the sense of minimizing BER and discuss their efficiency for various relaying scenarios. In Section 2.5, a comprehensive Monte-Carlo simulation study is presented to demonstrate the BER performance of the considered cooperation protocols with equal power allocation and optimum power allocation.

2.2 Transmission Model

We consider a single-relay scenario where terminals operate in half-duplex mode and are equipped with single transmit and receive antennas. As illustrated in Fig.2.1, three nodes source (S), relay (R), and destination (D) are assumed to be located in a two-dimensional plane where d_{SD}, d_{SR}, and d_{RD} denote the distances of source-to-destination (S→D), source-to-relay (S→R), and relay-to-destination (R→D) links, respectively and θ is the angle between lines S→R and R→D. To incorporate the effect of relay geometry in our model, we consider a channel model which takes into account both long-term free-space path loss and short-term Rayleigh fading. The path loss is modeled as

$$\text{Path Loss} = \frac{c}{d^{\alpha}} \tag{2.1}$$

where c is a constant that depends on the propagation environment, d is the propagation distance, and α is path loss coefficient. Typical values of α for various wireless environments can be found in [46]. Assuming the path loss between S→D to be unity, the relative gain of S→R and R→D links are defined [47], respectively, as

$$G_{SR} = \left(d_{SD}/d_{SR}\right)^{\alpha}, \tag{2.2}$$

$$G_{RD} = \left(d_{SD}/d_{RD}\right)^{\alpha}. \tag{2.3}$$

These ratios can be further related to each other by through law of cosines as

$$G_{SR}^{-2/\alpha} + G_{RD}^{-2/\alpha} - 2G_{SR}^{-1/\alpha}G_{RD}^{-1/\alpha}\cos\theta = 1. \tag{2.4}$$

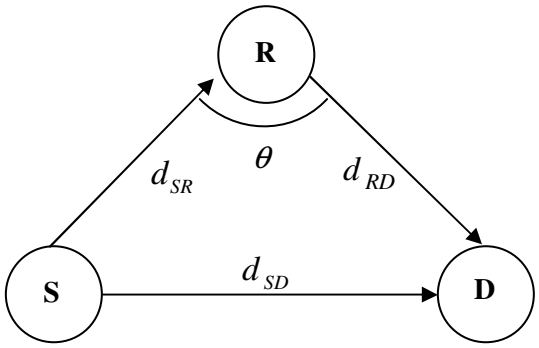

Figure 2.1 Relay-assisted transmission model.

2.2.1 Protocol I

In Protocol I, the source terminal communicates with the relay and destination during the first time slot. In the second time slot, both the relay and source terminals communicate with the destination terminal. Let x_1 denote the transmitted signal in the first time slot. We assume x_1 is the output of an M-PSK (Phase Shift Keying) modulator with unit energy. Considering path-loss effects, the received signals at the relay and the destination are given as

$$r_R = \sqrt{2G_{SR}K_T E}h_{SR}x_1 + n_R\,, \tag{2.5}$$

$$r_{D1} = \sqrt{2K_T E}h_{SD}x_1 + n_{D1}\,, \tag{2.6}$$

where n_R and n_{D1} are the independent samples of zero-mean complex Gaussian random variables with variance $N_0/2$ per dimension, which model the additive noise terms. h_{SR} and h_{RD} denote the zero-mean complex Gaussian fading coefficients with variances 0.5 per dimension, leading to a Rayleigh fading channel assumption. Here, the total energy (to be used by both source and relay terminals) is $2E$ during two time slots yielding an average power in proportion to E per time slot, i.e., assuming unit time duration. K_T is an optimization parameter and controls the fraction of power which is reserved for the source terminal's use in the first time slot, i.e., broadcasting phase. At the

relay, we assume that AaF under APS [12], [48] is used. The relay terminal normalizes the received signal r_R by a factor of

$$\sqrt{E_{n_R,h_{SR}}\left[\left|r_R\right|^2\right]} = \sqrt{2G_{SR}K_T E + N_0}\,, \tag{2.7}$$

where we have used $E_{h_{SR}}[|h_{SR}|^2]=1$ and $E_{n_R}[|n_R|^2]=N_0$. The relay re-transmits the signal during the second time slot. The source terminal simultaneously transmits x_2 using $2(1-K_T)K_S E$ where K_S is another optimization parameter and controls the fraction of power which is reserved for the source terminal's use in the second time slot, i.e., relaying phase. Therefore, the power used by the source in broadcasting and relaying phase is, respectively, $2K_T E$ and $2(1-K_T)K_S E$. Power used by the relay terminal is $2(1-K_T)(1-K_S)E$.

The received signal at the destination terminal is the superposition of transmitted signals by the relay and source terminals resulting in

$$r_{D2} = \sqrt{2(1-K_T)K_S E}\,h_{SD}x_2 + \sqrt{\frac{4G_{SR}G_{RD}K_T(1-K_T)(1-K_S)E^2}{2G_{SR}K_T E + N_0}}\,h_{RD}h_{SR}x_1 + \tilde{n}_{D2}\,, \tag{2.8}$$

where we define the effective noise term as

$$\tilde{n}_{D2} = \sqrt{\frac{2G_{RD}(1-K_T)(1-K_S)E}{2G_{SR}K_T E + N_0}}\,h_{RD}n_R + n_{D2}\,. \tag{2.9}$$

In the above, n_{D2} is modeled as a zero-mean complex Gaussian random variable with variance $N_0/2$ per dimension. h_{RD} is a zero-mean complex Gaussian fading coefficient with variances 0.5 per dimension, leading to a Rayleigh fading channel assumption similar to h_{SR} and h_{SD}. Conditioned on h_{RD}, $\tilde{n}_{D2}$ turns out to be complex Gaussian. We assume that the destination terminal normalizes the received signal given by (2.8) with $\sqrt{1+2G_{RD}(1-K_T)(1-K_S)E|h_{RD}|^2/(2G_{SR}K_T E+N_0)}$ [2], resulting in

$$r'_{D2} = \sqrt{A_1}\sqrt{E}\,h_{RD}h_{SR}x_1 + \sqrt{A_2}\sqrt{E}\,h_{SD}x_2 + n'_{D2}\,, \tag{2.10}$$

[2] This does not change the SNR, but simplifies the ensuing presentation [14].

where $n_{D2}^{'}$ is complex Gaussian random variable which has zero mean and variance of $N_0/2$ per dimension. In (2.10), A_1 and A_2 are defined, respectively, as

$$A_1 = A_{N1} \Big/ \left(A_D + |h_{RD}|^2 \right), \tag{2.11}$$

$$A_2 = A_{N2} \Big/ \left(A_D + |h_{RD}|^2 \right). \tag{2.12}$$

where

$A_{N1} = 2G_{SR}K_T$,

$A_{N2} = K_S \left(1 + 2G_{SR}K_T SNR\right) \Big/ \left[G_{RD} \left(1 - K_S\right) SNR \right]$,

$A_D = \left[1 + 2G_{SR}K_T SNR\right] \Big/ \left[2G_{RD} \left(1 - K_T\right)\left(1 - K_S\right) SNR \right]$

with $SNR = E/N_0$.

After setting up the relay-assisted transmission model for Protocol I given by (2.6) and (2.10), we now introduce space-time coding across the transmitted signals x_1 and x_2. For the case of single relay deployment as considered here, we use STBC designed for two transmit antennas, i.e., Alamouti's scheme [6]. The received signals at the destination terminal during the four time slots can be written in a compact matrix form as $\mathbf{r} = \mathbf{hX} + \mathbf{n}$ where $\mathbf{h} = \left[h_{SD} \quad h_{SR}h_{RD}\right]$, $\mathbf{n} = [n_{D1} \quad n_{D2}^{'} \quad n_{D3} \quad n_{D4}^{'}]$, and

$$\mathbf{X} = \begin{bmatrix} \sqrt{A_0}\sqrt{E}x_1 & \sqrt{A_2}\sqrt{E}x_2 & \sqrt{A_0E}x_2 & \sqrt{A_2}\sqrt{E}x_1^* \\ 0 & \sqrt{A_1}\sqrt{E}x_1 & 0 & -\sqrt{A_1}\sqrt{E}x_2^* \end{bmatrix} \tag{2.13}$$

Each entry of $\mathbf{n}$ is a zero-mean complex Gaussian random variable and $A_0 = 2K_T$. Since distributed implementation of repetition code offers the same rate of Alamouti code in the considered single-relay scenario[3], we also consider it as a possible candidate for the underlying distributed code. For the repetition code, $\mathbf{X}$ is given by

$$\mathbf{X} = \begin{bmatrix} \sqrt{A_0E}x_1 & \sqrt{A_2}\sqrt{E}x_1 & \sqrt{A_0E}x_2 & \sqrt{A_2}\sqrt{E}x_2 \\ 0 & \sqrt{A_1}\sqrt{E}x_1 & 0 & \sqrt{A_1}\sqrt{E}x_2 \end{bmatrix}. \tag{2.14}$$

[3] In distributed implementation of single-relay transmission, Alamouti's code is able to transmit two symbols in four time intervals resulting in a rate of 1/2 [14].

2.2.2 Protocol II

Protocol II realizes receive diversity in a distributed manner and does not involve transmit diversity. Therefore, unlike Protocol I which relies on two optimization parameters K_T and K_S, only K_T is relevant for Protocol II optimization. Let x_1 denote the transmitted signal. Considering path-loss effects, the received signals at the relay and destination are given as

$$r_R = \sqrt{2G_{SR}K_T E}h_{SR}x_1 + n_R, \tag{2.15}$$

$$r_{D1} = \sqrt{2K_T E}h_{SD}x_1 + n_{D1}. \tag{2.16}$$

There is no source-to-destination transmission in the second time slot. The received signal at destination is given by

$$r_{D2} = \sqrt{\left[4G_{SR}G_{RD}K_T\left(1-K_T\right)E^2\right]/\left[2G_{SR}K_T E + N_0\right]}h_{RD}h_{SR}x_1 + \tilde{n}_{D2}, \tag{2.17}$$

where the effective noise term is defined as

$$\tilde{n}_{D2} = \sqrt{\left[2G_{RD}\left(1-K_T\right)E\right]/\left[2G_{SR}K_T E + N_0\right]}h_{RD}n_R + n_{D2}. \tag{2.18}$$

$\tilde{n}_{D2}$ is complex Gaussian conditioned on h_{RD}. In a similar manner to the previous section, we normalize (2.17) such that additive noise term has a variance of N_0 which yields

$$r_{D2}^{'} = \sqrt{B_1}\sqrt{E}h_{SR}h_{RD}x_1 + n_{D2}^{'}, \tag{2.19}$$

where we define $B_1 = B_N/\left(B_D + \left|h_{RD}\right|^2\right)$ with $B_D = \left[1 + 2G_{SR}K_T SNR\right]/\left[2G_{RD}\left(1-K_T\right)SNR\right]$ and $B_N = 2G_{SR}K_T$. (2.16) and (2.19) can be written in matrix form as in the previous section where $\mathbf{X}$ now has the form of

$$\mathbf{X} = \begin{bmatrix} \sqrt{B_0}\sqrt{E}x_1 & 0 \\ 0 & \sqrt{B_1}\sqrt{E}x_1 \end{bmatrix} \tag{2.20}$$

with $B_0 = 2K_T$.

2.2.3 Protocol III

Protocol III is identical to Protocol I apart from the fact that the destination terminal chooses not to receive the direct source-to-destination transmission during the first time slot for reasons which are possibly imposed from the upper-layer networking protocols. For example, the destination terminal may be engaged in data transmission to another terminal during the first time slot. Following similar steps as in Section 2.2.1 for Protocol I, the received signals can be written in matrix form where $\mathbf{X}$ is now given by

$$\mathbf{X} = \begin{bmatrix} \sqrt{A_2}\sqrt{E}x_2 & \sqrt{A_2}\sqrt{E}x_1^* \\ \sqrt{A_1}\sqrt{E}x_1 & -\sqrt{A_1}\sqrt{E}x_2^* \end{bmatrix}. \tag{2.21}$$

For the repetition code, $\mathbf{X}$ takes the form of

$$\mathbf{X} = \begin{bmatrix} \sqrt{A_2}\sqrt{E}x_1 & \sqrt{A_2}\sqrt{E}x_2 \\ \sqrt{A_1}\sqrt{E}x_1 & \sqrt{A_1}\sqrt{E}x_2 \end{bmatrix}. \tag{2.22}$$

2.3 Union Bound on the BER performance

We consider BER performance as our objective function for power allocation problem under consideration. A union bound on the BER for coded systems is given by [49]

$$P_b \le \frac{1}{n}\sum_{\mathbf{X}} p(\mathbf{X}) \sum_{\mathbf{X}\neq\hat{\mathbf{X}}} q\left(\mathbf{X}\to\hat{\mathbf{X}}\right) P\left(\mathbf{X}\to\hat{\mathbf{X}}\right), \tag{2.23}$$

where $p(\mathbf{X})$ is the probability that codeword $\mathbf{X}$ is transmitted, $q\left(\mathbf{X}\to\hat{\mathbf{X}}\right)$ is the number of information bit errors in choosing another codeword $\hat{\mathbf{X}}$ instead of the original one, and n is the number of information bits per transmission. In (2.23), $P\left(\mathbf{X}\to\hat{\mathbf{X}}\right)$ is the probability of deciding in favour of $\hat{\mathbf{X}}$ instead of $\mathbf{X}$ and called as pairwise error probability (PEP). As reflected by (2.23), PEP is the building block for the derivation of union bounds to the error probability.

In this section, we derive PEP expressions for each protocol under consideration. A Chernoff bound on the (conditional) PEP is given by [5]

$$P\left(\mathbf{X}\to\hat{\mathbf{X}}|\mathbf{h}\right)\le\exp\left(\frac{-d^2\left(\mathbf{X},\hat{\mathbf{X}}|\mathbf{h}\right)}{4N_0}\right), \tag{2.24}$$

where the Euclidean distance (conditioned on fading channel coefficients) between $\mathbf{X}$ and $\hat{\mathbf{X}}$ is $d^2\left(\mathbf{X},\hat{\mathbf{X}}|\mathbf{h}\right)=\mathbf{h}\boldsymbol{\Delta}\,\mathbf{h}^{\mathrm{H}}$ with $\boldsymbol{\Delta}=\left(\mathbf{X}-\hat{\mathbf{X}}\right)\left(\mathbf{X}-\hat{\mathbf{X}}\right)^{\mathrm{H}}$. Recalling the definitions of $\mathbf{X}$ in (2.13), (2.20), (2.21) for different protocols and carrying out the expectation with respect to **h**, we obtain PEP expressions for Protocols I, II and III in the following:

2.3.1 PEP for Protocol I

Replacing (2.13) in (2.24), we have

$$P\left(\mathbf{X}\to\hat{\mathbf{X}}|\mathbf{h}\right)\le\exp\left\{\frac{-SNR\chi_1}{4}\left[\left(A_0+A_2\right)\left|h_{SD}\right|^2+A_1\left|h_{SR}\right|^2\left|h_{RD}\right|^2\right]\right\}, \tag{2.25}$$

with $\chi_1=\left|x_1-\hat{x}_1\right|^2+\left|x_2-\hat{x}_2\right|^2$. Averaging (2.25) with respect to $\left|h_{SR}\right|^2$ and $\left|h_{SD}\right|^2$ which follow exponential distribution, we obtain

$$P\left(\mathbf{X}\to\hat{\mathbf{X}}|h_{RD}\right)\le\left(1+\frac{SNR\left(A_0+A_2\right)\chi_1}{4}\right)^{-1}\left(1+\frac{SNRA_1\chi_1}{4}\left|h_{RD}\right|^2\right)^{-1}. \tag{2.26}$$

After some mathematical manipulation, we obtain

$$P\left(\mathbf{X}\to\hat{\mathbf{X}}\middle|h_{RD}\right)\le\delta_1\left(1+\alpha_1\frac{1}{\left|h_{RD}\right|^2+\lambda_1}+\beta_1\frac{1}{\left|h_{RD}\right|^2+\mu_1}\right). \tag{2.27}$$

Here, δ_1, λ_1, μ_1, α_1, and β_1 are defined, respectively, as

$$\delta_1=\left(1+\frac{SNR}{4}A_{N1}\chi_1\right)^{-1}\left(1+\frac{SNR}{4}A_0\chi_1\right)^{-1}, \tag{2.28}$$

$$\lambda_1=\left[A_D\left(1+\frac{SNR}{4}A_0\chi_1\right)+\frac{SNR}{4}A_{N2}\chi_1\right]\Bigg/\left(1+\frac{SNR}{4}A_0\chi_1\right), \tag{2.29}$$

$$\mu_1=A_D\Bigg/\left(1+\frac{SNR}{4}A_{N1}\chi_1\right), \tag{2.30}$$

$$\alpha_1 = \left[-\left(2A_D - \lambda_1 - \mu_1\right)\lambda_1 + A_D^2 - \lambda_1\mu_1 \right] \Big/ \left(\mu_1 - \lambda_1\right), \tag{2.31}$$

$$\beta_1 = \left[-\left(2A_D - \lambda_1 - \mu_1\right)\mu_1 + A_D^2 - \lambda_1\mu_1 \right] \Big/ \left(\lambda_1 - \mu_1\right), \tag{2.32}$$

where A_0, A_D, A_{N1}, and A_{N2} have been earlier introduced in our transmission model. Carrying out an expectation of (2.27) with respect to $|h_{RD}|^2$, we have

$$P\left(\mathbf{X} \to \hat{\mathbf{X}}\right) \le \delta_1 \left[1 + \alpha_1 \int_0^\infty \frac{1}{|h_{RD}|^2 + \lambda_1} \exp\left(-|h_{RD}|^2\right) d|h_{RD}|^2 + \beta_1 \int_0^\infty \frac{1}{|h_{RD}|^2 + \mu_1} \exp\left(-|h_{RD}|^2\right) d|h_{RD}|^2 \right]. \tag{2.33}$$

Eq. (2.33) has a similar form of [50- p.366, 3.384] and readily yields a closed-form solution as

$$P\left(\mathbf{X} \to \hat{\mathbf{X}}\right) \le \Psi_1(\chi_1) \triangleq \delta_1 \left[1 + \alpha_1 \exp(\lambda_1)\Gamma(0, \lambda_1) + \beta_1 \exp(\mu_1)\Gamma(0, \mu_1) \right] \tag{2.34}$$

where $\Gamma(.,.)$ denotes the incomplete gamma function [50].

It has been verified through a Monte-Carlo simulation that for various values of SNR and relay location the derived upper bound given by (2.34) lies within ~3 dB of the exact PEP expression (see Fig.2.2).

Assuming equal-power allocation case, (i.e., $K_T = 0.5$ and $K_S = 0.5$), equal distances among all nodes (i.e., $G_{SR} = G_{SD} = G_{RD} = 1$), and sufficiently high *SNR*, (2.34) reduces to

$$P\left(\mathbf{X} \to \hat{\mathbf{X}}\right) \le \left(\frac{SNR\chi_1}{4} \right)^{-2} \left[1.2 + \frac{4}{3} \exp\left(\frac{8}{SNR\chi_1} \right) \Gamma\left(0, \frac{8}{SNR\chi_1} \right) \right] \tag{2.35}$$

which illustrates that a diversity order of two is achievable.

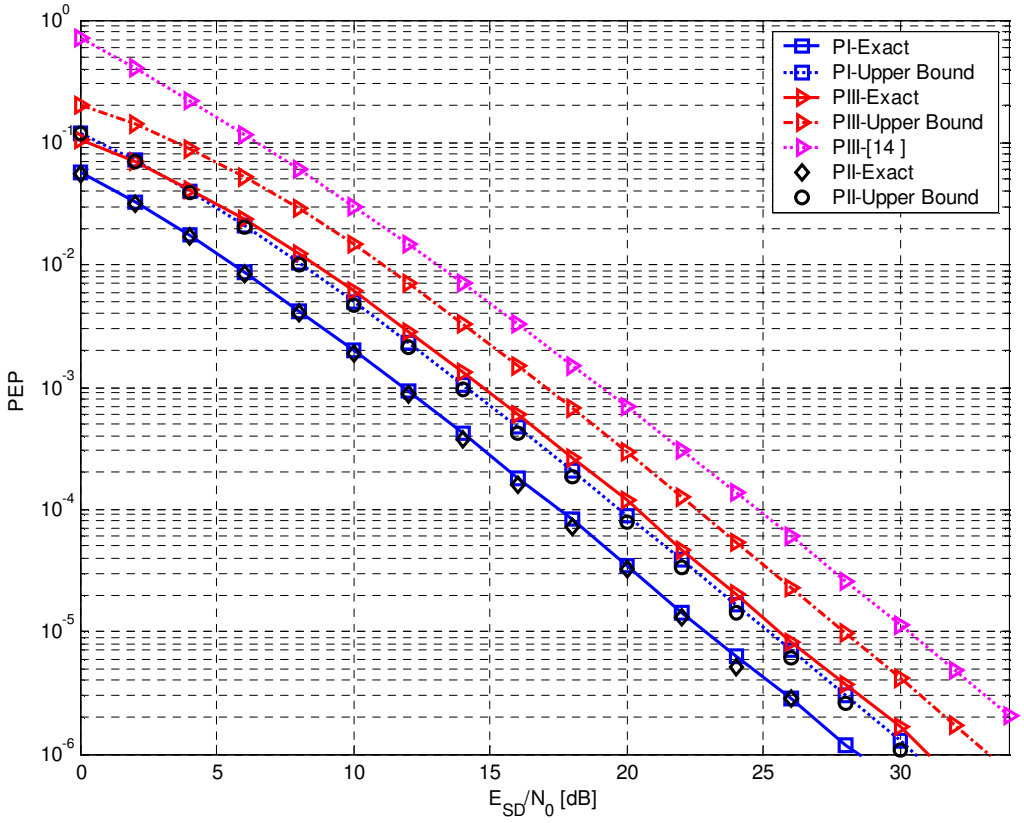

Figure 2.2 Comparison of exact and derived upper bounds on PEP.

2.3.2 PEP for Protocol II

Replacing (2.20) in (2.24) and averaging the resulting expression with respect to $|h_{SR}|^2$ and $|h_{SD}|^2$, we have

$$P\left(\mathbf{X}\to\hat{\mathbf{X}}|h_{RD}\right)\le\left(1+\frac{SNRB_0\chi_2}{4}\right)^{-1}\left(1+\frac{SNRB_1\chi_2}{4}|h_{RD}|^2\right)^{-1}, \tag{2.36}$$

with $\chi_2=|x_1-\hat{x}_1|^2$. After some mathematical manipulation, we obtain

$$P\left(\mathbf{X}\to\hat{\mathbf{X}}|h_{RD}\right)\le\delta_2\left(1+\frac{\beta_2}{|h_{RD}|^2+\lambda_2}\right). \tag{2.37}$$

Here, δ_2, β_2, and λ_2 are defined as

$$\delta_2 = \left(1+\frac{SNR}{4}B_0\chi_2\right)^{-1}\left(1+\frac{SNR}{4}B_N\chi_2\right)^{-1}, \tag{2.38}$$

$$\lambda_2 = B_D \Big/ \left(1+\frac{SNR}{4}B_N\chi_2\right). \tag{2.39}$$

$$\beta_2 = B_D - \lambda_2, \tag{2.40}$$

where B_0, B_D, and B_N have been earlier introduced in our transmission model. By averaging (2.37) over $|h_{RD}|^2$, we obtain the final form for PEP as

$$P\left(\mathbf{X}\to\hat{\mathbf{X}}\right) \le \Psi_2(\chi_2) \hat{=} \delta_2\left[1+\beta_2\exp(\lambda_2)\Gamma(0,\lambda_2)\right]. \tag{2.41}$$

Similar to the upper bound derived for Protocol I, this upper bound also lies within ~2 dB of the exact PEP expression. Under the assumptions of equal-power allocation, equal distances among all nodes, and sufficiently high SNR, (2.41) simplifies to

$$P\left(\mathbf{X}\to\hat{\mathbf{X}}\right) \le \left(\frac{SNR\chi_2}{4}\right)^{-2}\left[1+\exp\left(\frac{4}{SNR\chi_2}\right)\Gamma\left(0,\frac{4}{SNR\chi_2}\right)\right] \tag{2.42}$$

which illustrates that a diversity order of two is extracted. It should be further noted that if we use non-fading h_{RD} assumption (i.e., $h_{RD}=1$) as in [24], the final PEP has a similar form of (2.36). In this case, to minimize the resulting PEP, we need to maximize the summation of the sum and product of the SNRs in the direct and relaying links. This is related to the criteria in [24] which aim to maximize either the sum or the product of the SNRs.

2.3.3 PEP for Protocol III

Replacing (2.21) in (2.24) and averaging the resulting expression with respect to $|h_{SR}|^2$ and $|h_{SD}|^2$, we have

$$P\left(\mathbf{X}\to\hat{\mathbf{X}}\middle|h_{RD}\right) \le \left(1+\frac{SNRA_2\chi_3}{4}\right)^{-1}\left(1+\frac{SNRA_1\chi_3}{4}|h_{RD}|^2\right)^{-1}. \tag{2.43}$$

After some mathematical manipulation, we obtain

$$P\left(\mathbf{X}\to\hat{\mathbf{X}}\middle|h_{RD}\right)\le\delta_3\left(1+\alpha_3\frac{1}{|h_{RD}|^2+\lambda_3}+\beta_3\frac{1}{|h_{RD}|^2+\mu_3}\right), \tag{2.44}$$

where δ_3, μ_3, λ_3, α_3, and β_3 are defined as

$$\delta_3=\left(1+\frac{SNR}{4}A_{N1}\chi_3\right)^{-1}, \tag{2.45}$$

$$\lambda_3=A_D+\frac{SNR}{4}A_{N2}\chi_3, \tag{2.46}$$

$$\mu_3=A_D\Big/\left(1+\frac{SNR}{4}A_{N1}\chi_3\right), \tag{2.47}$$

$$\alpha_3=\left[-\left(2A_D-\lambda_3-\mu_3\right)\lambda_3+A_D^2-\lambda_3\mu_3\right]\Big/\left(\mu_3-\lambda_3\right), \tag{2.48}$$

$$\beta_3=\left[-\left(2A_D-\lambda_3-\mu_3\right)\mu_3+A_D^2-\lambda_3\mu_3\right]\Big/\left(\lambda_3-\mu_3\right). \tag{2.49}$$

By averaging (2.44) over $|h_{RD}|^2$, we obtain the final form for PEP as

$$P\left(\mathbf{X},\hat{\mathbf{X}}\right)\le\Psi_3\left(\chi_3\right)\triangleq\delta_3\left[1+\alpha_3\exp\left(\lambda_3\right)\Gamma\left(0,\lambda_3\right)+\beta_3\exp\left(\mu_3\right)\Gamma\left(0,\mu_3\right)\right]. \tag{2.50}$$

with $\chi_3=|x_1-\hat{x}_1|^2+|x_2-\hat{x}_2|^2$ [4]. The tightness of upper bound given by (2.50) is similar to that of Protocol I (See Fig.2.2). For comparison purpose, we also include the plot of PEP expression derived in [14]. Our derived PEP is 2 dB tighter than the one of [14]. Under the assumption of equal-power allocation, high SNR, and equal distances among all nodes, (2.50) simplifies to

$$P\left(\mathbf{X}\to\hat{\mathbf{X}}\right)\le\left(\frac{SNR\chi_3}{8}\right)^{-2}\exp\left(\frac{8}{SNR\chi_3}\right)\Gamma\left(0,\frac{8}{SNR\chi_3}\right), \tag{2.51}$$

which shows that a diversity order of two is available. For $G_{SR}/G_{RD}<<1$, i.e., relay is close to destination, it can be shown that (2.51) reduces to

---

[4] Both Protocols I and III are built upon Alamouti code. Therefore, $\chi_1=\chi_3$.

$$P\left(\mathbf{X}\to\hat{\mathbf{X}}\right)\le\left(\frac{SNR\chi_3}{4}\right)^{-1}. \tag{2.52}$$

This demonstrates that Protocol III with equal power allocation suffers diversity loss for a scenario where the relay is close to destination. We will later demonstrate that optimum power allocation guarantees full diversity for Protocol III regardless of the relay location.

2.4 Optimum Power Allocation

As noted in Section 2.3, the objective function in our optimization problem is the union bound on BER. Replacing PEP expressions given by (2.34), (2.41), (2.50), respectively, for Protocols I, II and III, in the BER bound given by (2.23), we obtain the objective functions to be used for power allocation. The specific form of BER expressions depends on the modulation scheme and underlying code. For example, if BPSK is used as the modulation scheme, upper bounds on BER scheme can be calculated as

$$P_{b1}\le\Psi_1(\chi_1=2)+\Psi_1(\chi_1=4), \tag{2.53}$$

$$P_{b2}\le\Psi_2(\chi_2=4), \tag{2.54}$$

$$P_{b3}\le\Psi_3(\chi_3=2)+\Psi_3(\chi_3=4), \tag{2.55}$$

for Protocols I, II, and III respectively. If QPSK is used, the upper bounds on BER are given as

$$P_{b1}\le\Psi_1(\chi_1=2)+3\Psi_1(\chi_1=4)+3\Psi_1(\chi_1=6)+\Psi_1(\chi_1=8), \tag{2.56}$$

$$P_{b2}\le\Psi_2(\chi_2=2)+\Psi_2(\chi_2=4), \tag{2.57}$$

$$P_{b3}\le\Psi_3(\chi_3=2)+3\Psi_3(\chi_3=4)+3\Psi_3(\chi_3=6)+\Psi_3(\chi_3=8). \tag{2.58}$$

Similar bounds can be easily found for higher order PSK schemes. We need to minimize the resulting BER expressions with respect to the power allocation parameters K_T and K_S ($0<K_T,K_S<1$). These expressions are found to be convex functions with respect to optimization parameters K_T and K_S. Convexity of the functions under consideration guarantees that local

minimum found through optimization will be indeed a global minimum. Unfortunately, an analytical solution for power allocation values in the general case is very difficult, if not infeasible. In the rest, we follow two approaches: First, we pursue numerical optimization of union BER bounds to find out the optimal values of K_T and K_S. For this purpose, we have used Matlab optimization toolbox command "fmincon" designed to find the minimum of a given constrained nonlinear multivariable function [54], [55]. Second, we impose certain assumptions on the relay locations, consider non-fading R→D link, and derive optimal allocation values analytically for Protocols II and III based on the simplified PEPs. Our results demonstrate that analytical solutions largely coincide with numerical results although the former have been obtained under some simplifying assumptions.

Under non-fading R→D channel assumption (i.e., $h_{RD}=1$), optimum value of K_T for Protocol II can be found by differentiating (2.36) and equating it to zero. Assuming $G_{SR}\approx 1$ and $G_{RD}>>1$ (i.e., relay is close to destination), we find

$$K_T=\frac{\left(4G_{RD}-1\right)\left(2G_{RD}SNR+1\right)-\sqrt{\left(2G_{RD}SNR+1\right)\left(8{G_{RD}}^2+16{G_{RD}}^2SNR+2G_{RD}SNR+1\right)}}{8G_{RD}SNR\left(G_{RD}-1\right)}. \qquad (2.59)$$

Under the assumption of $G_{SR}/G_{RD}=0\text{dB}$ (i.e., relay is equidistant from source and destination), we have

$$K_T=\frac{2SNR-1+\sqrt{1.18+3.5SNR+4SNR^2}}{6SNR}. \qquad (2.60)$$

Under non-fading R→D channel assumption, optimum values of K_T and K_S for Protocol III can be found by differentiating (2.43) and equating it to zero. Assuming large values of SNR, $G_{SR}\approx 1$ and $G_{RD}>>1$, the optimum values are

$$K_T=\frac{3G_{RD}-\sqrt{G_{RD}\left(G_{RD}+8\right)}}{4\left(G_{RD}-1\right)}, \qquad (2.61)$$

$$K_S = \frac{4 - G_{RD} + \sqrt{G_{RD}\left(G_{RD}+8\right)}}{8}. \tag{2.62}$$

Under the assumption of $G_{SR} >> 1$ and $G_{RD} \approx 1$ (i.e., relay is close to source), we have

$$K_T = \frac{2}{3+\sqrt{8G_{SR}+1}}, \tag{2.63}$$

$$K_S = \frac{4G_{SR} - 1 + \sqrt{8G_{SR}+1}}{8G_{SR}}. \tag{2.64}$$

For the particular case of $G_{SR}/G_{RD} = 0\text{dB}$ (i.e., the relay is equidistant from source and destination terminals), we obtain $K_T = 1/3$ and $K_S = 3/4$. Finally, we note that an analytical solution for Protocol I is intractable even under the considered simplifying assumptions.

In Table 2.1, we present optimum values of K_T and K_S (obtained through numerical optimization) for various values of G_{SR}/G_{RD} which reflects the effect of relay location. More negative this ratio is, more closely the relay is placed to destination terminal. On the other hand, positive values of this ratio indicate that the relay is more close to source terminal. For Protocol I, we observe from Table 2.1.a that

- When the relay is close to destination, optimum values of K_T are ~ 0.95, and those of K_S are ~0. These values indicate that it is better to spend most of power in broadcast phase, and in the relaying phase available power (i.e., $1 - K_T$) should be dedicated to the relay terminal.
- When relay is equidistant from source and destination, the optimum value of K_T is ~2/3 which means that 66 % of power should be spent in the broadcast phase. The optimum value of K_S is still ~0 which indicates that all available power should be dedicated to the relay terminal in the relaying phase.
- When relay is close to source and system is operating in low SNR region (0-10 dB), optimum values of K_T and K_S are the same as in previous case, but in higher SNR region (>10 dB) the optimum value of K_S increases with increasing SNR while that of K_T decreases.

For Protocol II, we observe from Table 2.1.b that

- When relay is equidistant or close to source, ~66% of power is required by the source to achieve optimum performance. This perfectly matches to the analytical result obtained from (2.60).
- When relay is close to destination, ~95% of power should be used in broadcast phase. This can be readily compared to (2.59) which yields very similar results. For example, for $G_{SR}/G_{RD} = -30\text{dB}$ and $SNR = 20\text{dB}$, K_T is equal to 0.97.

For Protocol III, we observe from Table 2.1.c that

Optimum values of K_S and K_T are ~1 and ~0.5 for negative values of G_{SR}/G_{RD} ratio (in dB). This is in contrast with small values of K_S observed for Protocol I. Here, it should be noted that Protocol I is able to guarantee a diversity order of two even with equal power allocation owing to the existence of S→D link in the relaying phase. However, the diversity order of Protocol III with equal power allocation reduces to one for scenarios where relay is close to destination. Such large values of K_S in the optimized Protocol III aim to balance the S→D and R→D links so that diversity order of two can be extracted, guaranteeing the full diversity. We also note that our analytical derivations give similar results to those obtained through numerical optimization. For example, (2.61) and (2.62) yield $K_S = 0.99$ and $K_T = 0.49$ for $G_{SR}/G_{RD} = -30\text{dB}$.

- For equidistant nodes, optimum values of K_T and K_S through numerical optimization are found to be ~ 0.26 and ~0.75, respectively. These results are also in line with our analytical derivations for this particular relay location.
- When relay is close to source, numerical optimization yields K_T ~0 and K_S ~0.6. These are similar to our analytical results which can be obtained from (2.63) and (2.64). For example, assuming $G_{SR}/G_{RD} = 30\text{dB}$, (2.63) and (2.64) yield $K_T = 0.02$ and $K_S = 0.51$.

Table 2.1 Power allocation parameters for distributed Alamouti code.

(a) Protocol I

SNR [dB]	$G_{SR}/G_{RD} = -30$dB		$G_{SR}/G_{RD} = 0$dB		$G_{SR}/G_{RD} = 30$dB	
	K_T	K_S	K_T	K_S	K_T	K_S
5	0.9535	0.0000	0.6648	0.0000	0.6336	0.0000
10	0.9516	0.0000	0.6501	0.0000	0.6153	0.0000
15	0.9503	0.0000	0.6417	0.0000	0.5812	0.0586
20	0.9493	0.0000	0.6358	0.0000	0.3680	0.3652
25	0.9486	0.0000	0.6315	0.0000	0.3682	0.3583
30	0.9479	0.0000	0.6280	0.0000	0.3608	0.3599

(b) Protocol II

SNR [dB]	$G_{SR}/G_{RD} = -30$dB	$G_{SR}/G_{RD} = 0$dB	$G_{SR}/G_{RD} = 30$dB
	K_T	K_T	K_T
5	0.9551	0.6728	0.6466
10	0.9530	0.6580	0.6267
15	0.9517	0.6493	0.6156
20	0.9507	0.6432	0.6081
25	0.9499	0.6385	0.6025
30	0.9492	0.6348	0.5982

(c) Protocol III

SNR [dB]	$G_{SR}/G_{RD} = -30$dB		$G_{SR}/G_{RD} = 0$dB		$G_{SR}/G_{RD} = 30$dB	
	K_T	K_S	K_T	K_S	K_T	K_S
5	0.9276	0.0722	0.2697	0.7707	0.0236	0.6532
10	0.4765	0.9984	0.2660	0.7565	0.0223	0.6034
15	0.4780	0.9984	0.2631	0.7484	0.0433	0.6066
20	0.4787	0.9984	0.2609	0.7427	0.0464	0.5999
25	0.4792	0.9984	0.2590	0.7384	0.0490	0.5950
30	0.4795	0.9983	0.2575	0.7349	0.0515	0.5911

In Fig. 2.3, we demonstrate performance gains in power efficiency (as predicted by the derived PEP expressions) achieved by optimum power allocation (OPA) over equal power allocation (EPA) for a target BER of 10^{-3} assuming QPSK modulation. The performance gains are presented as a function of G_{SR}/G_{RD}. In Fig.2.3.a given for Protocol I, we observe performance improvements of ~0.4dB and 0.3dB at $G_{SR}/G_{RD} = 0$ dB and $G_{SR}/G_{RD} = 30$ dB, respectively. Advantages of OPA are more pronounced for negative values of G_{SR}/G_{RD}. For example, an improvement of ~2.5dB is observed for $G_{SR}/G_{RD} =$ -30 dB. It is clear from this figure that although power optimization helps in all cases, it is more rewarding in scenarios where relay is close to destination. In Fig.2.3.b given for Protocol II, we observe performance improvements up to ~2.6dB for negative values of G_{SR}/G_{RD}. For positive values, it is observed that OPA and EPA performance curves converge to each other. In Fig.3.c given for Protocol III, we observe significant performance improvements for both negative and positive G_{SR}/G_{RD} values. In particular, the performance improvements are ~8.4dB and ~2.9dB at $G_{SR}/G_{RD} = -30$dB and $G_{SR}/G_{RD} =$30dB, respectively. The change in characteristic behavior of Protocol III in comparison to those of Protocols I and II should be also noted. This is actually not unexpected; recall that Protocol III realizes a distributed transmit diversity scheme, so it is expected to perform good when relay is close to source mimicking a virtual transmit antenna array. Protocol II implements receive diversity, so it is expected to perform good when relay is close to destination mimicking a virtual receive antenna array. Protocol I is a combination of both Protocol II and Protocol III. It is observed from our results that the advantages of receive diversity are dominating in this hybrid version.

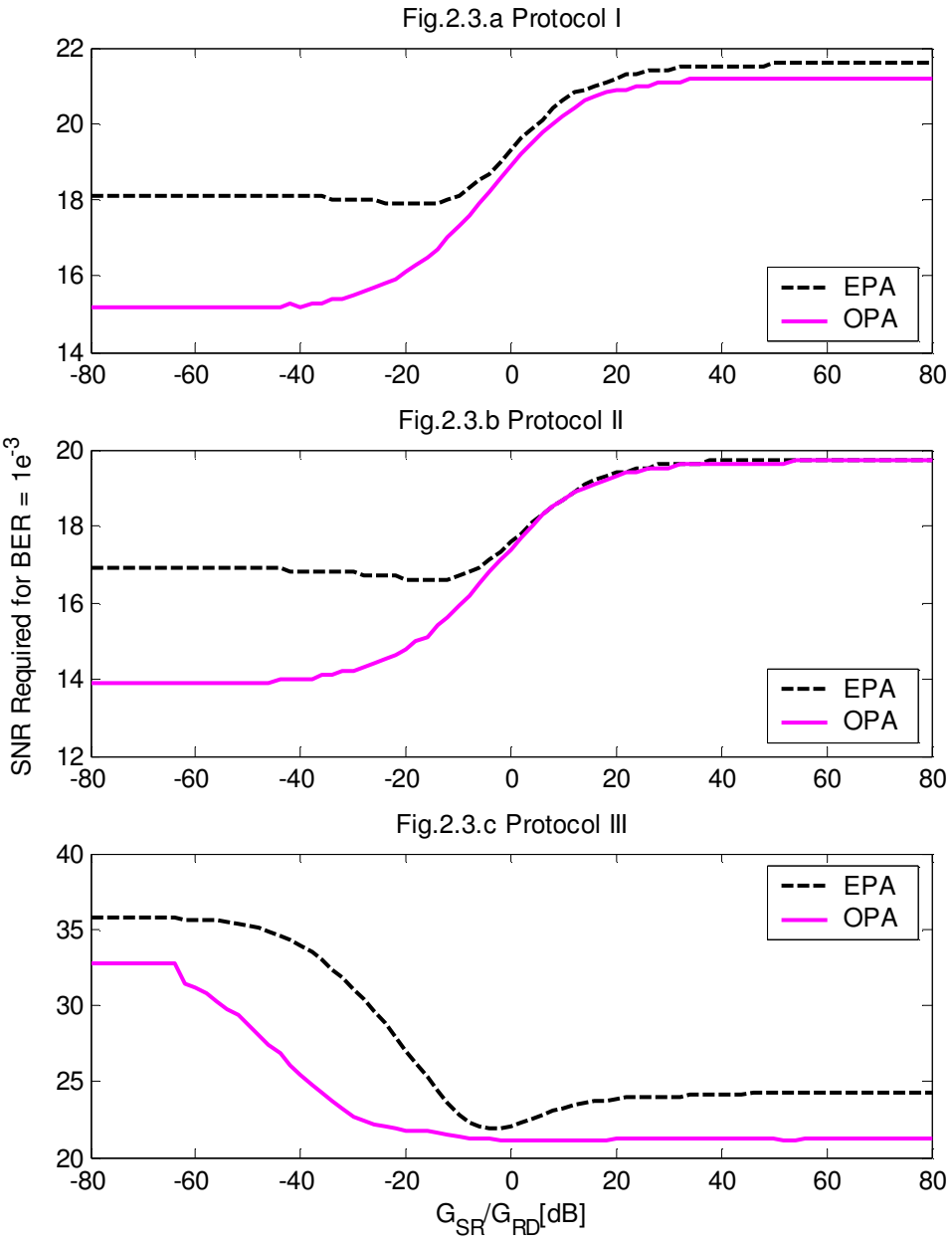

Figure 2.3 SNR required to achieve BER of 10^{-3} for Protocols I, II and III.

2.5 Simulation Results

To further confirm the performance gains of OPA promised by the derived expressions, we have conducted a Monte Carlo simulation study to compare the BER performance of the considered protocols with EPA and OPA. Our simulation results for Protocol I are presented in Fig. 2.4 where we assume QPSK modulation and $\theta=\pi$. We observe performance improvements of 2.5dB, 0.4dB, and 0.29dB at a target BER of 10^{-3} for $G_{SR}/G_{RD}=-30\text{dB}$, 0dB and 30dB respectively. These are similar to performance gains predicted for Protocol I through our PEP expressions. Similar confirmation holds for the other two protocols and those simulation results are not included here due to the space limitations.

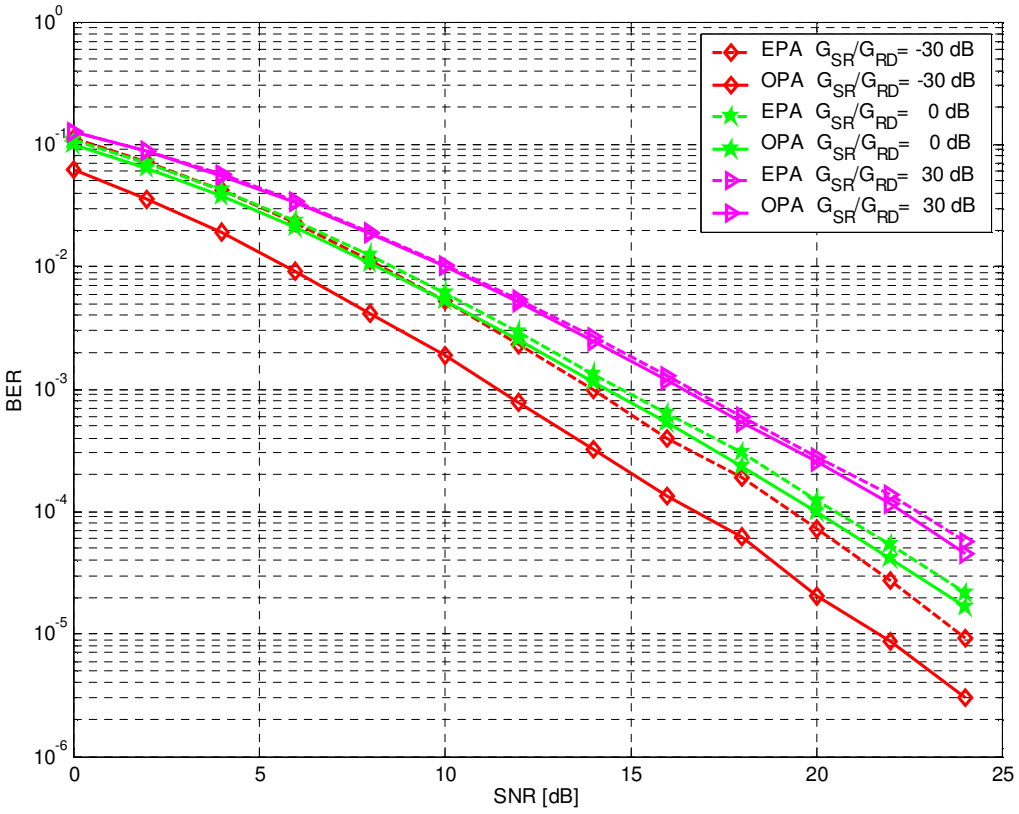

Figure 2.4 Simulated BER performance of Protocol I for different values of G_{SR}/G_{RD}.

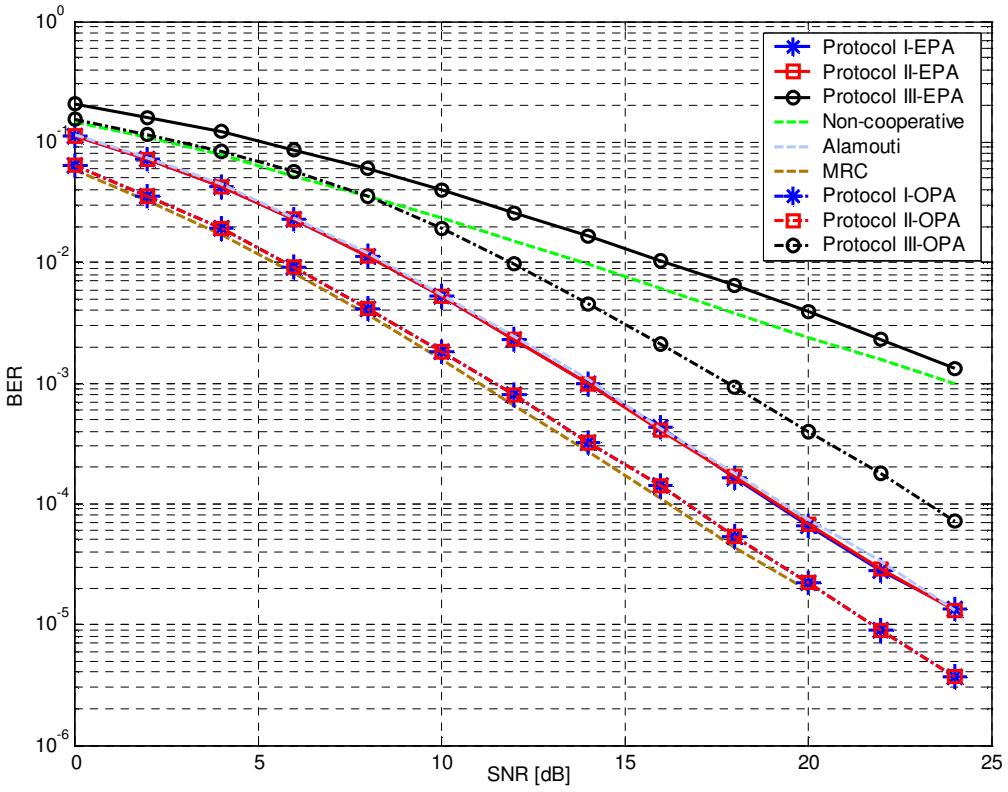

Figure 2.5 Performance comparison of Protocols I, II and III with EPA and OPA ($G_{SR}/G_{RD} = -30\text{dB}$).

Fig. 2.5 presents a performance comparison of three protocols with EPA and OPA assuming $G_{SR}/G_{RD} = -30\text{dB}$. As benchmarks, we include the performance of non-cooperative direct transmission (i.e., no relaying), Alamouti code, and maximal ratio combining (MRC) with two co-located antennas. It should be noted that the inclusion of co-located antenna scenarios help us demonstrate how close the "virtual" antenna implementations can come to their co-located counterparts. The performance of MRC and Alamouti code provide practical lower bounds for Protocol II and Protocol III, which are distributed receive and transmit diversity schemes. To make a fair comparison between cooperative and benchmark schemes which achieve rates of 1/2 and 1 respectively, direct transmission and co-located antenna scenarios are simulated with BPSK. Under

EPA assumption, we observe that Protocol I and Protocol II have a similar performance and outperform Protocol III whose diversity is limited to one for the considered $G_{SR}/G_{RD} = -30\text{dB}$ [5] confirming our earlier observation in (2.52). Suffering severely from the low SNR in source-to-relay link, Protocol III is even outperformed by direct transmission under the same throughput constraint and is far inferior to its co-located counterpart, i.e., Alamouti scheme. We observe that optimized version of Protocol III achieves a diversity order of two and outperforms direct transmission after SNR=8dB. Unlike Protocol III, Protocols I and II guarantee full diversity under EPA assumption, however their performance is still 3dB away from the MRC performance. Under OPA assumption, Protocol II is able to operate just 0.4 dB away from the MRC bound.

In the following, we discuss the choice of the underlying distributed code (i.e., Alamouti vs. repetition code) for Protocols I and III. As earlier noted, repetition code provides a rate of 1/2 which is the same as distributed implementation of STBC (Alamouti) code for the single-relay scenario under consideration. From the codeword matrix definition given by (2.22), it can be easily argued that repetition code will not extract spatial diversity under Protocol III. Therefore, STBC is the obvious choice for Protocol III.

On the other hand, we observe from Fig. 2.6 that both repetition code and STBC present a similar performance under EPA for Protocol I. OPA-STBC brings only a small performance improvement over OPA-repetition code[6]. Therefore, both codes can be possibly used in conjunction with Protocol I. We should, however, remind that our discussion here focuses on the single-relay case. For relay network scenarios with more than one relay, the rate loss due to repetition code might exceed that attributable to STBCs [11]. For example, if three relays are available to assist communication then repetition code can achieve a rate of 1/4 while that of G4 [7] is 1/3.

---

[5] We should note that Protocol III under EPA is able to collect a diversity order of two for $G_{SR}/G_{RD} = 0$ and 30dB , but its performance is still inferior to Protocol I and Protocol II.

[6] The PEP derivations for repetition code are omitted here due to the space limitations, but OPA values can be found in Table 2.2.

Table 2.2 Power allocation parameters for distributed repetition code under Protocol I.

SNR	$G_{SR}/G_{RD} = -30\text{dB}$		$G_{SR}/G_{RD} = 0\text{dB}$		$G_{SR}/G_{RD} = 30\text{dB}$	
[dB]	K_T	K_S	K_T	K_S	K_T	K_S
5	0.9644	0.2035	0.5106	0.4687	0.0346	0.5721
10	0.9643	0.2030	0.5104	0.4597	0.0300	0.5600
15	0.9577	0.5122	0.5445	0.4121	0.0768	0.5219
20	0.9734	0.2847	0.4421	0.4114	0.0681	0.4761
25	0.9734	0.3064	0.5317	0.4112	0.0647	0.4957
30	0.9743	0.2776	0.5475	0.4069	0.1372	0.4598

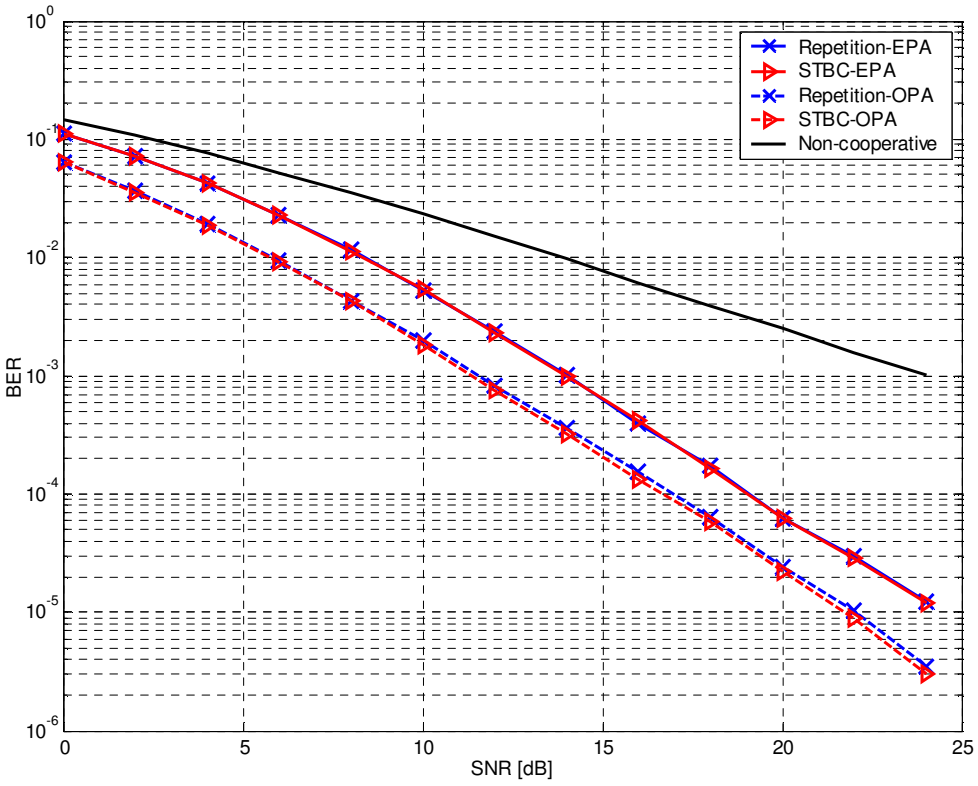

Figure 2.6 Performance of Protocol I with repetition and Alamouti codes ($G_{SR}/G_{RD} = -30\text{dB}$).

Chapter 3
Power Allocation for DaF Relaying

3.1 Introduction

In this chapter, we address the problem of power allocation in a multi-relay network with DaF relaying. The multi-relay network under consideration uses relay selection. First, we propose a relay selection criterion based on an open-loop architecture. It does not require any feedback unlike [31] which relies on power allocation by the source node through feedback information. It further does not require any error detection mechanism (e.g., CRC) at relay nodes in contrast to [29], [30]. In our scheme, the destination node chooses the best relay based on the minimum of source-to-relay and relay-to-destination SNRs at the end of broadcasting phase and allows the selected relay to participate only if the minimum of its source-to-relay and relay-to-destination link SNRs is greater than SNR of the direct link. We derive closed-form SER performance expressions for the multi-relay network scenario with the proposed relay selection algorithm. We assume arbitrary relay locations, thereby avoiding the symmetrical scenario of [31] which is a simplifying assumption, yet somewhat impractical in real-life situations. We further formulate a power allocation problem to minimize SER and demonstrate that error rate performance can be improved by optimally distributing the power between the source and selected relay. Extensive Monte-Carlo simulations are also presented to collaborate on the analytical results.

The chapter is organized as follows: In Section 3.2, we describe the multi-relay cooperative network under consideration with DaF relaying and relay selection. In Section 3.3, we derive SER for multi-relays with arbitrary locations. In Section 3.4, we formulate the power allocation problem and provide results demonstrating advantages of optimized power allocation over the equal power allocation. In Section 3.5, we present simulation results and also discuss some issues related to practical implementation.

3.2 Transmission Model

We consider a multi-relay scenario with N relay nodes. Source, relay and destination nodes operate in half-duplex mode and are equipped with single transmit and receive antennas. As illustrated in Fig.3.1, all the nodes are assumed to be located in a two-dimensional plane where d_{SD}, d_{SR_i}, and d_{R_iD}, $i=1,2...N$ denote the distances of source-to-destination (S→D), source-to-relay (S→R_i), and relay-to-destination (R_i→D) links respectively. To incorporate the effect of relay geometry into our model, we consider an aggregate channel model which takes into account both long-term path loss and short-term Rayleigh fading. The path loss is proportional to $d^{-\alpha}$ where d is the propagation distance and α is path loss coefficient. Normalizing the path loss in S→D to be unity, the relative geometrical gains of S→R_i and R_i→D links are defined as $G_{SR_i}=\left(d_{SD}/d_{SR_i}\right)^{\alpha}$ and $G_{R_iD}=\left(d_{SD}/d_{R_iD}\right)^{\alpha}$. They can be further related to each other by law of cosines, i.e., $G_{SR_i}^{-2/\alpha}+G_{R_iD}^{-2/\alpha}-2G_{SR_i}^{-1/\alpha}G_{R_iD}^{-1/\alpha}\cos\left(\theta_i\right)=1$ where θ_i is the angle between lines S→R_i and R_i→D [47]. The fading coefficients for S→D, S→R_i, and R_i→D links are denoted by h_{SD}, h_{SR_i}, and h_{R_iD}, respectively and are modeled as zero-mean complex Gaussian random variables with variance of 1 leading to a Rayleigh fading channel model.

Let x be a modulation symbol taken from an M-PSK. Considering path-loss effects, the received signals in the first time slot at destination and i^{th} relay nodes are given by

$$r_{D1}=\sqrt{K_S P}h_{SD}x+n_{D1}, \tag{3.1}$$

$$r_{R_i}=\sqrt{G_{SR_i}K_S P}h_{SR_i}x+n_{R_i}, \tag{3.2}$$

where P is the total transmit power shared by the source and relay nodes. K_S is an optimization parameter for power allocation and denotes the fraction of power used by the source node in the broadcasting phase. The remaining power is reserved for relay transmission and power of the selected

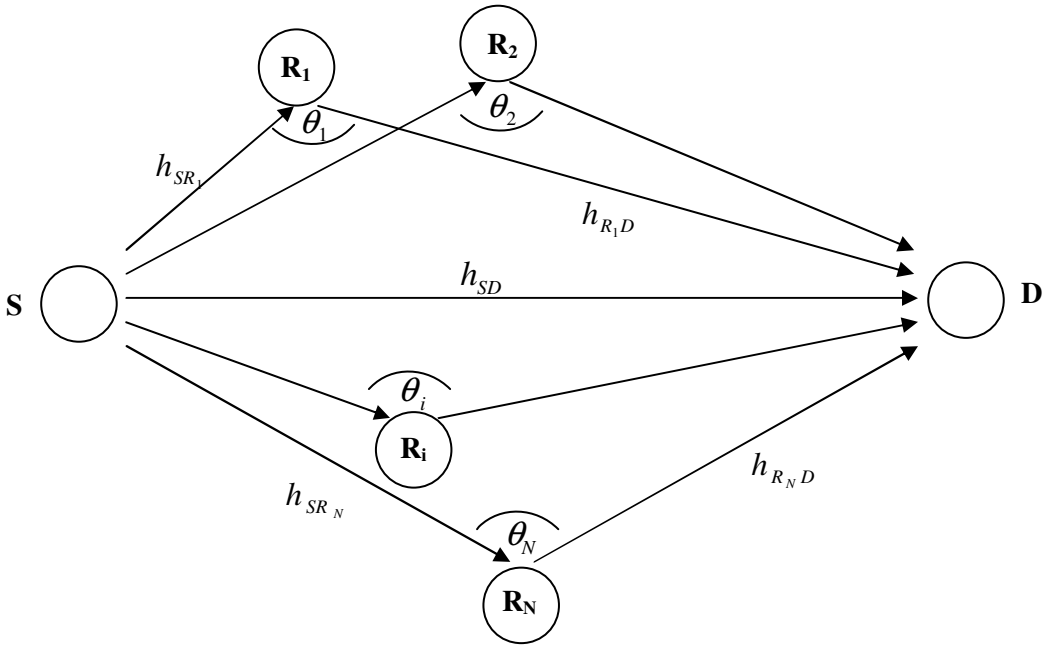

Figure 3.1 Multi-relay network.

relay is controlled by an optimization parameter K_i, $i=1,2,...N$ (which will be later discussed in Section 3.4). In (3.1)-(3.2), n_{R_i} and n_{D1} model the additive noise terms and are assumed to be complex Gaussian with zero mean and variance of N_0.

Similar to previous work [29]-[31], it is assumed that the destination node has estimates of h_{SD}, h_{SR_i} and h_{R_iD}. Assuming a slow fading channel, h_{R_iD} can be estimated in advance. Since channel estimation is outside the scope of this work, we assume that perfect channel information is available at destination. Let λ_{SD}, λ_{SR_i}, and λ_{R_iD} denote the instantaneous SNRs in S→D, S→R_i, and R_i→D links respectively. In our scheme, the destination first chooses the best relay based on the following criteria

$$R_{sel} = \arg\max_{R_i} \left\{ \min\left(\lambda_{SR_i}, \lambda_{R_iD}\right) \right\}, \tag{3.3}$$

where "sel" denotes the index for the selected relay. Then, the destination node instructs the selected relay to participate in cooperation phase only if SNR in direct link is less than the minimum of the SNRs in the selected relaying path, i.e.,

$$\lambda_{SD} < \lambda_{\max} \triangleq \min\left(\lambda_{SR_{sel}}, \lambda_{R_{sel}D}\right). \tag{3.4}$$

Otherwise, the selected relay node will not participate in cooperation phase. If allowed to cooperate, the relay node performs decoding and transmits re-encoded symbol $\hat{x}$ in the second time slot. The signal received at destination node is therefore given by

$$r_{D2} = \sqrt{G_{R_{sel}D} K_{sel} P} h_{R_{sel}D} \hat{x} + n_{D2}, \tag{3.5}$$

where n_{D2} models the additive Gaussian noise term and $K_{sel} = K_{i|i=sel}$. The destination node then combines the received signals given by (3.1) and (3.5) using MRC and decodes the symbol transmitted by source.

3.3 SER Derivation

In this section, we derive the SER performance for the multi-relay cooperative scheme under consideration. Defining $\boldsymbol{\lambda} = \left[\lambda_{SD} \quad \lambda_{\max} \quad \lambda_{SR_{sel}} \quad \lambda_{R_{sel}D}\right]$, a conditional SER expression can be given as

$$P\left(e|\boldsymbol{\lambda}\right) = P_{n-coop} P_{e|direct} + P_{coop} P_{e|coop}, \tag{3.6}$$

where $P_{n-coop} = P\left(\lambda_{SD} > \lambda_{\max}\right)$ is the probability that the selected relay is not qualified to participate in cooperation phase and $P_{coop} = 1 - P_{n-coop}$ is the probability of cooperation. $P_{e|direct}$ denotes the SER for direct S→D transmission and $P_{e|coop}$ denotes the SER when the cooperation takes place.

If cooperation does not take place, the overall SER is simply equal to the SER of direct link and is given by

$$P_{e|direct} = \beta\left(\lambda_{SD}\right) \tag{3.7}$$

where $\beta(.)$ is given by [53]

$$\beta(x)=\frac{1}{\pi}\int_{0}^{(M-1)\pi/M}\exp\left(-\frac{gx}{\sin^2\eta}\right)d\eta, \tag{3.8}$$

with $g=\sin^2(\pi/M)$

If cooperation takes place, we need to calculate $P_{e|coop}$ which is given by

$$P_{e|coop}=P_{e\_sel}P_{e|e\_sel}+\left(1-P_{e\_sel}\right)P_{e|c\_sel}, \tag{3.9}$$

where $P_{e\_sel}=\beta\left(\lambda_{SR_{sel}}\right)$ denotes the probability of the selected relay to make a decoding error. If the selected relay makes an incorrect decision, the corresponding conditional SER is calculated as $P_{e|e\_sel}=\beta\left(\left|\lambda_{SD}+e\lambda_{R_{sel}D}\right|^2/\left(\lambda_{SD}+\lambda_{R_{sel}D}\right)\right)$. In the calculation of $P_{e|e\_sel}$, we use $\hat{x}=e\,x$ to take into account for the error at the relay. We can actually approximate this probability by 1, because, under the assumption that relay is qualified for cooperation (i.e., $\lambda_{\max}>\lambda_{SD}$), an incorrect decision at destination is much more likely than a correct one. On the other hand, if the selected relay has decoded correctly, the SER is given by $P_{e|c\_sel}=\beta\left(\lambda_{R_{sel}D}+\lambda_{SD}\right)$. Replacing all above related definitions in (3.6), we have

$$\begin{aligned}P(e|\boldsymbol{\lambda})=&\underbrace{P\left(\lambda_{SD}>\lambda_{\max}\right)\beta\left(\lambda_{SD}\right)}_{T_0}+\underbrace{P\left(\lambda_{SD}<\lambda_{\max}\right)\beta\left(\lambda_{SR_{sel}}\right)}_{T_1}\\&+\underbrace{P\left(\lambda_{SD}<\lambda_{\max}\right)\left[1-\beta\left(\lambda_{SR_{sel}}\right)\right]\beta\left(\lambda_{R_{sel}D}+\lambda_{SD}\right)}_{T_2}\end{aligned}. \tag{3.10}$$

To find the unconditional SER, one needs to take an expectation of (3.10) with respect to $\boldsymbol{\lambda}$. This requires to find the probability density functions (pdfs) of variables $\lambda_{\max}$, $\lambda_{SR_{sel}}$, and $\lambda_{R_{sel}D}$. This is quite difficult and would probably not yield closed form expressions. Therefore, we pursue an alternative approach here: It is easier to find the conditional pdfs of $\lambda_{\max}$, $\lambda_{SR_{sel}}$, and $\lambda_{R_{sel}D}$ conditioned on the event that i^{th} relay node is selected. We first calculate these conditional pdfs and obtain the corresponding conditional SER. The unconditional SER P_e is then obtained performing an

expectation over all possible events. Let ξ_i denote the event $\lambda_{\max} = \lambda_{SR_i}$ and ξ_i^C denote the event $\lambda_{\max} = \lambda_{R_iD}$. P_e can be calculated as

$$P_e = \sum_{i=1}^{N} \left[P\left(e \middle| \xi_i\right) \Pr\left(\xi_i\right) + P\left(e \middle| \xi_i^C\right) \Pr\left(\xi_i^C\right) \right]. \tag{3.11}$$

The pdfs of $\lambda_{\max}$, $\lambda_{SR_{sel}}$, and $\lambda_{R_{sel}D}$ conditioned on event ξ_i and ξ_i^C, and the probabilities of these events are provided in Appendix A. Using these conditional pdfs, we approximate P_e as

$$P_e \cong \sum_{i=1}^{N} \left[\sum\nolimits_{\sigma \in \Delta_i} \Pr\left(\sigma\right) \right] \left[\Phi_0 + \sum_{k=1}^{2} \left\{ \Phi_k \Pr\left(\mu_i\right) + \Phi_k^C \Pr\left(\mu_i^C\right) \right\} \right], \tag{3.12}$$

where correlation of μ_i and σ is ignored. Calculations of $\Pr\left(\sigma\right), \Pr\left(\mu_i\right)$ and $\Pr\left(\mu_i^C\right)$ are provided in Appendix A while calculations of Φ_0, Φ_k, and Φ_k^C, $k = 1,2$ are given in Appendix B. Using the results from Appendixes, we obtain the final SER expression as

$$P_e \cong \sum_{i=1}^{N} \Pr\left(i = sel\right) \left\{ \Phi_0 + \frac{\Lambda_{R_iD}}{\Lambda_{SR_i} + \Lambda_{R_iD}} \left(\Phi_1 + \Phi_2\right) + \frac{\Lambda_{SR_i}}{\Lambda_{SR_i} + \Lambda_{R_iD}} \left(\Phi_1^C + \Phi_2^C\right) \right\}, \tag{3.13}$$

$$\begin{aligned}
&= \sum_{i=1}^{N} \Pr\left(i = sel\right) \times \left[F_1 \left\{ \Psi_{SD}\left(\alpha_{\eta_1}\right) \Psi_{\max}\left(\alpha_{\eta_1} - \frac{1}{\Lambda_{SD}} \right) \right\} \right. \\
&\quad + \frac{\Lambda_{R_iD}}{\Lambda_{SR_i} + \Lambda_{R_iD}} F_1 \left\{ \Psi_{\max}\left(\alpha_{\eta_1}\right) - \Psi_{\max}\left(\alpha_{\eta_1} - \frac{1}{\Lambda_{SD}} \right) \right\} \\
&\quad + \frac{\Lambda_{R_iD}}{\Lambda_{SR_i} + \Lambda_{R_iD}} F_1 \left\{ \Psi_{SD}\left(\alpha_{\eta_1}\right) \Psi_{R_iD}\left(\alpha_{\eta_1}\right) \left(\Psi_{\max}\left(\alpha_{\eta_1}\right) - \Psi_{\max}\left(\alpha_{\eta_1} - \frac{1}{\Lambda_{SD}} \right) \right) \right\} \\
&\quad - \frac{\Lambda_{R_iD}}{\Lambda_{SR_i} + \Lambda_{R_iD}} F_2 \left\{ \Psi_{SD}\left(\alpha_{\eta_1}\right) \Psi_{R_iD}\left(\alpha_{\eta_1}\right) \left(\Psi_{\max}\left(\alpha_{\eta_1} + \alpha_{\eta_2}\right) - \Psi_{\max}\left(\alpha_{\eta_1} + \alpha_{\eta_2} - \frac{1}{\Lambda_{SD}} \right) \right) \right\} \\
&\quad + \frac{\Lambda_{SR_i}}{\Lambda_{SR_i} + \Lambda_{R_iD}} F_1 \left\{ \Psi_{SR_i}\left(\alpha_{\eta_1}\right) \left(\Psi_{\max}\left(\alpha_{\eta_1} - \frac{1}{\Lambda_{SR_i}} \right) - \Psi_{\max}\left(\alpha_{\eta_1} - \frac{1}{\Lambda_{SD}} - \frac{1}{\Lambda_{SR_i}} \right) \right) \right\} \\
&\quad + \frac{\Lambda_{SR_i}}{\Lambda_{SR_i} + \Lambda_{R_iD}} F_1 \left\{ \Psi_{SD}\left(\alpha_{\eta_1}\right) \left(\Psi_{\max}\left(\alpha_{\eta_1}\right) - \Psi_{\max}\left(\alpha_{\eta_1} - \frac{1}{\Lambda_{SD}} \right) \right) \right\} \\
&\quad \left. - \frac{\Lambda_{SR_i}}{\Lambda_{SR_i} + \Lambda_{R_iD}} F_2 \left\{ \Psi_{SD}\left(\alpha_{\eta_1}\right) \Psi_{SR_i}\left(\alpha_{\eta_2}\right) \left(\Psi_{\max}\left(\alpha_{\eta_1} - \frac{1}{\Lambda_{SR_i}} \right) - \Psi_{\max}\left(\alpha_{\eta_1} - \frac{1}{\Lambda_{SD}} - \frac{1}{\Lambda_{SR_i}} \right) \right) \right\} \right]
\end{aligned} \tag{3.14}$$

where $\Psi_{SR_i}(.)$ and $\Psi_{R_iD}(.)$ are the MGFs of λ_{SR_i} and λ_{R_iD}, respectively and α_{η_k} is defined as

$$\alpha_{\eta_k} = -\frac{g}{\sin^2 \eta_k}, \quad k = 1,2, \tag{3.15}$$

In the above $F_1\{.\}$ and $F_2\{.\}$ are defined by

$$F_1\{f(\eta)\} = \frac{1}{\pi} \int_0^{\frac{(M-1)\pi}{M}} f(\eta)\, d\eta, \tag{3.16}$$

$$F_2\{f(\eta_1,\eta_2)\} = \frac{1}{\pi^2} \int_0^{\frac{(M-1)\pi}{M}} \left[\int_0^{\frac{(M-1)\pi}{M}} f(\eta_1,\eta_2)\, d\eta_1 \right] d\eta_2 . \tag{3.17}$$

We conclude this section by demonstrating the achievable diversity of our scheme. An approximate value of Φ_0 can be found by inserting $\eta_1 = \eta_2 = \pi/2$ [7] for BPSK. Inserting $\eta_1 = \pi/2$ in (3.14), we have

$$\Phi_0 = F_1\left\{ \Psi_{SD}\left(\alpha_{\frac{\pi}{2}} \right) \Psi_{\max}\left(\alpha_{\frac{\pi}{2}} - \frac{1}{\Lambda_{SD}} \right) \right\}. \tag{3.18}$$

Since $\alpha_{\pi/2} = -g$, (3.18) reduces to

$$\begin{aligned} \Phi_0 &= \Psi_{SD}(-g)\, \Psi_{\max}\left(-g - \frac{1}{\Lambda_{SD}} \right) \\ &= (1 + g\Lambda_{SD})^{-1} \prod_{i=1}^{N} \left[1 + \Lambda_i \left(g + \frac{1}{\Lambda_{SD}} \right) \right]^{-1}. \end{aligned} \tag{3.19}$$

For $\Lambda_{SD} = \Lambda_{SR_i} = \Lambda_{R_iD} = \Lambda$ and large values of SNR, it can be further approximated as

$$\Phi_0 \approx (g\Lambda)^{-1} \left[1 - N(g\Lambda)^{-1} \right] \prod_{i=1}^{N} \left[\frac{\Lambda}{2} g \right]^{-1}. \tag{3.20}$$

Similarly, taking the upper bounds of Φ_1 and Φ_1^C and assuming high SNR, we can show that

[7] The value of $\eta_1 = \pi/2$ gives an upper bound for the integral in (3.16), but Φ_1, Φ_2, Φ_1^C and Φ_2^C are the functions of sum and difference of integrals in the form of (3.16) with different arguments. This makes the following result an approximation, not an upper or lower bound.

$$\begin{aligned}\Phi_1 &\approx \prod_{i=1}^{N}(\Lambda_i g)^{-1} - \prod_{i=1}^{N}\left[\left(\frac{\Lambda}{2}\right)^{-1}\left(g+\frac{1}{\Lambda}\right)^{-1}\right] \\ &= \left[1-\left(1+\frac{1}{g\Lambda}\right)^{-N}\right]\prod_{i=1}^{N}\left(\frac{\Lambda}{2}g\right)^{-1} \\ &\approx N(g\Lambda)^{-1}\prod_{i=1}^{N}\left(\frac{\Lambda}{2}g\right)^{-1}\end{aligned}, \tag{3.21}$$

$$\begin{aligned}\Phi_1^C &\approx (\Lambda g)^{-1}\left[\prod_{i=1}^{N}\left[\frac{\Lambda}{2}\left(g+\frac{1}{\Lambda}\right)\right]^{-1} - \prod_{i=1}^{N}\left[\frac{\Lambda}{2}\left(g+\frac{2}{\Lambda}\right)\right]^{-1}\right]. \\ &\approx N(\Lambda g)^{-2}\prod_{i=1}^{N}\left(\frac{\Lambda}{2}g\right)^{-1}\end{aligned} \tag{3.22}$$

For Φ_2 and Φ_2^C, we get

$$\begin{aligned}\Phi_2 &\approx (g\Lambda_{SD})^{-1}(g\Lambda_{R_iD})^{-1}\left[\prod_{i=1}^{N}\left(\frac{\Lambda}{2}g\right)^{-1} - \prod_{i=1}^{N}\left\{\frac{\Lambda}{2}\left(g+\frac{1}{\Lambda}\right)\right\}^{-1} - \prod_{i=1}^{N}(\Lambda g)^{-1} + \prod_{i=1}^{N}\left\{\frac{\Lambda}{2}\left(2g+\frac{1}{\Lambda}\right)\right\}^{-1}\right] \\ &\approx (g\Lambda)^{-2}\left[N(g\Lambda)^{-1}\prod_{i=1}^{N}\left(\frac{\Lambda}{2}g\right)^{-1} - N(2g\Lambda)^{-1}\prod_{i=1}^{N}\left(\frac{\Lambda}{2}g\right)^{-1}\right] \\ &\approx N(g\Lambda_{SD})^{-3}\prod_{i=1}^{N}\left(\frac{\Lambda}{2}g\right)^{-1}\end{aligned}. \tag{3.23}$$

$$\begin{aligned}\Phi_2^C &\approx (g\Lambda_{SD})^{-1}\left[\prod_{i=1}^{N}(\Lambda_i g)^{-1} - \prod_{i=1}^{N}\left\{\Lambda_i\left(g+\frac{1}{\Lambda_{SD}}\right)\right\}^{-1}\right] \\ &\quad -(g\Lambda_{SD})^{-1}(g\Lambda_{SR_i})^{-1}\left[\prod_{i=1}^{N}(2\Lambda_i g)^{-1} - \prod_{i=1}^{N}\left\{\Lambda_i\left(2g+\frac{1}{\Lambda_{SD}}\right)\right\}^{-1}\right]. \\ &\approx (g\Lambda)^{-2}N\prod_{i=1}^{N}\left(\frac{\Lambda}{2}g\right)^{-1} \\ &\quad -(g\Lambda)^{-3}N\prod_{i=1}^{N}(\Lambda g)^{-1}\end{aligned} \tag{3.24}$$

Through (3.20)-(3.24), we observe that a diversity order of $N+1$ is achieved.

3.4 Optimum Power Allocation

As shown in the previous section, the proposed relay selection scheme is able to extract the full diversity. However, further performance improvement over EPA is possible through OPA. In the following, we pursue two directions for performance optimization.

3.4.1 OPA-I

We assume that power is divided between source and the selected relay node irrespective of relay location. In this case, power of the source and relay node are given by $K_S P$ and $\left(1-K_S\right)P$, respectively. The optimization problem can be formulated as

$$\min_{s.t.\ 0<K_s<1} P_e(K_S), \tag{3.25}$$

where $P_e(.)$ is the SER expression given by (3.14).

3.4.2 OPA-II

We assume that power is divided among source and relay nodes taking into account location of relay nodes. Power of the source is $K_S P$ and power of each relay node is $K_i P,\ i=1,2,...,N$, such that $K_S+\sum_{i=1}^{N} P_i K_i = 1$. Recall that P_i has been earlier defined and denotes the probability of i^{th} relay node being selected. The optimization problem now takes the form of

$$\min_{s.t.\ K_S+\sum_{i=1}^{N} P_i K_i=1} P_e(K_S, K_1, K_2, ..., K_N). \tag{3.26}$$

Analytical solutions for (3.25) and (3.26) are unfortunately very difficult to obtain, if not infeasible. Therefore, we resort to numerical optimization [54], [55]. It should be also noted that this optimization problem needs not to be solved in real-time for practical systems, because the optimization does not depend on the instantaneous channel information or the input data. As an example, Table 3.1 tabulates the power allocation values for a two-relay scenario assuming various relay locations.

Table 3.1 OPA values for a two-relay network.

(a) **OPA-I**

SNR [dB]	$G_{SR_1}/G_{R_1D} = -30\text{dB}$ $G_{SR_2}/G_{R_2D} = 30\text{dB}$	$G_{SR_1}/G_{R_1D} = -30\text{dB}$ $G_{SR_2}/G_{R_2D} = 0\text{dB}$	$G_{SR_1}/G_{R_1D} = -30\text{dB}$ $G_{SR_2}/G_{R_2D} = -30\text{dB}$
	K_S	K_S	K_S
5	0.9762	0.7714	0.9774
10	0.7262	0.7676	0.9793
15	0.6835	0.7686	0.9795
20	0.6718	0.7691	0.9795
25	0.6626	0.7644	0.9790
30	0.6671	0.7179	0.9691

(b) **OPA- II**

SNR [dB]	$G_{SR_1}/G_{R_1D} = -30\text{dB}$ $G_{SR_2}/G_{R_2D} = 30\text{dB}$			$G_{SR_1}/G_{R_1D} = -30\text{dB}$ $G_{SR_2}/G_{R_2D} = 0\text{dB}$			$G_{SR_1}/G_{R_1D} = -30\text{dB}$ $G_{SR_2}/G_{R_2D} = -30\text{dB}$		
	K_S	K_1	K_2	K_S	K_1	K_2	K_S	K_1	K_2
5	0.8108	0.0252	0.6392	0.8415	0.0266	0.3828	0.9821	0.0265	0.0265
10	0.8148	0.0233	0.6341	0.8506	0.0249	0.3692	0.9831	0.0251	0.0251
15	0.8152	0.0231	0.6335	0.8553	0.0246	0.3619	0.9832	0.0249	0.0249
20	0.8155	0.0228	0.6332	0.8553	0.0246	0.3619	0.9832	0.0249	0.0249
25	0.8155	0.0228	0.6332	0.8553	0.0246	0.3619	0.9832	0.0249	0.0249
30	0.8155	0.0228	0.6332	0.8553	0.0246	0.3619	0.9832	0.0249	0.0249

3.5 Numerical Results and Discussion

In this section, we first provide numerical results for the derived closed-form SER expression and compare them with Monte-Carlo simulation results. Then, we present the performance with OPA comparing with EPA and demonstrating the effect of optimization on the SER performance. We assume path loss exponent $\alpha = 2$, $\theta_i = \pi$, and 4-PSK modulation scheme.

In Fig. 3.2, we plot the SER expression given by (3.14) along with the simulation results. We assume EPA, therefore have $K_S = K_1 = K_2 = \cdots = 0.5$. We consider scenarios with 2, 3, and 4 relays with the following geometrical gains:

- Two-relay network with $G_{SR_i}/G_{R_iD} = \{-30, 0\}$ dB.

- Three-relay network with $G_{SR_i}/G_{R_iD} = \{-30, 0, 30\}$ dB.
- Four-relay network with $G_{SR_i}/G_{R_iD} = \{-30, 0, 30, -10\}$ dB.

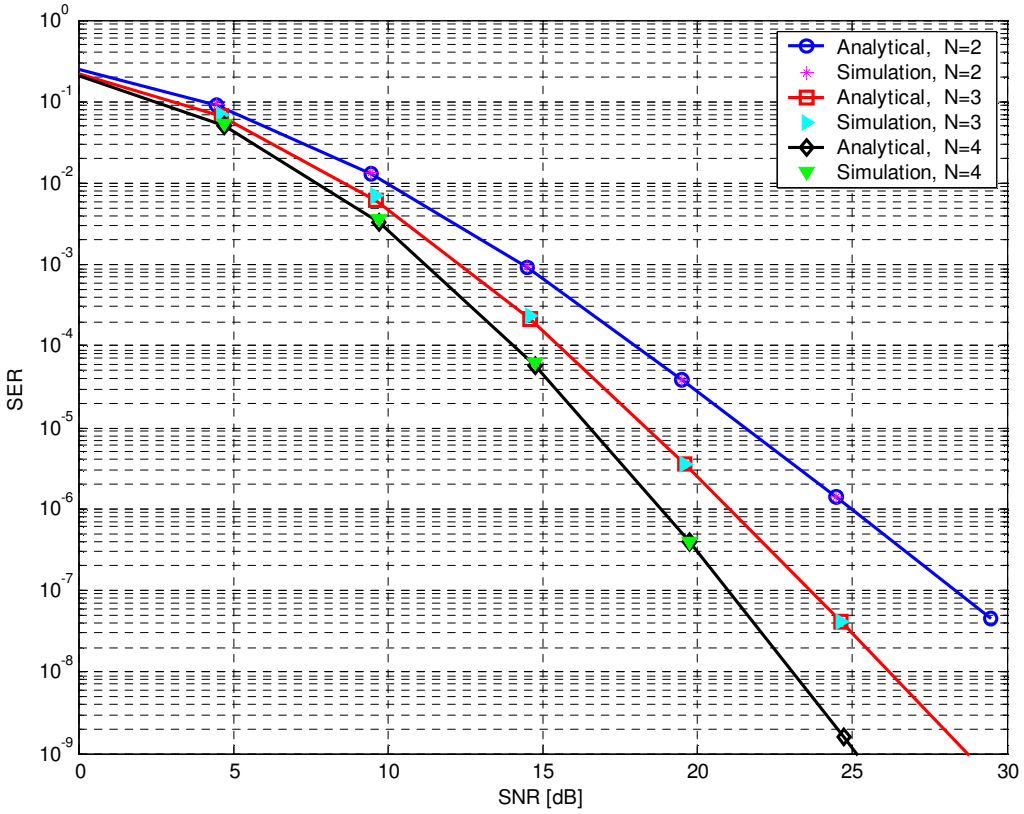

Figure 3.2 Comparison of derived SER expression with simulation results.

As observed from Fig. 3.2, our approximate analytical expressions provide an identical match (within the thickness of the line) to the simulation results. It can be also observed that diversity orders of 3, 4, and 5 are extracted indicating the full diversity for the considered number of relays and confirming our earlier observation.

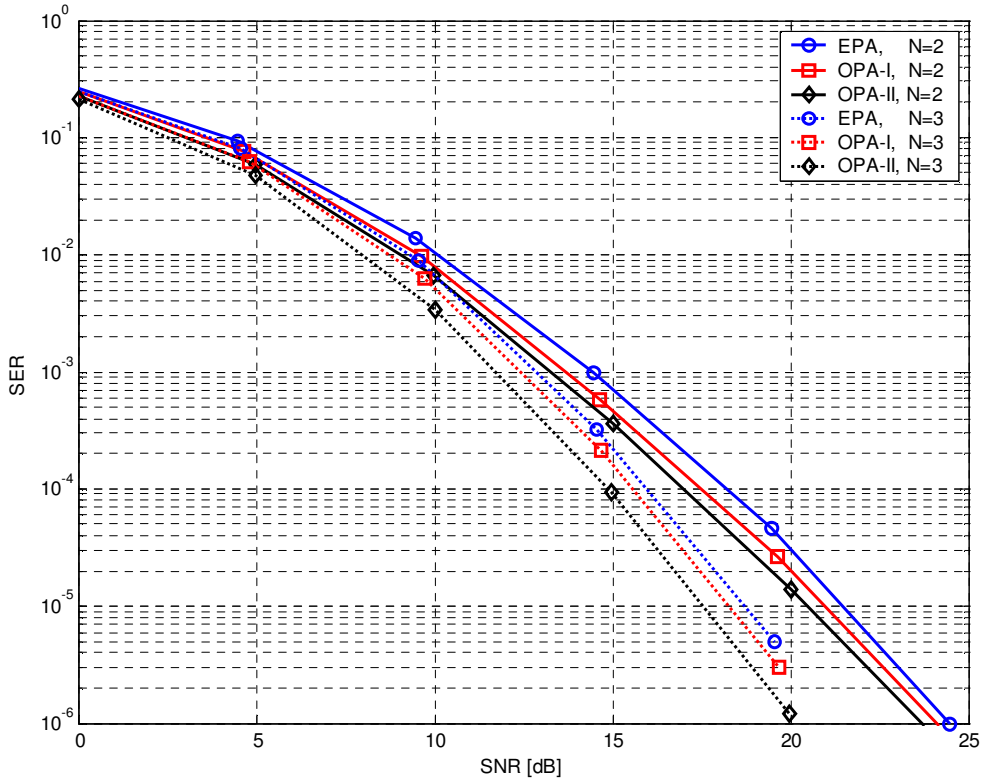

Figure 3.3 SER performance of 2- and 3-relay networks with EPA and OPA.

Although the multi-relay network with proposed relay selection method can extract the full diversity, further performance improvement is possible through OPA. To demonstrate the effect of OPA, we consider the following scenarios in Fig.3.3.

- Two-relay network with $G_{SR_1}/G_{R_1D} = 0$ dB (i.e., first relay is in the middle) and $G_{SR_2}/G_{R_2D} = -30$ dB (i.e., second relay is close to destination).
- Three-relay network with $G_{SR_1}/G_{R_1D} = -30$ dB (i.e., first relay is close to destination), $G_{SR_2}/G_{R_2D} = 30$ dB (i.e., second relay is close to source), and $G_{SR_3}/G_{R_3D} = -10$ dB (i.e., third relay is close to destination, but not as close as the first one).

For the two-relay network, we observe performance improvements of 0.75dB and 1.2dB for a target BER of 10^{-3} through OPA-I and OPA-II, respectively. For the three-relay network, OPA-I yields 0.42dB improvement while OPA-II results in an improvement of 1.14dB. These results clearly illustrate that OPA-II outperforms OPA-I taking advantage of the additional information on relay locations.

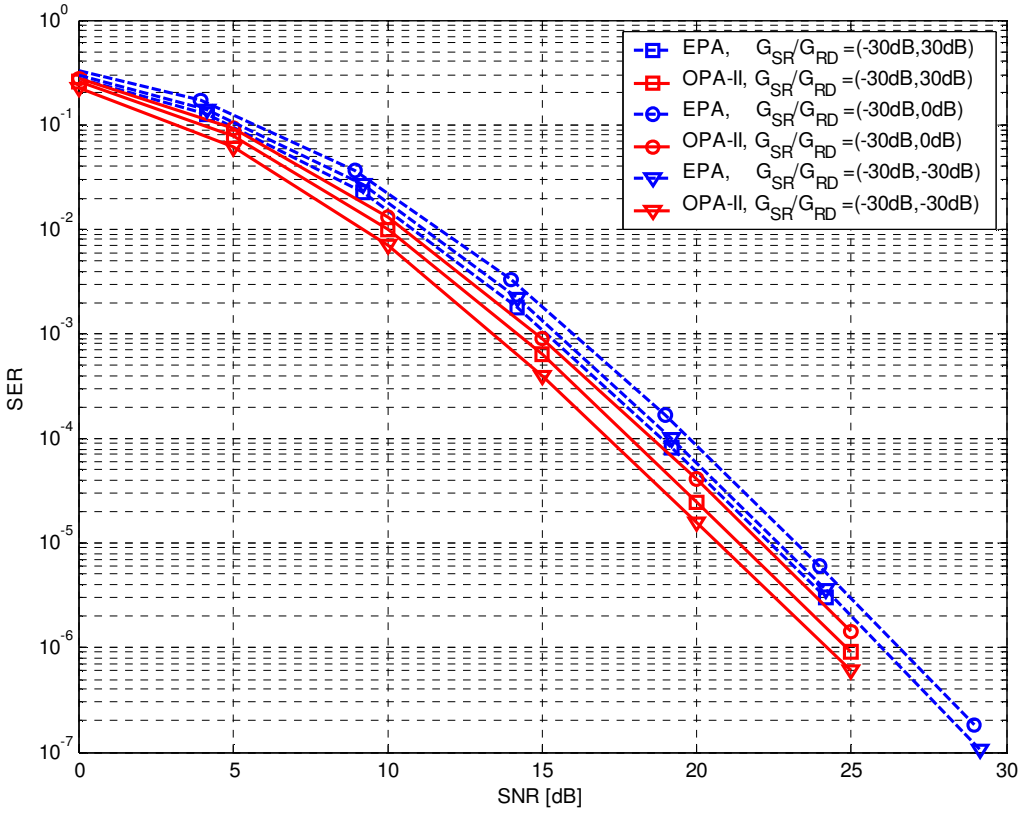

Figure 3.4 SER performance of a 2-relay network with EPA and OPA-II for various relay locations.

In Fig. 3.4, we further compare EPA and OPA-II for a two-relay network for various relay locations:

- First relay is close to source (i.e., $G_{SR_1}/G_{R_1D} = 30$ dB), while second relay is close to destination (i.e., $G_{SR_1}/G_{R_1D} = -30$ dB)
- One relay is equidistant from source and destination (i.e. $G_{SR_1}/G_{R_1D} = 0$ dB) while the other relay is close to destination (i.e., $G_{SR_1}/G_{R_1D} = -30$ dB).
- Both relays are close to destination (i.e., $G_{SR_1}/G_{R_1D} = G_{SR_2}/G_{R_2D} = -30$ dB).

It can be observed from Fig. 3.4 that system performance with EPA gets better when both relays are close to source. On the other hand, we observe a reverse effect in OPA-II where a better performance is achieved when relays are close to destination. Power allocation becomes more rewarding when relays are away from source. For example, when one relay is close to source and one is close to destination we get an improvement of 1dB, but when both relays are close to destination the performance improvement climbs up to 2dB.

In Fig. 3.5, we compare the performance of our proposed DaF multi-relay scheme (assuming OPA-II) with other existing DaF schemes (optimized if available) in the literature. The competing schemes are listed as

- Relay selection without any error detection or threshold (RS),
- Relay selection with 16-bit CRC in a frame length of 1024 bits (RS-CRC)[29],
- All relays participating without any error detection or threshold (AP)[8]
- All relays participating with 16-bit CRC in a frame length of 1024 bits (AP-CRC),
- Relay selection with static threshold (RS-STH) [31],
- *Genie* bound: Relay selection with symbol-by-symbol genie-assisted receiver at relay (RS-GEN), i.e., the genie relay knows whether or not it has decoded symbol correctly[9] participates in the cooperation phase only if it has correctly decoded

[8] This is referred as "fixed relaying" in [12].
[9] Genie-assisted receiver is assumed to only have knowledge of the symbol transmitted by source. It does not have any knowledge of channel.

The selection criteria used in RS-STH is based on the modified harmonic mean as described in [31] with optimized values of power allocation parameters. In all other selection schemes, the relay selection criterion is based on (3.3). Table 3.2 summarizes implementation aspects of the competing cooperation schemes.

Table 3.2 Different cooperation schemes for an *N*-relay network.

"Local" CSI of a certain node is defined as the CSI of a link which terminates at that node (e.g., CSI of S→Ri is local information for ith relay). "Global" CSI describes the situation when information about all the channels is available at a certain node.

	Diversity	**CSI requirement**	**Rate**	**Comments**
AP	Partial	Local CSI	$\frac{1}{N+1}$	Simple implementation, poor performance.
AP-CRC	Full	Local CSI	1 to $\frac{1}{N+1}$	Requires CRC at relay.
RS-CRC	Full	Global CSI at destination	1 to $\frac{1}{2}$	Requires CRC at relay.
RS-STH	Full	Global CSI at source	1 to $\frac{1}{2}$	Requires feedback channel to the source.
Proposed	Full	Global CSI at destination	1 to $\frac{1}{2}$	Requires neither feedback nor CRC. Requires only feedforward channel. This can be even avoided by distributed timer implementation (See Section 3.5)

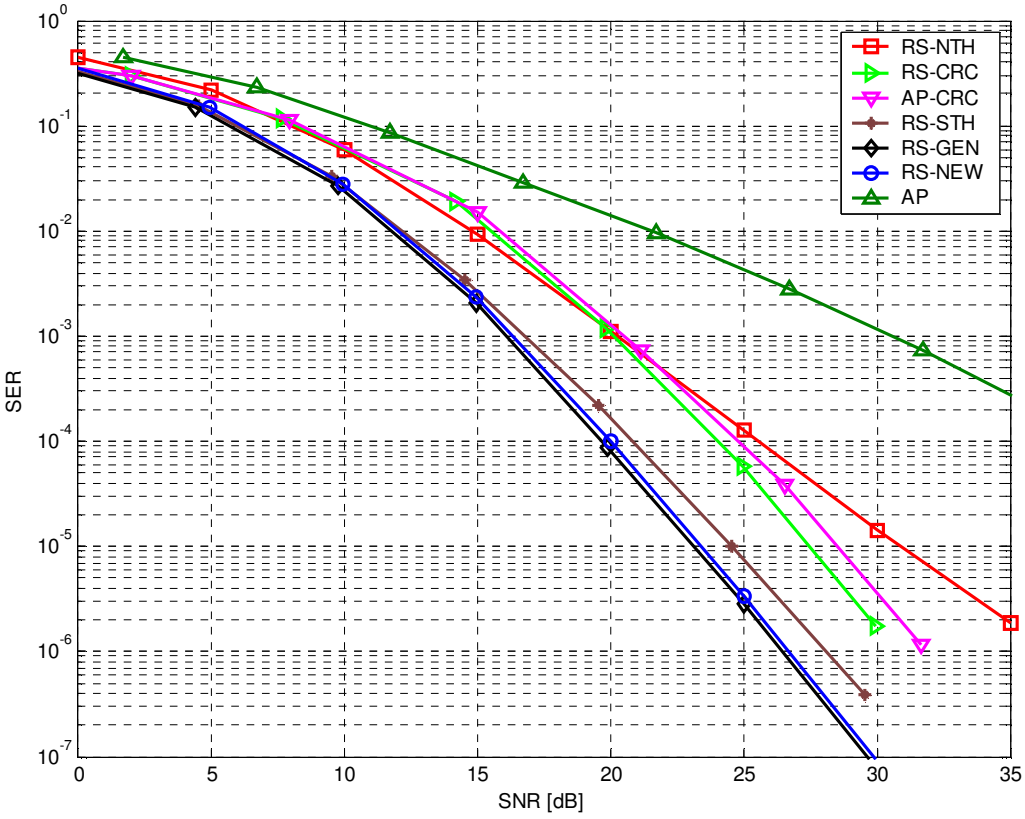

Figure 3.5 Comparison of the proposed scheme with other cooperative schemes for a channel block length of 512 symbols.

Fig.3.5 illustrates the performance of aforementioned cooperation schemes for a channel block length of 512 symbols. It is clearly observed that RS-GEN performance is the best, as expected, among all the considered schemes and presents an idealistic lower bound on the performance of other schemes. AP scheme where all relays participate without any error detection mechanism at relays performs the worst. For the considered relay location, it does not provide any diversity advantage. RS scheme outperforms AP and is able to extract a diversity order of two. The use of CRC could potentially improve the performance of both AP and RS. As observed from Fig.6, both schemes with

CRC (i.e., AP-CRC and RS-CRC) take advantage of the full diversity and significantly outperform their counterparts without CRC. It should be noted that the implementation of RS-CRC requires maximum two time slots while AP-CRC might require more time slots (i.e., each relay with correct CRC needs an orthogonal time slot for transmission). RS-STH scheme where relay selection is performed with a static threshold is able to outperform the RS-CRC and AP-CRC schemes and avoid the use for CRC in its implementation. Our proposed scheme outperforms all previous schemes and its performance lies within 0.3 dB of the genie performance bound.

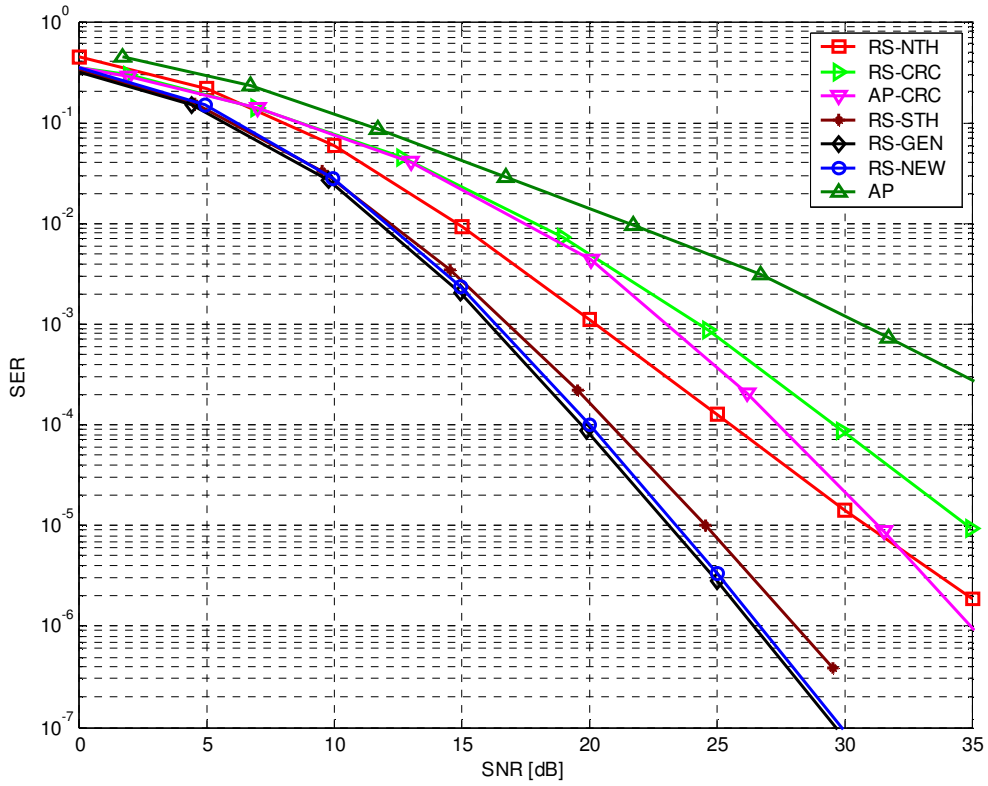

Figure 3.6 Comparison of the proposed scheme with other cooperative schemes for a channel block length of 128 symbols.

Fig. 3.6 illustrates the performance of the above schemes for a channel block length of 128 symbols. The performance of cooperative schemes which rely only on CSI (i.e. AP, RS, RS-STH, RS-NEW) remain unchanged, while that of schemes which rely also on decoded bits at relay nodes (i.e., AP-CRC, RS-CRC) demonstrates dependency on channel block length. Particularly CRC-assisted schemes suffer a significant degradation if channel varies within CRC frame. Compared to Fig. 3.5, we also observe from Fig. 3.6 that the performance of AP-CRC now becomes better than that of RS-CRC.

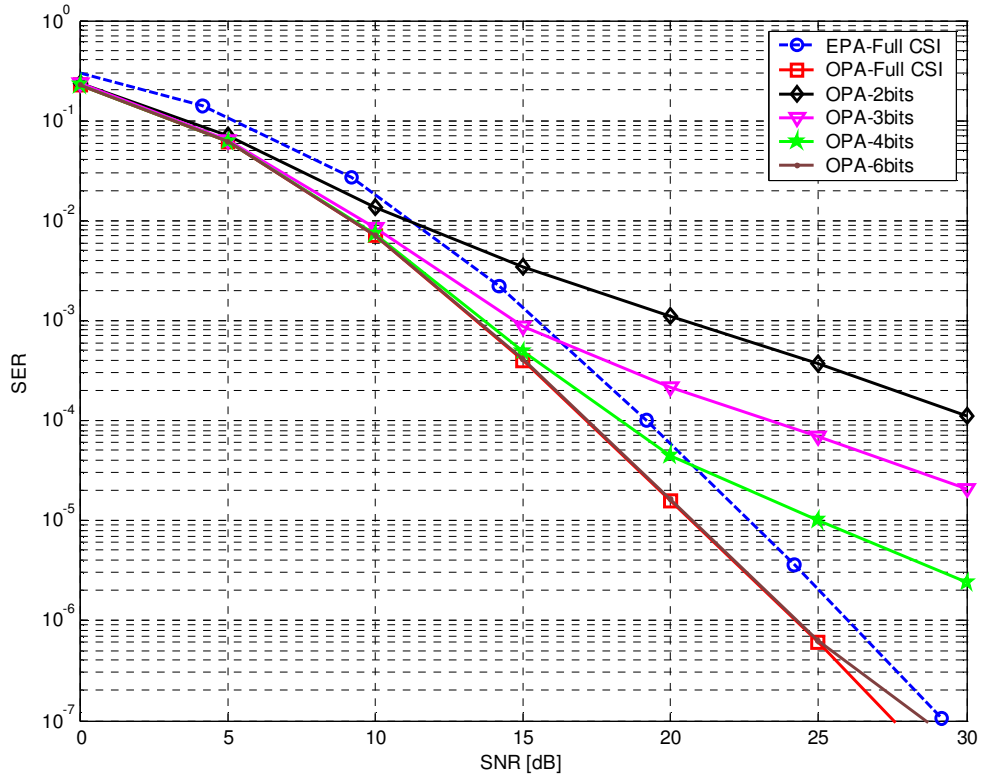

Figure 3.7 Effect of h_{SRi} quantization on the performance of the proposed scheme.

As earlier mentioned, the proposed relay selection algorithm does not require any feedback information. It, however, requires CSI of S→R_i links at the destination node. This requires transmission of h_{SR_i} from each relay to destination. Since the transfer of analog CSI requires sending an infinite number of bits, a control channel with limited number of feedforward bits can be used in practical implementation. To demonstrate the effect of quantization, we provide simulation results in Fig. 3.7 where h_{SRi} is quantized using 2, 3, 4, and 6 bits with a non-uniform quantizer optimized for Rayleigh distributed input [56]. It is observed from Fig. 3.7 that as low as 6 bits would be enough to obtain a good match to the ideal case.

As a final note, we would like to point out that this feedforward channel can be also avoided if one prefers a distributed implementation of relay selection algorithm similar to [29]. This alternative implementation requires the deployment of timers at relay and destination nodes. The algorithm steps are summarized as follows:

1. Set the timer at each relay node proportional to $\left|h_{SR_i}\right|^2$ and $N+1$ timers at the destination node proportional to $\left|h_{SD}\right|^2$ and $\left|h_{R_iD}\right|^2, i=1,2,\cdots,N$, respectively.
2. Whenever a timer expires at any of the relay nodes, it informs the destination.
3. If destination receives an expiration message from the i^{th} relay node, it forces its timer corresponding to i^{th} relay (i.e., proportional to $\left|h_{R_iD}\right|^2$) to expire.
4. The destination timer which expires at the end is used to make a decision about the participation of relay in cooperation phase. If any of the timers corresponding to $\left|h_{R_iD}\right|^2$ expires at the end, then this relay is selected and destination informs the selected relay. If the timer corresponding to $\left|h_{SD}\right|^2$ expires at the end, then no relay is allowed to cooperate.

It should be also emphasized that, unlike [29] built upon a similar timer deployment, the proposed scheme requires no h_{R_iD} at the relay node and is able to work without error detection mechanism in source-to-relay link.

Chapter 4
Power Allocation for Multiple Source Nodes over Frequency-Selective Channels

4.1 Introduction

Most of the current literature on cooperative OFDMA focuses on resource allocation problem based on rate maximization. A common assumption in these works is the availability of CSI at transmitter which requires a close-loop implementation. In contrast, this work focuses an open-loop cooperative OFDMA system which avoids the need of CSI at transmitter side. We are interested in analyzing the error rate performance of such a system and determining power allocation and relay selection methods to improve the system performance. Our contributions in this chapter are summarized in the following:

- We derive a closed-form approximate symbol error rate (SER) expression for the uplink of OFDMA network with K sources (S_k, $k = 1, 2, \cdots, K$) and M relays (R_m, $m = 1, 2, \cdots, M$).
- Based on the SER expression, we demonstrate that achievable diversity order for each $\mathrm{S_k} \rightarrow \mathrm{D}$ communication link can take different values depending on the location of relays. Specifically, we find out that the diversity orders are $\left(L_{S_k D}+1\right)+\sum_{m=1}^{M} \min\left(L_{S_k R_m}+1, L_{R_m D}+1\right)$, $\left(L_{S_k D}+1\right)+\sum_{m=1}^{M}\left(L_{R_m D}+1\right)$ and $\left(L_{S_k D}+1\right)+\sum_{m=1}^{M}\left(L_{S_k R_m}+1\right)$ for the cases when the relay nodes are located in the middle, close to the source nodes, and close to destination, respectively. Here, $L_{S_k D}+1$, $L_{S_k R_m}+1$, and $L_{R_m D}+1$ are the channel lengths of source-to-destination, source-to-m^{th} relay, and m^{th} relay-to-destination links, respectively.
- We propose open-loop power allocation rules (based on the availability of relay location information) which brings performance improvement of 3.3dB.

- We devise a simple relay selection algorithm which improves the throughput of the system by utilizing the local CSI at destination.
- We present a comprehensive Monte Carlo simulation study to corroborate our analytical results for the OFDMA system under consideration.

The rest of the chapter is organized as follows: In Section 4.2, we introduce the relay-assisted channel and transmission model for OFDMA system. In Section 4.3, we derive a SER expression for the system under consideration. In Section 4.4, we present diversity order analysis for various relay locations which are further confirmed via Monte-Carlo simulations in Section 4.5. In Section 4.6, we discuss optimum power allocation and relay selection for potential performance improvements.

4.2 Transmission and Channel Model

We consider the uplink of a broadband wireless communication system where K source nodes send their information to a single destination with the help of M relays (Fig. 4.1). All nodes are equipped with single antennas and the relay nodes operate in half-duplex mode i.e., relays cannot receive and transmit simultaneously. Underlying communication links are assumed to be subject to quasi-static Rayleigh frequency-selective fading. OFDMA (along with pre-coding [57]) is used to combat frequency selectivity of the channel as well as to eliminate interference between the transmitting nodes. We assume a total number of N orthogonal frequency carriers and each source is assigned $P = N / K$ carriers. To ensure that each source benefits from the available multipath diversity, N is chosen large enough such that P is greater than the maximum of all the channel lengths. We assume DaF relaying with error detection mechanism in source-to-relay link. This ensures that only correct data is forwarded by the relay nodes to avoid error propagation.

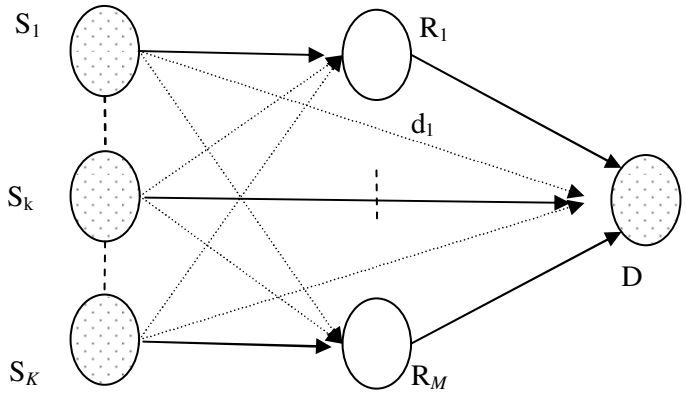

Figure 4.1 Relay-assisted transmission model.

The transmission takes place in two phases. In the first phase, the sources nodes transmit their information using the non-overlapping carriers assigned to them. The received signals $\mathbf{r}_{D_0}$ at the destination and $\mathbf{r}_m$ at the m^{th} relay are given by

$$\mathbf{r}_{D_0} = \sum_{k=1}^{K} \sqrt{G_{S_k D} P_{S_k}}\, \mathbf{H}_{S_k D} \mathbf{Q}^{\mathrm{H}} \mathbf{C}_k \mathbf{\Theta}_k \mathbf{x}_k + \mathbf{n}_{D_0}\,, \tag{4.1}$$

$$\mathbf{r}_m = \sum_{k=1}^{K} \sqrt{G_{S_k R_m} P_{S_k}}\, \mathbf{H}_{S_k R_m} \mathbf{Q}^{\mathrm{H}} \mathbf{C}_k \mathbf{\Theta}_k \mathbf{x}_k + \mathbf{n}_m\,,\ m = 1, 2, \cdots, M \tag{4.2}$$

where the related variables are defined as follows:

- P_{S_k} is the fraction of total power P assigned to the k^{th} source node. For equal power allocation, $P_{S_k} = P/(N+K)$.
- $\mathbf{x}_k \in \mathbb{C}^{n_k}$ is the signal vector transmitted by the k^{th} source node. Constellation set $\mathbb{C}$ is either chosen as M-PSK or M-QAM modulation and n_k is the number of symbols transmitted by the k^{th} source.
- $\mathbf{\Theta}_k$ is the $n_k \times n_k$ pre-coding matrix defined as in [57].

- $\mathbf{C}_k$ is the $N \times n_k$ carrier mapping matrix which contains all zero elements except for one non-zero element in each row. $\mathbf{C}_k(i,j)=1$ is used to map the i^{th} carrier to the j^{th} data symbol of $\mathbf{x}_k$. It is assumed that carrier assignments to different source nodes are pre-determined.
- $\mathbf{H}_{S_kD} = circ(\mathbf{h}_{S_kD})$ where $\mathbf{h}_{S_kD} = \left[h_{S_kD}(0), h_{S_kD}(1), \cdots, h_{S_kD}(L_{S_kD})\right]^{\mathrm{T}}$ is the channel response from the k^{th} source node to the destination . The elements of $\mathbf{h}_{S_kD}$ are assumed to be independent identically distributed (i.i.d) zero mean Gaussian random variables with variance of $1/(L_{S_kD}+1)$,
- $\mathbf{H}_{S_kR_m} = circ(\mathbf{h}_{S_kR_m})$ where $\mathbf{h}_{S_kR_m} = \left[h_{S_kR_m}(0), h_{S_kR_m}(1), \cdots, h_{S_kR_m}(L_{S_kR_m})\right]^{\mathrm{T}}$ is the channel response from the k^{th} source node to the m^{th} relay node. The elements of $\mathbf{h}_{S_kR_m}$ are assumed to be i.i.d zero mean Gaussian random variables with variance of $1/(L_{S_kR_m}+1)$,
- $\mathbf{n}_{D_0}$ and $\mathbf{n}_m$ represent the additive Gaussian noise terms, i.e., $\mathbf{n}_{D_0} \sim \mathbb{CN}(0, \mathbf{I}_N)$, $\mathbf{n}_m \sim \mathbb{CN}(0, \mathbf{I}_N)$ $m = 1, 2, \cdots, M$
- $G_{S_kR_m}$ and G_{R_mD} represent the geometrical gains [47] of the link $S_k \rightarrow R_m$ and $R_m \rightarrow D$ relative to the path loss between S_1 and D [10].

At the destination and the relay nodes, received signals are pre-multiplied by $\mathbf{Q}$. By this pre-multiplication, OFDM along with introduction of cyclic prefix (CP) converts the transmission into the set of parallel channels with non-overlapping subsets assigned to different source nodes. The coefficients of these parallel channels are the frequency responses of channels evaluated at the assigned carrier frequencies. After pre-multiplication by $\mathbf{Q}$, we have

$$\mathbf{z}_{D_0} = \mathbf{Q}\mathbf{r}_{D_0} = \sum_{k=1}^{K} \sqrt{G_{S_kD} P_{S_k}}\, \mathbf{D}_{S_kD} \mathbf{C}_k \mathbf{\Theta}_k \mathbf{x}_k + \mathbf{Q}\mathbf{n}_{D_0}, \tag{4.3}$$

$$\mathbf{z}_m = \mathbf{Q}\mathbf{r}_m = \sum_{k=1}^{K} \sqrt{G_{S_kR_m} P_{S_k}}\, \mathbf{D}_{S_kR_m} \mathbf{C}_k \mathbf{\Theta}_k \mathbf{x}_k + \mathbf{Q}\mathbf{n}_m, \tag{4.4}$$

Where $\mathbf{D}_{S_kD} = \mathbf{Q}\mathbf{H}_{S_kD}\mathbf{Q}^{\mathrm{H}}$ and $\mathbf{D}_{S_kR_m} = \mathbf{Q}\mathbf{H}_{S_kR_m}\mathbf{Q}^{\mathrm{H}}$.

[10] Without loss of generality, we assume that S_1 is the most distant source from the destination.

During the relaying phase, only the relay nodes which are able to correctly decode[11] the received information are permitted to forward them to the destination. They transmit one-by-one in orthogonal time slots[12]. Therefore, the duration of whole transmission varies between two and $M+1$ time slots. It is assumed that sources are silent during the relaying phase. Let Δbe the set of relays which are able to decode correctly and δ is the cardinality of set Δ. The received signals at the destination are given by

$$\mathbf{r}_{D_m} = \sqrt{G_{R_mD} P_{R_m}} \mathbf{H}_{R_mD} \mathbf{Q}^{\mathrm{H}} \mathbf{x}_m + \mathbf{n}_{D_m}, \ \forall m \in \Delta \tag{4.5}$$

where the related variables are defined as follows:

- P_{R_m} is the fraction of total power P assigned to the m^{th} relay node.
- $\mathbf{x}_m = \sum_{k=1}^{K} \mathbf{C}_k \mathbf{\Theta}_k \hat{\mathbf{x}}_{m,k}$ with $\hat{\mathbf{x}}_{m,k}$ denoting the decoded message of the k^{th} source node at the m^{th} relay node.
- $\mathbf{H}_{R_mD} = circ\left(\mathbf{h}_{R_mD}\right)$ where $\mathbf{h}_{R_mD} = \left[h_{R_mD}(0), h_{R_mD}(1), \cdots, h_{R_mD}\left(L_{R_mD}\right)\right]^{\mathrm{T}}$ is the channel response from the m^{th} relay node to the destination. The elements of $\mathbf{h}_{R_mD}$ are assumed to be i.i.d. zero mean Gaussian random variables with variance of $1/\left(L_{R_mD}+1\right)$.

After pre-multiplication (4.5) by $\mathbf{Q}$, we have

$$\mathbf{z}_{D_m} = \mathbf{Q}\mathbf{r}_{D_m} = \sqrt{G_{R_mD} P_{R_m}} \mathbf{D}_{R_mD} \mathbf{x}_m + \mathbf{Q}\mathbf{n}_{D_m}, \ m = 1, 2, \cdots, M \tag{4.6}$$

where $\mathbf{D}_{R_mD} = \mathbf{Q}\mathbf{H}_{R_mD}\mathbf{Q}^{\mathrm{H}}$. The $\delta+1$ signals in (4.3) and (4.5) are combined at the destination using MRC before performing ML decoding. Since a pre-coder is used at transmitter, ML decoder is required to decode a block of at least $L_{\max}+1$ symbols, where $L_{\max}+1$ is the maximum of all channel lengths.

[11] In practice, this can be done through an error detection mechanism such as CRC.

[12] Alternatively, distributed space time block codes can be used by relays to transmit simultaneously, but it will increase the system complexity as well it can possibly reduce the through put as rate-one codes are available for two transmitters only.

4.3 Derivation of SER

In this section, we derive a SER expression for the OFDMA system under consideration. Overall SER of the system is given by

$$P_e = \frac{1}{K}\sum_{k=1}^{K} P_k(e), \tag{4.7}$$

where $P_k(e)$ is the symbol error rate for the data received from the k^{th} source at the destination. To calculate $P_k(e)$, let $A_k = \{\alpha_k(1), \alpha_k(2), \cdots, \alpha_k(M)\}$ denote the set of M variables $\alpha_k(m)$. The variable $\alpha_k(m)$ represents the outcome of decoding at relays, i.e.,

$$\alpha_k(m) = \begin{cases} 1 & \text{No decoding error in mesage from } \mathrm{S}_k \text{ at } \mathrm{R}_m \\ 0 & \text{otherwise} \end{cases}. \tag{4.8}$$

Then SER for the k^{th} source can be calculated as $P_k(e)$

$$P_k(e) = \sum_{\forall A_k}\left[\left\{\prod_{\forall \alpha_k(m)=0} P_{S_k R_m}(e)\right\}\left\{\prod_{\forall \alpha_k(m)=1} P_{S_k R_m}(c)\right\} P_k\left(e|A_k\right)\right], \tag{4.9}$$

where $P_k\left(e|A_k\right)$ is the SER at destination conditioned on a given particular value of set A_k, $P_{S_k R_m}(e)$ is the probability of error in the $\mathrm{S}_k \rightarrow \mathrm{R}_m$ link, and $P_{S_k R_m}(c)$ is the probability of error-free transmission in the $\mathrm{S}_k \rightarrow \mathrm{R}_m$ link.

Calculation of $P_k\left(e|A_k\right)$: $P_k\left(e|A_k\right)$ can be upper bounded using union bound [8] as

$$P_k\left(e|A_k\right) \le \frac{1}{n_k}\sum_{\mathbf{x}_k} p(\mathbf{x}_k) \sum_{\mathbf{x}_k \neq \bar{\mathbf{x}}_k} q(\mathbf{x}_k \rightarrow \bar{\mathbf{x}}_k)\Pr(\mathbf{x}_k \rightarrow \bar{\mathbf{x}}_k | A_k), \tag{4.10}$$

where $p(\mathbf{x}_k)$ is the probability that codeword $\mathbf{x}_k$ is transmitted, $q(\mathbf{x}_k \rightarrow \bar{\mathbf{x}}_k)$ is the number of information symbol errors in choosing another codeword $\bar{\mathbf{x}}_k$ instead of the original one, and n_k is the number of information symbols per transmission. In (4.10), $P(\mathbf{x}_k \rightarrow \bar{\mathbf{x}}_k)$ is the PEP and denotes the probability of deciding in favour of $\bar{\mathbf{x}}_k$ instead of $\mathbf{x}_k$. From (4.3) and (4.6), PEP for the k^{th} source is given by

$$\Pr\left(\mathbf{x}_k \to \bar{\mathbf{x}}_k \,|A_k\right) = E_{\mathbf{h}_{S_kD},\mathbf{h}_{R_mD}}\left[Q\left(\sqrt{\Gamma_{S_kD}\left\|\mathbf{D}_{S_kD}\mathbf{y}_k\right\|_F + \sum_{\forall\alpha_k(m)=1}\Gamma_{R_mD}\left\|\mathbf{D}_{R_mD}\mathbf{y}_k\right\|_F}\right)\right], \tag{4.11}$$

where $\Gamma_{S_kD} = G_{S_kD}P_{S_k}$, $\Gamma_{R_mD} = G_{R_mD}P_{R_m}$, and $\mathbf{y}_k = \mathbf{C}_k\boldsymbol{\Theta}_k\left(\mathbf{x}_k - \bar{\mathbf{x}}_k\right)$. Using Cherrnoff bound [5] in (4.11), we obtain

$$\Pr\left(\mathbf{x}_k \to \bar{\mathbf{x}}_k \,|A_k\right) \le \frac{1}{2}E_{\mathbf{h}_{S_kD}}\left[\exp\left(-\frac{\Gamma_{S_kD}\left\|\mathbf{D}_{S_kD}\mathbf{y}_k\right\|_F}{2}\right)\right]E_{\mathbf{h}_{S_kD}}\left[\exp\left(-\frac{\sum_{\forall\alpha_k(m)=1}\Gamma_{R_mD}\left\|\mathbf{D}_{R_mD}\mathbf{y}_k\right\|_F}{2}\right)\right]. \tag{4.12}$$

By defining $\mathbf{U}_{S_kD} = \mathrm{diag}\left(\mathbf{y}_k\right)\mathbf{V}_{S_kD}$, the first term on the right side of (4.12) can be evaluated as

$$E_{\mathbf{h}_{S_kD}}\left[\exp\left(-\frac{\Gamma_{S_kD}}{2}\left\|\mathbf{D}_{S_kD}\mathbf{C}_k\boldsymbol{\Theta}_k\left(\mathbf{x}_k - \bar{\mathbf{x}}_k\right)\right\|_F\right)\right] = E_{\mathbf{h}_{S_kD}}\left[\exp\left(-\frac{\Gamma_{S_kD}}{2}\mathbf{h}_{S_kD}^H\mathbf{U}_{S_kD}^H\mathbf{U}_{S_kD}\mathbf{h}_{S_kD}\right)\right],$$
$$= \prod_{i=0}^{L_{S_kD}}\left(1 + \lambda_{S_kD}^i\frac{\Gamma_{S_kD}}{2}\right)^{-1}$$

where $\lambda_{S_kD}^i$, $i = 0,1,\cdots,L_{S_kD}$ are the eigenvalues of $\mathbf{U}_{S_kD}^{\mathrm{H}}\mathbf{U}_{S_kD}$. In a similar fashion, we can take expectation in the second term of (4.12). Replacing the resulting expressions in (4.12), we have

$$\Pr\left(\mathbf{x}_k \to \bar{\mathbf{x}}_k \,|A_k\right) \le \frac{1}{2}\prod_{i=0}^{L_{S_kD}}\left(1 + \lambda_{S_kD}^i\frac{\Gamma_{S_kD}}{2}\right)^{-1}\prod_{\forall\alpha_k(m)=1}\left[\prod_{i=0}^{L_{R_mD}}\left(1 + \lambda_{R_mD}^i\frac{\Gamma_{R_mD}}{2}\right)^{-1}\right] \tag{4.13}$$

where $\lambda_{R_mD}^i$, $i = 0,1,\cdots,L_{R_mD}$ denote the eigenvalues of $\mathbf{U}_{R_mD}^{\mathrm{H}}\mathbf{U}_{R_mD}$ associated with $\mathrm{R_m}\to\mathrm{D}$ link. Inserting (4.13) in (4.10), we have

$$P_k\left(e\,|A_k\right) \le \frac{1}{2n_k}\sum_{\mathbf{x}_k}p\left(\mathbf{x}_k\right)\sum_{\mathbf{x}_k\neq\bar{\mathbf{x}}_k}q\left(\mathbf{x}_k\to\bar{\mathbf{x}}_k\right)\prod_{i=0}^{L_{S_kD}}\left(1 + \lambda_{S_kD}^i\frac{\Gamma_{S_kD}}{2}\right)^{-1}\prod_{\forall\alpha_k(m)=1}\left[\prod_{i=0}^{L_{R_mD}}\left(1 + \lambda_{R_mD}^i\frac{\Gamma_{R_mD}}{2}\right)^{-1}\right]. \tag{4.14}$$

Calculation of $P_{S_kR_m}\left(e\right)$: The probability of error in the $\mathrm{S}_k\to\mathrm{R}_m$ link $P_{S_kR_m}\left(e\right)$ can be calculated following the similar steps as we used for the calculation of $P_k\left(e\,|A_k\right)$. By using union bound [8] and Cherrnoff bound [5], upper bound on $P_{S_kR_m}\left(e\right)$ is

$$P_{S_kR_m}(e) \le E_{\mathbf{h}_{S_kR_m}}\left[\frac{1}{n_k}\sum_{\mathbf{x}_k} p(\mathbf{x}_k)\sum_{\mathbf{x}_k\neq\bar{\mathbf{x}}_k} q(\mathbf{x}_k\to\hat{\mathbf{x}}_k)\Pr\left[\mathbf{x}_k\to\hat{\mathbf{x}}_k\,\middle|\,\mathbf{h}_{S_kR_m}\right]\right]$$

$$\cong \frac{1}{2n_k}\sum_{\mathbf{x}_k} p(\mathbf{x}_k)\sum_{\mathbf{x}_k\neq\bar{\mathbf{x}}_k} q(\mathbf{x}_k\to\hat{\mathbf{x}}_k)E_{\mathbf{h}_{S_kR_m}}\left[\exp\left(-\frac{\Gamma_{S_kR_m}\left\|\mathbf{D}_{S_kR_m}\mathbf{y}_k\right\|_F}{2}\right)\right]$$

$$= \frac{1}{2n_k}\sum_{\mathbf{x}_k} p(\mathbf{x}_k)\sum_{\mathbf{x}_k\neq\bar{\mathbf{x}}_k} q(\mathbf{x}_k\to\hat{\mathbf{x}}_k)\prod_{i=0}^{L_{S_kR_m}}\left(1+\lambda_{S_kR_m}^{i}\frac{\Gamma_{S_kR_m}}{2}\right)^{-1}, \tag{4.15}$$

where $\Gamma_{S_kR_m} = G_{S_kR_m}P_{S_k}$ and $\lambda_{S_kR_m}^{i}$, $i=0,1,\cdots,L_{S_kR_m}$ are the eigenvalues of $\mathbf{U}_{S_kR_m}^{\mathrm{H}}\mathbf{U}_{S_kR_m}$ with $\mathbf{U}_{S_kR_m} = \mathrm{diag}\left(\boldsymbol{\Theta}_k(\mathbf{x}_k-\bar{\mathbf{x}}_k)\right)\mathbf{V}_{S_kR_m}$. Inserting (4.14) and (4.15) in (4.9) and noting $P_{S_kR_m}(c) = 1-P_{S_kR_m}(e)$, we have $P_k(e)$

$$P_k(e) \cong \sum_{\forall A_k}\left[\left\{\prod_{\forall\alpha_k(m)=0}\left(\frac{1}{2n_k}\sum_{\mathbf{x}_k} p(\mathbf{x}_k)\sum_{\mathbf{x}_k\neq\bar{\mathbf{x}}_k} q(\mathbf{x}_k\to\hat{\mathbf{x}}_k)\prod_{i=0}^{L_{S_kR_m}}\left(1+\lambda_{S_kR_m}^{i}\frac{\Gamma_{S_kR_m}}{2}\right)^{-1}\right)\right\}\right.$$

$$\times\left\{\prod_{\forall\alpha_k(m)=1}\left(1-\frac{1}{2n_k}\sum_{\mathbf{x}_k} p(\mathbf{x}_k)\sum_{\mathbf{x}_k\neq\bar{\mathbf{x}}_k} q(\mathbf{x}_k\to\hat{\mathbf{x}}_k)\prod_{i=0}^{L_{S_kR_m}}\left(1+\lambda_{S_kR_m}^{i}\frac{\Gamma_{S_kR_m}}{2}\right)^{-1}\right)\right\}$$

$$\left.\times\left\{\frac{1}{2n_k}\sum_{\mathbf{x}_k} p(\mathbf{x}_k)\sum_{\mathbf{x}_k\neq\bar{\mathbf{x}}_k} q(\mathbf{x}_k\to\bar{\mathbf{x}}_k)\prod_{i=0}^{L_{S_kD}}\left(1+\lambda_{S_kD}^{i}\frac{\Gamma_{S_kD}}{2}\right)^{-1}\prod_{\forall\alpha_k(m)=1}\left(\prod_{i=0}^{L_{R_mD}}\left(1+\lambda_{R_mD}^{i}\frac{\Gamma_{R_mD}}{2}\right)^{-1}\right)\right\}\right], \tag{4.16}$$

Replacing this in (4.7) yields the SER.

4.4 Diversity Order Analysis

In this section, we discuss the achievable diversity orders through the derived SER expression. Note that SER is dominated by the shortest error. Let $\lambda_{S_kD}^{i}$ and $\lambda_{R_mD}^{i}$ denote the eigenvalues corresponding to the shortest error event.

4.4.1 Case 1: Relays are in the middle (i.e., $\Gamma_{S_kR_m} \approx \Gamma_{R_mD}$)

Under this assumption, we can approximate $P_k(e|A_k)$ as

$$P_k(e|A_k) \cong \text{constant} \times \Gamma^{-(L_{S_kD}+1)}\prod_{\forall\alpha_k(m)=1}\Gamma^{-(L_{R_mD}+1)}. \tag{4.17}$$

assuming high SNR, and $\Gamma_{S_kD} \approx \Gamma_{S_kR} \approx \Gamma_{R_mD} \approx \Gamma$. Similar to (4.17), we can show

$$P_{S_kR_m}(e) \cong \text{constant} \times \Gamma^{-\left(L_{S_kR_m}+1\right)}. \tag{4.18}$$

Inserting these approximations in (4.16), $P_k(e)$ becomes

$$P_k(e) \cong \text{constant} \times \Gamma^{-\left(L_{S_kD}+1\right)} \times \sum_{\forall A_k}\left[\left\{\left\{\prod_{\forall \alpha_k(m)=0} \Gamma^{-\left(L_{S_kR_m}+1\right)}\right\}\prod_{\forall \alpha_k(m)=1}\left(1-\text{constant} \times \Gamma^{-\left(L_{S_kR_m}+1\right)}\right)\Gamma^{-\left(L_{R_mD}+1\right)}\right\}\right]$$

Noting that $\left(1-\text{constant} \times \Gamma^{-\left(L_{S_kR_m}+1\right)}\right)\Gamma^{-\left(L_{R_mD}+1\right)}$ is dominated by the second term for high SNR, we can approximate $P_k(e)$ as

$$P_k(e) \cong \text{constant} \times \Gamma^{-\left(L_{S_kD}+1\right)} \times \sum_{\forall A_k}\left[\left\{\prod_{\forall \alpha_k(m)=0} \Gamma^{-\left(L_{S_kR_m}+1\right)}\right\}\left\{\prod_{\forall \alpha_k(m)=1} \Gamma^{-\left(L_{R_mD}+1\right)}\right\}\right]. \tag{4.19}$$

Rearranging the terms in (4.19), we get

$$\begin{aligned} P_k(e) \cong \text{constant} \times \Gamma^{-\left(L_{S_kD}+1\right)} \times \Bigg[& \sum_{\forall A_k \mid \alpha_k(1)=0}\left\{\Gamma^{-\left(L_{S_kR_1}+1\right)}\Gamma^{-\sum\limits_{\substack{\forall \alpha_k(m)=0 \\ m\neq 1}}\left(L_{S_kR_m}+1\right)-\sum\limits_{\substack{\forall \alpha_k(m)=1 \\ m\neq 1}}\left(L_{R_mD}+1\right)}\right\} \\ & + \sum_{\forall A_k \mid \alpha_k(1)=1}\left\{\Gamma^{-\left(L_{R_1D}+1\right)}\Gamma^{-\sum\limits_{\substack{\forall \alpha_k(m)=0 \\ m\neq 1}}\left(L_{S_kR_m}+1\right)-\sum\limits_{\substack{\forall \alpha_k(m)=1 \\ m\neq 1}}\left(L_{R_mD}+1\right)}\right\}\Bigg], \end{aligned} \tag{4.20}$$

By defining A_{k-1} as the set with all the elements of A_k except the first element, we get

$$P_k(e) \cong \text{constant} \times \Gamma^{-\left(L_{S_kD}+1\right)} \times \left(\Gamma^{-\left(L_{S_kR_1}+1\right)}+\Gamma^{-\left(L_{R_1D}+1\right)}\right)\sum_{\forall A_{k-1}}\left\{\Gamma^{-\sum\limits_{\substack{\forall \alpha_k(m)=0 \\ m\neq 1}}\left(L_{S_kR_m}+1\right)-\sum\limits_{\substack{\forall \alpha_k(m)=1 \\ m\neq 1}}\left(L_{R_mD}+1\right)}\right\}, \tag{4.21}$$

Noting the fact that diversity is determined by the term with the smallest negative power, we can use $\Gamma^{-\left(L_{S_kR_1}+1\right)}+\Gamma^{-\left(L_{R_1D}+1\right)}\approx\Gamma^{-\min\left(L_{S_kR_1}+1,L_{R_1D}+1\right)}$ and (4.21) becomes

$$P_k(e)\cong\text{constant}\times\Gamma^{-\left(L_{S_kD}+1\right)}\times\Gamma^{-\min\left(L_{S_kR_1}+1,L_{R_1D}+1\right)}\left[\sum_{\forall A_k\mid\alpha_k(1)=0}\left\{\Gamma^{-\sum_{\forall\alpha_k(m)=0,\,m\neq1}\left(L_{S_kR_m}+1\right)}\Gamma^{-\sum_{\forall\alpha_k(m)=1,\,m\neq1}\left(L_{R_mD}+1\right)}\right\}+\sum_{\forall A_k\mid\alpha_k(1)=1}\left\{\Gamma^{-\sum_{\forall\alpha_k(m)=0,\,m\neq1}\left(L_{S_kR_m}+1\right)}\Gamma^{-\sum_{\forall\alpha_k(m)=1,\,m\neq1}\left(L_{R_mD}+1\right)}\right\}\right], \tag{4.22}$$

Similarly by defining $A_{k-n},n=1,2,\cdots M$ as the set with all the of A_k except the first n elements, rearranging terms, and repeating the above steps, we obtain

$$P_k(e)\cong\text{constant}\times\Gamma^{-\left(L_{S_kD}+1\right)}\times\Gamma^{-\sum_{m=1}^{M}\min\left(L_{S_kR_m}+1,L_{R_mD}+1\right)}. \tag{4.23}$$

The above result shows that diversity order of $d=\left(L_{S_kD}+1\right)+\sum_{m=1}^{M}\min\left(L_{S_kR_m}+1,L_{R_mD}+1\right)$ is achievable.

4.4.2 Case 2: Relays close to source (i.e., $\Gamma_{S_kR}\gg\Gamma_{R_mD}$)

If all of the source-to-relay links have very good SNRs i.e., $\Gamma_{S_kR}\gg\Gamma_{R_mD}$, the SER in these links becomes negligible. In this case, all the terms in the outer summation of (4.9) become zero except the last term which corresponds to $A_k=\left\{\alpha_k(m)=1,\forall m\right\}$, resulting in overall SER as

$$P_k(e)=\frac{1}{2n_k}\sum_{\mathbf{x}_k}p(\mathbf{x}_k)\sum_{\mathbf{x}_k\neq\bar{\mathbf{x}}_k}q(\mathbf{x}_k\to\bar{\mathbf{x}}_k)\prod_{i=0}^{L_{S_kD}}\left(1+\lambda_{S_kD}^{i}\frac{\Gamma_{S_kD}}{2}\right)^{-1}\prod_{m=1}^{M}\left(\prod_{i=0}^{L_{R_mD}}\left(1+\lambda_{R_mD}^{i}\frac{\Gamma_{R_mD}}{2}\right)^{-1}\right), \tag{4.24}$$

We can approximate $P_k(e)$ as

$$P_k(e)\leq\text{constant}\times\prod_{i=0}^{L_{S_kD}}\left(1+\lambda_{S_kD}^{i}\frac{\Gamma_{S_kD}}{2}\right)^{-1}\prod_{m=1}^{M}\left(\prod_{i=0}^{L_{R_mD}}\left(1+\lambda_{R_mD}^{i}\frac{\Gamma_{R_mD}}{2}\right)^{-1}\right). \tag{4.25}$$

This shows that a diversity order of $d=\left(L_{S_kD}+1\right)+\sum_{m=1}^{M}\left(L_{R_mD}+1\right)$ is achievable.

4.4.3 Case 3: Relays close to destination ($\Gamma_{S_kR_m} \ll \Gamma_{R_mD}$)

Similar to the previous case, if relay-to-destination links have very good SNRs i.e., $\Gamma_{S_kR} \ll \Gamma_{R_mD}$, the SER in these links becomes negligible. Therefore, all the terms in the outer summation of (4.9) become zero except the first term which corresponds to $A_k = \{\alpha_k(m) = 0, \forall m\}$. The overall SER is then given by

$$P_k(e) \cong \left\{ \prod_{m=1}^{M} \left(\frac{1}{2n_k} \sum_{\mathbf{x}_k} p(\mathbf{x}_k) \sum_{\mathbf{x}_k \neq \hat{\mathbf{x}}_k} q(\mathbf{x}_k \to \hat{\mathbf{x}}_k) \prod_{i=0}^{L_{S_kR_m}} \left(1 + \lambda_{S_kR_m}^{i} \frac{\Gamma_{S_kR_m}}{2} \right)^{-1} \right) \right\} \times \left\{ \frac{1}{2n_k} \sum_{\mathbf{x}_k} p(\mathbf{x}_k) \sum_{\mathbf{x}_k \neq \bar{\mathbf{x}}_k} q(\mathbf{x}_k \to \bar{\mathbf{x}}_k) \prod_{i=0}^{L_{S_kD}} \left(1 + \lambda_{S_kD}^{i} \frac{\Gamma_{S_kD}}{2} \right)^{-1} \right\}, \tag{4.26}$$

This can be further approximated, by considering the shortest error event only, as

$$P_k(e) \leq \text{constant} \times \prod_{i=0}^{L_{S_kD}} \left(1 + \lambda_{S_kD}^{i} \frac{\Gamma_{S_kD}}{2} \right)^{-1} \prod_{m=1}^{M} \left(\prod_{i=0}^{L_{S_kR_m}} \left(1 + \lambda_{S_kR_m}^{i} \frac{\Gamma_{S_kR_m}}{2} \right)^{-1} \right). \tag{4.27}$$

From (4.27), it can be observed that a diversity order of $d = (L_{S_kD} + 1) + \sum_{m=1}^{M} (L_{S_kR_m} + 1)$ is achievable.

4.5 Comparison of the derived and simulated SER

To further confirm our analytically derived results, we have conducted Monte Carlo simulations. The results are given for 4-QAM modulation. Number of carriers N is chosen to be the minimum number of carriers required to communicate i.e., $N = K(L_{\max} + 1)$. For example if the maximum of all channel lengths is $L_{\max} = 2$, at least $N = 6$ carriers are required for two source nodes to communicate with destination using orthogonal carriers and at the same time benefit from multipath diversity through pre-coding [57].

In Fig. 4.2, we present the comparison of simulated and analytical SER curves obtained for different number of relays. We consider two source nodes both of which are equidistant from destination and assume relay(s) is (are) closer to sources. Each link is assumed to have the same

channel length and equal to 2. It can be observed from Fig. 4.2 that simulated and derived results have the same slopes. It can be checked that a diversity order of 6, 9, and 12 are, respectively, achieved for one, two and three relays. The discrepancy between simulated and derived expression is ~1.6dB for a target SNR of 10^{-3}. This mainly comes from Cherrnoff and union bounds used for the calculation of (4.14) and (4.15).

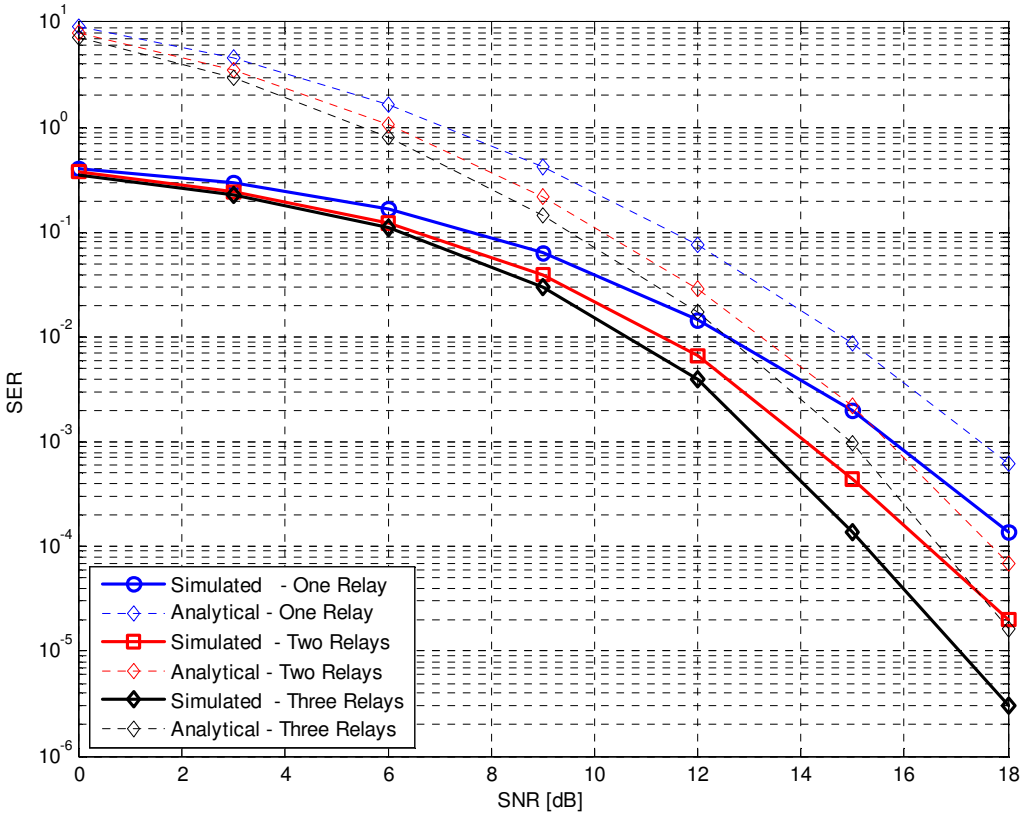

Figure 4.2 Comparison of simulated and analytical SER for 4-QAM with one, two, and three relays.

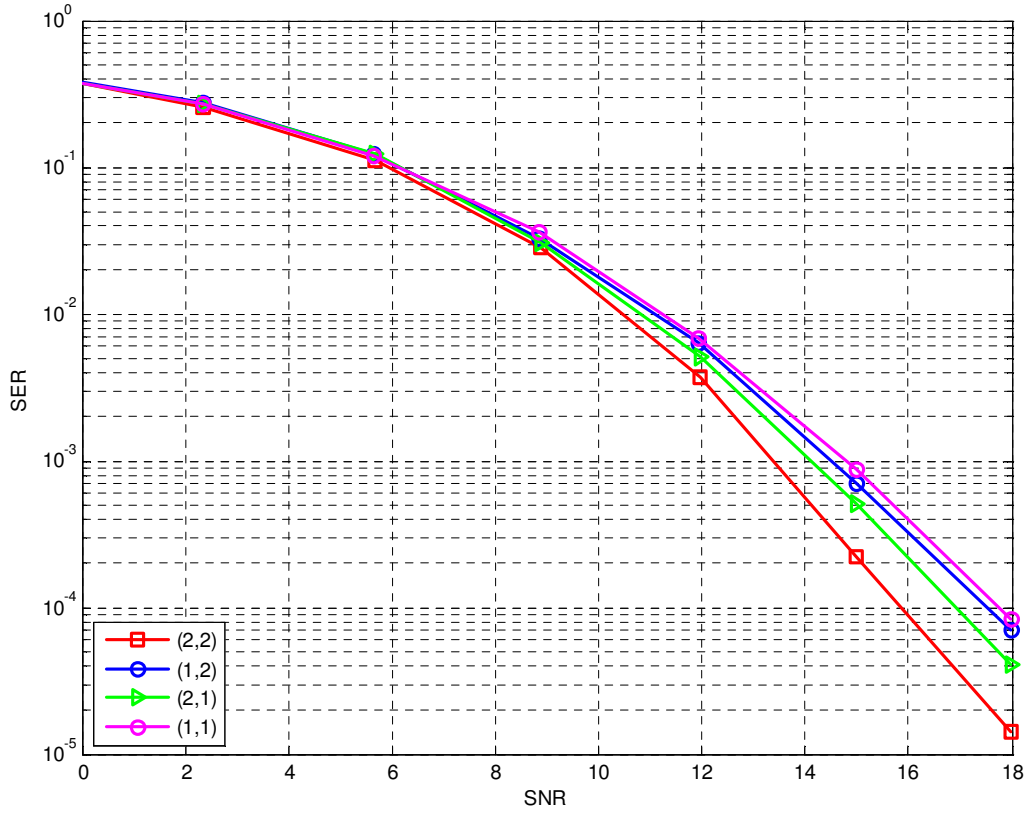

Figure 4.3 Simulated SER for various values of $\left(L_{S_1R_1}, L_{R_1D}\right)$ and $G_{S_1R_1}/G_{R_1D} = 0\text{dB}$.

Figs. 4.3-4.5 present the simulated SER for different values of $G_{S_mR_k}/G_{R_kD}$ for two source nodes and single relay scenario assuming different combinations of channel lengths. Particularly, we consider four representative scenarios with the following channel lengths: $\left(L_{S_1R_1}, L_{R_1D}\right) = (2,2)$ $\left(L_{S_1R_1}, L_{R_1D}\right) = (1,2)$ $\left(L_{S_1R_1}, L_{R_1D}\right) = (1,2)$ and $\left(L_{S_1R_1}, L_{R_1D}\right) = (1,1)$. We assume $L_{SD} = 2$. In Fig. 4.3, illustrated for $G_{S_1R_1}/G_{R_1D} = 0\text{dB}$, a diversity order of 6 is achieved only for $\left(L_{S_1R_1}, L_{R_1D}\right) = (2,2)$, for other three cases we get a diversity order of 5. This confirms our earlier derived result, i.e., $d = \left(L_{S_kD} + 1\right) + \sum_{m=1}^{M} \min\left(L_{S_kR_m} + 1, L_{R_mD} + 1\right)$.

In Fig. 4.4, we assume $G_{S_1R_1}/G_{R_1D} = 30\text{dB}$. In this case, a diversity order of 6 is achieved for the first two cases i.e., $\left(L_{S_1R_1}, L_{R_1D}\right) = (2,2)$ and $\left(L_{S_1R_1}, L_{R_1D}\right) = (1,2)$, but for other two cases with

$L_{R_1D}=1$, diversity order of 5 is achieved. This confirms our analytical result that diversity order of $d=\left(L_{S_kD}+1\right)+\sum_{m=1}^{M}\left(L_{R_mD}+1\right)$ is expected when relay is close to source. Similarly for $G_{S_1R_1}/G_{R_1D}=-30\text{dB}$ (illustrated in Fig. 4.5), we observe a diversity order of 6 for and $\left(L_{S_1R_1},L_{R_1D}\right)=(2,2)$ and $\left(L_{S_1R_1},L_{R_1D}\right)=(2,1)$ while a diversity order 5 is obtained for $\left(L_{S_1R_1},L_{R_1D}\right)=(1,2)$ and $\left(L_{S_1R_1},L_{R_1D}\right)=(1,1)$. These observations are in line with the earlier derived result of $d=\left(L_{S_kD}+1\right)+\sum_{m=1}^{M}\left(L_{S_kR_m}+1\right)$.

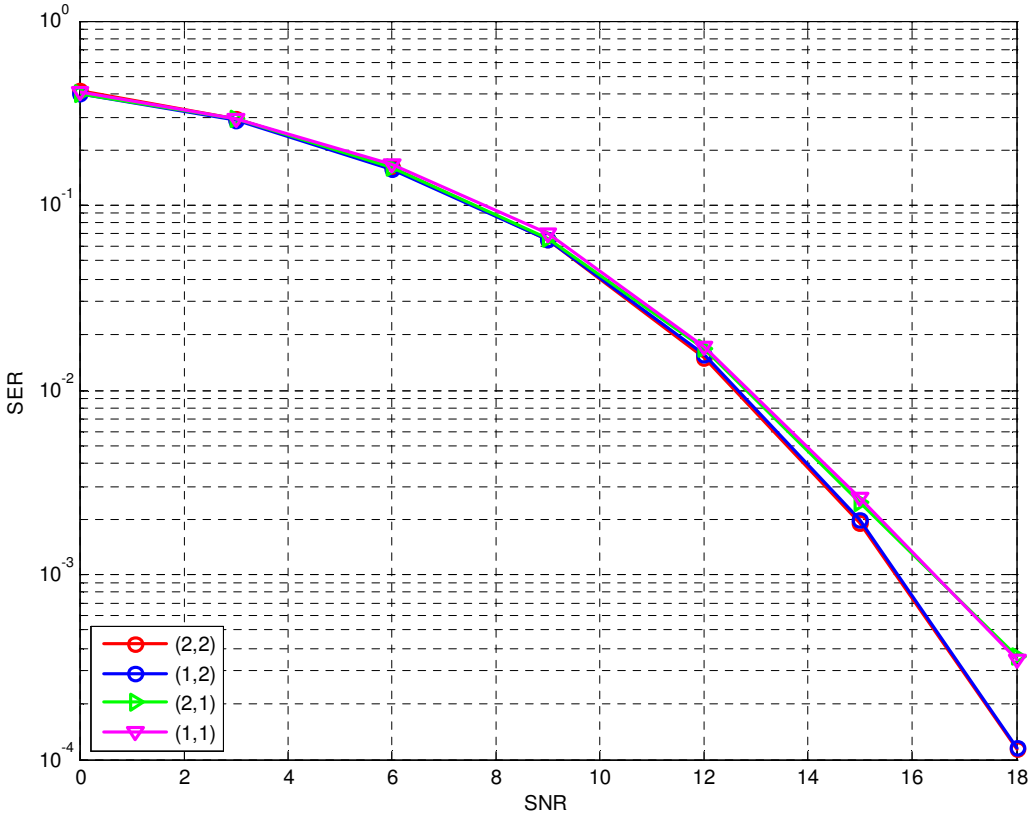

Figure 4.4 Simulated SER for various values of $\left(L_{S_1R_1},L_{R_1D}\right)$ and $G_{S_1R_1}/G_{R_1D}=30\text{dB}$.

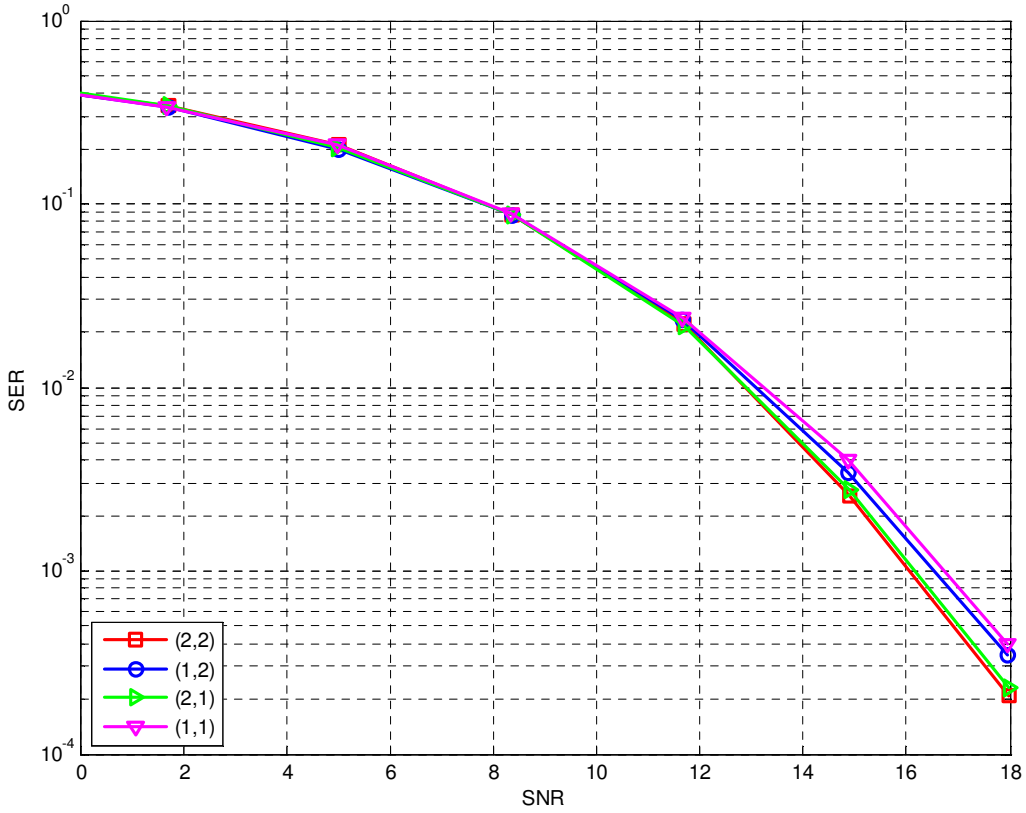

Figure 4.5 Simulated SER for various values of $\left(L_{S_1R_1}, L_{R_1D}\right)$ and $G_{S_1R_1}/G_{R_1D} = -30\text{dB}$.

4.6 Power Allocation and Relay Selection

In the previous sections, we have shown that a rich diversity is already available. It is possible to further improve the performance of cooperative communications through appropriate techniques particularly inherent to distributed schemes. In this section, we will discuss power allocation and relay selection as two potential methods for performance improvement.

4.6.1 Optimum Power Allocation

It has been demonstrated in earlier chapters that optimized power allocation has significant effect on the error rate performance of cooperative systems. By distributing the available power to the transmitting nodes based on their respective locations, not only we have performance improvement, but also we can reduce unnecessary interference created by transmitting nodes to co-existing wireless systems. In the following we formulate an optimum power allocation problem to minimize the derived SER expression given by (4.7). This can be expressed as

$$\arg \min_{P_{S_k}, P_{R_m}} \frac{1}{K} \sum_{k=1}^{K} P_k(e), \tag{4.28}$$

$$\text{s.t. } \sum_{k=1}^{K} P_{S_k} + \sum_{m=1}^{M} P_{R_m} = P. \tag{4.29}$$

An analytical solution for the above optimization is very difficult. In the rest, we pursue numerical optimization to find out the optimal values. In Table 4.1, as an example, we present optimum values of P_{S_1}/P, P_{S_2}/P, and P_{R_m}/P for one and two relays assuming $G_{S_1R_1}/G_{R_1D} = -30\text{dB}$ with two source nodes. We observe from Table 4.1 that for negative values of $G_{S_kR_m}/G_{R_mD}$, i.e., when relay(s) is (are) close to destination, a large fraction of power is allocated to source.

Table 4.1 Power allocation parameters for 4-QAM with one source, one and two relays.

SNR [dB]	**One relay**			**Two relays**			
	$G_{S_kR_1}/G_{R_1D} = -30\text{dB}, k = 1,2$			$G_{S_kR_m}/G_{R_mD} = -30\text{dB}, k = 1,2, \text{m} = 1,2$			
	P_{S_1}/P	P_{S_2}/P	P_{R_1}/P	P_{S_1}/P	P_{S_2}/P	P_{R_1}/P	P_{R_2}/P
0	0.4995	0.4995	0.0010	0.4990	0.4990	0.0010	0.0010
3	0.4995	0.4995	0.0010	0.4990	0.4990	0.0010	0.0010
6	0.4995	0.4995	0.0010	0.4990	0.4990	0.0010	0.0010
9	0.4995	0.4995	0.0010	0.4990	0.4990	0.0010	0.0010
12	0.4989	0.4989	0.0021	0.4981	0.4981	0.0019	0.0019
15	0.4989	0.4989	0.0023	0.4980	0.4980	0.0020	0.0020
18	0.4989	0.4989	0.0022	0.4980	0.4980	0.0020	0.0020

Fig. 4.6 presents the SNR required to obtain SER of 10^{-3} for various values of $G_{S_1R_m}/G_{R_mD}$. It is evident from this figure that OPA is more rewarding for negative values of $G_{S_1R_1}/G_{R_1D}$. Fig. 4.7 presents the simulation results to compare the performance of EPA and OPA. We consider one and two relays and we assume that relay(s) is (are) close to the destination, i.e., $G_{S_1R_i}/G_{R_iD} = -30\text{dB}, i=1,2$. We can observe from Fig. 4.7 that performance gains of 2dB and 3.3 dB are, respectively, achieved for one and two relays at a target SER of 10^{-3}.

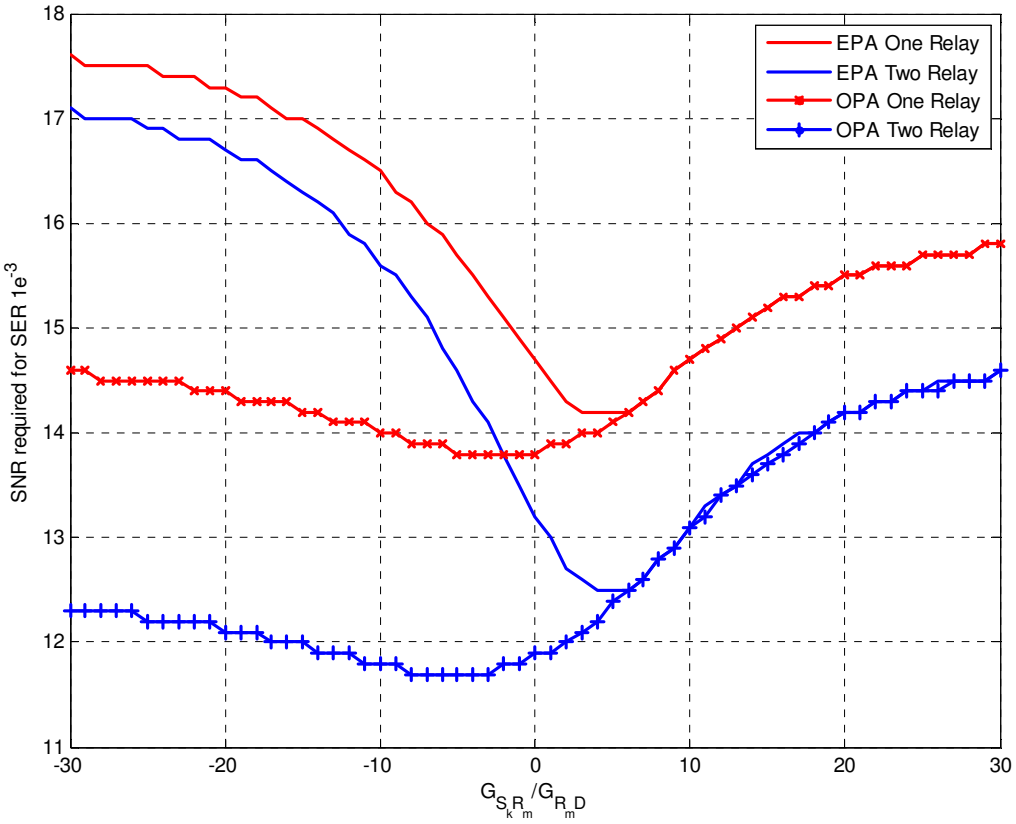

Figure 4.6 SNR required to achieve SER of 10^{-3}.

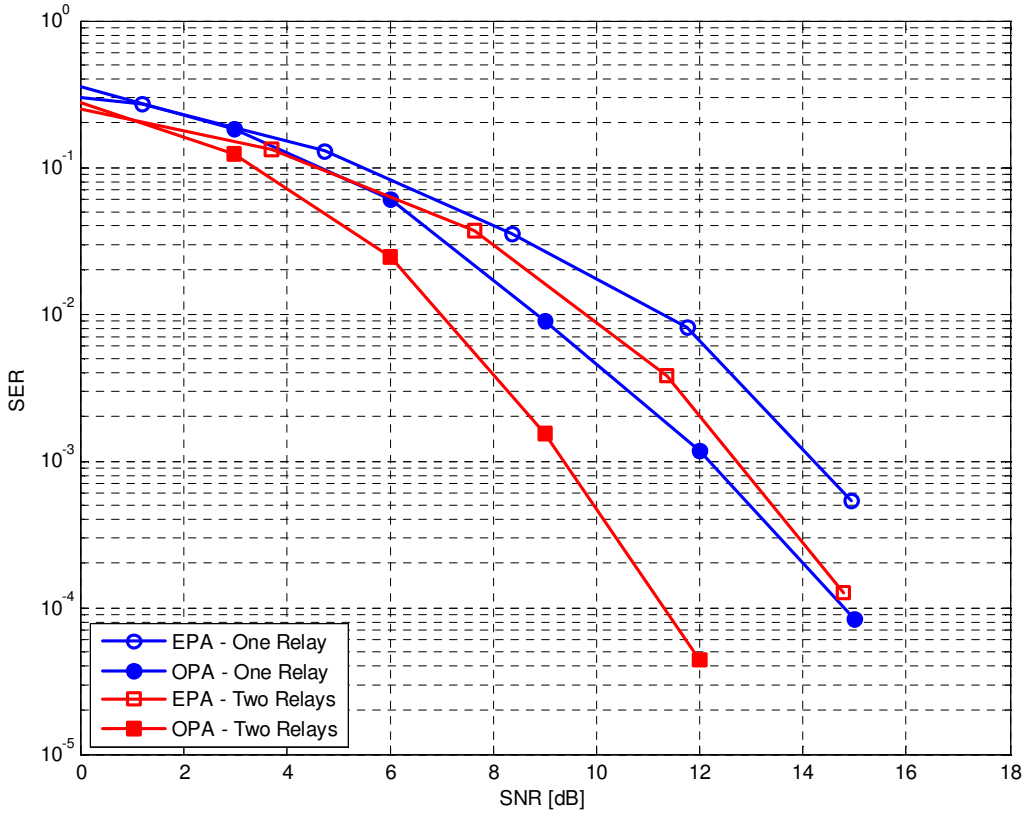

Figure 4.7 SER performance of EPA and OPA for one and two relays.

4.6.2 Relay Selection

Relay selection [29], [30] is a powerful technique to achieve higher throughput, because it requires fewer time slots to complete transmission of one block. In the relay selection (RS) scheme, only one selected relay transmits the information received during the broadcasting phase. This makes RS scheme to complete the transmission in at maximum two time slots. The relay selection algorithm utilizes only CSI at destination (i.e., $\mathbf{h}_{R_m D}$). The relay with maximum $\left\|\mathbf{h}_{R_m D}\right\|_{\mathrm{F}}$, is selected by destination and instructed to participate in the second phase.

In Fig. 4.8, we present simulation results for RS scheme and compare it with all participants (AP) scheme. We assume two source nodes with two and three relay nodes. Results show that SER performance of RS scheme is within 0.1dB of AP scheme along with the better throughput which is inherent to RS.

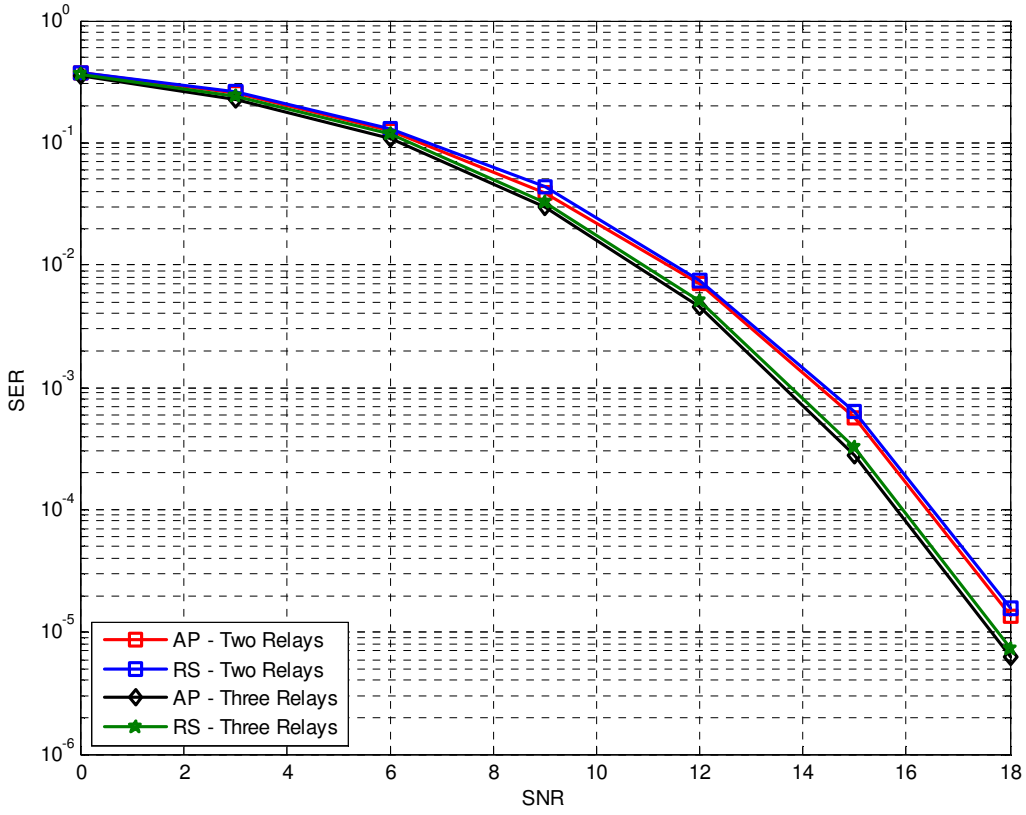

Figure 4.8 SER performance of AP and RS for one and two relays.

Chapter 5
Conclusions and Future Work

5.1 Introduction

In this final chapter, we summarize the contributions of the work presented in this dissertation and discuss some potential extensions to our work.

5.2 Contributions

Different from conventional point-to-point communications, cooperative communication allows nodes in a wireless network to share their resources through distributed transmission/processing. In this dissertation, we have presented a comprehensive performance analysis for cooperative communication techniques. Our analysis has spanned from a simple three-node cooperative communication system to a more sophisticated and practical broadband network. We have employed our derived analytical performance expressions to develop optimum power allocation methods.

We have started with the analysis of a three-node cooperative communication system. For this single-relay scenario, we have investigated optimum power allocation methods for AaF relaying assuming Protocols I, II, III of [14]. For each cooperation protocol, we have derived union bounds on the BER performance which are then used to optimally allocate the power among cooperating nodes in broadcasting and relaying phases. In comparison to their original counterparts, optimized protocols demonstrate significant performance gains depending on the relay geometry. Our results further provide a detailed comparison among Protocols I, II and III which give insight into the performance of these protocols incorporating the effects of relay location and power allocation.

In the second part of research, we have proposed a simple relay selection method for multi-relay networks with DaF relaying. The proposed method avoids the use of error detection methods at relay nodes and does not require close-loop implementation with feedback information to the source. Its implementation however requires channel state information of source-to-relay channels at the

destination. This can be easily done in practice through a feedforward channel from the relay to the destination. We also describe an alternative distributed implementation based on the deployment of timers at the relay and destination nodes. Our SER performance analysis for a cooperative network with N relays has demonstrated that the proposed relay-selection method is able to extract the full diversity order of N+1. We have further formulated two power allocation strategies to minimize the SER. Optimum power allocation has brought performance improvements up to 2dB for a two-relay scenario depending on the relays location. Our simulation results have also demonstrated that the proposed scheme outperforms its competitors and performs only 0.3dB away from the genie performance bound.

In the final part of our work, we have derived a closed-form approximate SER expression for the uplink of a cooperative OFDMA system with K sources and M relays. We have demonstrated that achievable diversity order for each $\mathrm{S}_k \rightarrow \mathrm{D}$ communication link can take different values depending on the location of relays. For example, a diversity order of $\left(L_{S_k D}+1\right)+\sum_{m=1}^{M}\min\left(L_{S_k R_m}+1, L_{R_m D}+1\right)$ is available when the relay nodes are located in the middle. On the other hand, diversity orders of $\left(L_{S_k D}+1\right)+\sum_{m=1}^{M}\left(L_{R_m D}+1\right)$ and $\left(L_{S_k D}+1\right)+\sum_{m=1}^{M}\left(L_{S_k R_m}+1\right)$ are, respectively, achieved for the cases when the relay nodes are close to the source nodes and close to destination, respectively. We have further discussed power allocation and relay selection schemes for the OFDMA system under consideration. Optimized power allocation brings performance improvements up to 3.3dB depending on the relay location.

5.3 Future Work

Conventional cooperation schemes work in "one-way mode" and suffer from spectral loss due to repetitive transmissions from relays. "Two-way relaying" [58]-[62], also referred as "bi-directional communication", has emerged as a powerful technique to recover the spectral loss inherent to one-way cooperation. In two-way relaying, two terminals exchange their information with the help of

relay(s). In the first transmission phase, both terminals simultaneously transmit their information which is received at relay as the superposition of two signals. In the second phase, the relay(s) forward(s) the signal received in the first phase. Each of the two terminals can extract information of its counterpart by subtracting its own signal which is already known. This makes two-way communication possible in two time slots as compared to one-way communication which requires four time slots to exchange the same information in half-duplex mode. The theory and tools developed in this dissertation can be applied to analyze and optimization of two-way relaying. Initial results can be found in [63].

Another possible research venue is to consider power allocation in asynchronous cooperative communication systems. Most of the existing literature on cooperative diversity is based on the assumption of perfect synchronization among cooperating nodes. Unlike a conventional space-time coded system where multiple antennas are co-located and fed by a local oscillator, the relay nodes are geographically dispersed and each of them relies on its local oscillator. Therefore, cooperative schemes need to be implemented taking into account this asynchronous nature. To address such issues, Li and Xia [64] have introduced a family of space-time trellis codes based on the stack construction which is able to achieve the full cooperative diversity order without the idealistic synchronization assumption. On the other hand, motivated by non-coherent differential space-time coding, Oggier and Hassibi [65] have presented a coding strategy for cooperative networks which does not require channel knowledge. Kiran and Rajan [66] have further proposed a cooperative scheme which assumes partial channel information, i.e., only destination has knowledge of relay-to-destination channel. Although initial work on the topic of asynchronous cooperative communication systems exists, optimum power allocation for such systems remains an open problem.

Appendices

Appendix A

In this appendix, we calculate marginal pdf of $\lambda_{\max}$ and joint pdf of $\lambda_{SR_{sel}}$ and $\lambda_{R_{sel}D}$ which are required to take expectation of (3.10). Let us define $\lambda_i = \min\left(\lambda_{SR_i}, \lambda_{R_iD}\right)$. Under the Rayleigh fading assumption, both λ_{SR_i} and λ_{R_iD} follow exponential distribution. Therefore λ_i has also exponential distribution with expected value as

$$\frac{1}{\Lambda_i} = \frac{1}{\Lambda_{SR_i}} + \frac{1}{\Lambda_{R_iD}}. \tag{A-1}$$

Let Δ denote the set of permutations of {1, 2, ..., N}, $\Pr(\sigma)$ denote the probability of one particular permutation $\sigma \in \Delta$, and $\lambda_{(i)}$ denote the ordered sequence of λ_i s, i.e., $\lambda_{(1)} > \lambda_{(2)} > \lambda_{(3)} > ..... > \lambda_{(N)}$. It can be shown [67] that we can transform $\lambda_{(i)}$ s into a set of new conditionally independent variables V_n such that

$$\lambda_{(i)} = \sum_{n=i}^{N} A_n V_n$$

where $A_n = \left(\sum_{m=1}^{n} \Lambda_m^{-1}\right)^{-1}$. The joint pdf of V_n is given by

$$f_{\mathbf{V}}\left(\{V_n\}_{n=1}^{N}\right) = \sum_{\sigma \in S} \Pr\{\sigma\} f_{\mathbf{V}|\sigma}\left(\{V_n\}_{n=1}^{N} | \sigma\right), \tag{A-2}$$

where

$$\Pr\{\sigma\} = \prod_{k=1}^{N} \frac{1}{\Gamma_{\sigma_k}} \left(\sum_{m=1}^{k} \frac{1}{\Gamma_{\sigma_m}} \right)^{-1}, \tag{A-3}$$

$$f_{V_n|\sigma}\left(V_n | \sigma\right) = \begin{cases} \dfrac{1}{\Gamma_n} \exp\left(-\dfrac{V_n}{\Gamma_n}\right), & 0 < V_n < \infty \\ 0, & \text{otherwise} \end{cases}. \tag{A-4}$$

In the above, Γ_n s are defined as

$$\Gamma_n = \left(\sum_{m=1}^{n} \frac{1}{\Lambda_m} \right) \left(\sum_{m=1}^{n} \frac{1}{\Lambda_{\sigma_m}} \right)^{-1}.$$

The above transformation of variables enables us to find the moment generating function (MGF) of variable $\lambda_{\max} = \lambda_{(1)} = \sum_{n=1}^{N} A_n V_n$ as $\Psi_{\max}\left(s|\sigma\right) = \prod_{n=1}^{N} \left(1 - sA_n\Gamma_n\right)^{-1}$.

For probabilities of event ξ_i and ξ_i^C, we first define $\Delta_i \subset \Delta$ as the set of all the permutations for which i is the first element. Then we have $\Pr\left(i = sel\right) = \sum_{\sigma \in \Delta_i} \Pr\left(\sigma\right)$ which denotes the probability of i^{th} relay node being selected. Let μ_i denote the event of $\lambda_{SR_i} < \lambda_{R_iD}$ and μ_i^C its complementary event, i.e., $\lambda_{SR_i} > \lambda_{R_iD}$. The probabilities of these two events are approximated[13] as

$$\Pr\left(\xi_i\right) \cong \Pr\left(i = sel\right) \Pr\left(\mu_i\right), \tag{A-5}$$

$$\Pr\left(\xi_i^C\right) \cong \Pr\left(i = sel\right) \Pr\left(\mu_i^C\right), \tag{A-6}$$

with

$$\Pr\left(\mu_i\right) = \frac{\Lambda_{R_iD}}{\Lambda_{SR_i} + \Lambda_{R_iD}}. \tag{A-7}$$

$$\Pr\left(\mu_i^C\right) = \frac{\Lambda_{SR_i}}{\Lambda_{SR_i} + \Lambda_{R_iD}}, \tag{A-8}$$

In the above, Λ_{R_iD} and Λ_{SR_i} are the average values of received SNRs and are given by $\Lambda_{R_iD} = E\left[\lambda_{R_iD}\right] = G_{R_iD} K_i \left(E/N_0\right)$ and $\Lambda_{SR_i} = E\left[\lambda_{SR_i}\right] = G_{SR_i} K_S \left(E/N_0\right)$. Now let us calculate the joint pdf of $\lambda_{SR_{sel}}$ and $\lambda_{R_{sel}D}$ conditioned on the event ξ_i and ξ_i^C. For ξ_i, we have $\lambda_{SR_i} = \lambda_{\max}$, thus conditional statistics of $\lambda_{SR_{sel}}$ and $\lambda_{R_{sel}D}$ are given by

$$MGF\left(\lambda_{SR_{sel}}\right) = MGF\left(\lambda_{\max}\right), \tag{A-9}$$

and

[13] Exact value of first can be calculated as $\Pr\left(\xi_i\right) = \Pr\left(\lambda_{R_iD} > \lambda_{SR_i} > \lambda_k, \quad \forall k \neq i\right)$.

$$f_{R_{sel}D}\left(\lambda\middle|\xi_i\right)=\begin{cases}\dfrac{1}{\Lambda_{R_iD}}\exp\left(-\dfrac{\lambda}{\Lambda_{R_iD}}\right) & \lambda_{R_{sel}D}\geq\lambda_{\max}\\ 0 & \text{otherwise}\end{cases}. \tag{A-10}$$

The conditional statistics of the two variables swap for event ξ_i^C. For this case, we have $\lambda_{SR_i}>\lambda_{RiD}=\lambda_{\max}$. Thus conditional statistics of $\lambda_{SR_{sel}}$ and $\lambda_{RD_{sel}}$ are obtained as

$$f_{SR_{sel}}\left(\lambda\middle|\xi_i^C\right)=\begin{cases}\dfrac{1}{\Lambda_{SR_i}}\exp\left(-\dfrac{\lambda}{\Lambda_{SR_i}}\right) & \lambda_{SR_{sel}}\geq\lambda_{\max}\\ 0 & \text{otherwise}\end{cases}, \tag{A-11}$$

and

$$MGF\left(\lambda_{R_{sel}D}\right)=MGF\left(\lambda_{\max}\right). \tag{A-12}$$

For the calculations in Appendix B, we also require MGFs for λ_{SD}, λ_{SR_i}, and λ_{R_iD}. These MGFs are given respectively by

$$\Psi_{SD}\left(s\right)=\left(1+s\Lambda_{SD}\right)^{-1}. \tag{A-13}$$

$$\Psi_{SR_i}\left(s\right)=\left(1+s\Lambda_{SR_i}\right)^{-1}. \tag{A-14}$$

$$\Psi_{R_iD}\left(s\right)=\left(1+s\Lambda_{R_iD}\right)^{-1}. \tag{A-15}$$

Appendix B

In this appendix, we present the details of how the expectation of three terms of (3.10) is carried out. For first term, since λ_{SD} follows an exponential distribution under the considered Rayleigh fading assumption, we have

$$\Phi_0 = E_{\lambda}[T_0] = \int_{\lambda_{\max}}^{\infty} \beta(\lambda) f_{\lambda_{SD}}(\lambda) d\lambda .$$

Using the definition of $\beta(.)$ from (3.8), we have

$$\Phi_0 = F_1\left\{ \Psi_{SD}(\alpha_{\eta_1}) e^{-\lambda_{\max}\left(\frac{1}{\Lambda_{SD}} - \alpha_{\eta_1}\right)} \right\}. \tag{B-1}$$

where α_{η_1}, and $F_1\{.\}$ are earlier defined by (3.16) and (3.17). In (B-1), $\Psi_{SD}(.)$ and $\Psi_{\max}(.)$ are MGFs of λ_{SD} and $\lambda_{\max}$. Averaging over $\lambda_{\max}$ yields

$$\Phi_0 = F_1\left\{ \Psi_{SD}(\alpha_{\eta_1}) \Psi_{\max}\left(\alpha_{\eta_1} - \frac{1}{\Lambda_{SD}} \right) \right\}. \tag{B-2}$$

In the following, we present the details of how the expectation of second and third term of (3.11) is carried out for events ξ_i and ξ_i^C.

Case I (Event ξ_i)**:** From (3.10), we have T_1 for this event as

$$T_1 = P(\lambda_{SD} < \lambda_{\max}) \beta(\lambda_{\max}) .$$

Taking expectation with respect to λ_{SD}, we have

$$E_{\lambda_{SD}}[T_1] = \left(1 - e^{-\frac{\lambda_{\max}}{\Lambda_{SD}}} \right) \beta(\lambda_{\max}) . \tag{B-3}$$

Inserting $\beta(.)$ from (3.8) in (B-6) and further taking expectation with respect to $\lambda_{\max}$, we obtain

$$\Phi_1 = E_{\boldsymbol{\lambda}}\left[T_1\right] = F_1\left(\Psi_{\max}\left(\alpha_{\eta_1}\right) - \Psi_{\max}\left(\alpha_{\eta_1} - \frac{1}{\Lambda_{SD}}\right)\right). \tag{B-4}$$

On the other hand, T_2 is given by

$$T_2 = P\left(\lambda_{SD} < \lambda_{\max}\right)\left[1 - \beta\left(\lambda_{SR_{sel}}\right)\right]\beta\left(\lambda_{R_{sel}D} + \lambda_{SD}\right). \tag{B-5}$$

Inserting $\beta(.)$ in (B-5) and taking expectation with respect to λ_{SD} and $\lambda_{R_{sel}D}$ using pdf given by (A-10), we obtain

$$E_{\lambda_{SD},\ \lambda_{R_{sel}D}}\left[T_2\right] = F_1\left(\Psi_{SD}\left(\alpha_{\eta_1}\right)\left(1 - e^{-\frac{\lambda_{\max}}{\Lambda_{SD}}}\right)\Psi_{R_iD}\left(\alpha_{\eta_1}\right)e^{-\frac{\lambda_{\max}}{\Lambda_{R_iD}}}\left(1 - \beta\left(\lambda_{\max}\right)\right)\right). \tag{B-6}$$

Finally taking expectation with respect to $\lambda_{\max}$, we have

$$\begin{aligned}\Phi_2 &= E_{\boldsymbol{\lambda}}\left[T_2\right] \\ &= F_1\left(\Psi_{SD}\left(\alpha_{\eta_1}\right)\Psi_{R_iD}\left(\alpha_{\eta_1}\right)\left[\Psi_{\max}\left(\alpha_{\eta_1} - \frac{1}{\Lambda_{R_iD}}\right) - \Psi_{\max}\left(\alpha_{\eta_1} - \frac{1}{\Lambda_{R_iD}} - \frac{1}{\Lambda_{SD}}\right)\right]\right) \\ &\quad - F_2\left(\Psi_{SD}\left(\alpha_{\eta_1}\right)\Psi_{R_iD}\left(\alpha_{\eta_1}\right)\left[\Psi_{\max}\left(\alpha_{\eta_1} + \alpha_{\eta_2} - \frac{1}{\Lambda_{R_iD}}\right) - \Psi_{\max}\left(\alpha_{\eta_1} + \alpha_{\eta_2} - \frac{1}{\Lambda_{R_iD}} - \frac{1}{\Lambda_{SD}}\right)\right]\right)\end{aligned} \tag{B-7}$$

Case II (Event ξ_i^C)**:** From (3.10), we have T_1 for this event as

$$T_1 = P\left(\lambda_{SD} < \lambda_{\max}\right)\beta\left(\lambda_{SR_{sel}}\right). \tag{B-8}$$

Averaging (B-8) over λ_{SD}, we obtain

$$E_{\lambda_{SD}}\left[T_1\right] = \left(1 - e^{-\frac{\lambda_{\max}}{\Lambda_{SD}}}\right)\beta\left(\lambda_{SR_{sel}}\right).$$

Using the definition of $\beta(.)$ and taking the expectation over $\lambda_{SR_{sel}}$, we obtain

$$E_{\lambda_{SD},\ \lambda_{SR_{sel}}}\left[T_1\right] = F_1\left(\Psi_{SR_i}\left(\alpha_{\eta_1}\right)\left(1 - e^{-\frac{\lambda_{\max}}{\Lambda_{SD}}}\right)e^{-\lambda_{\max}\left(-\alpha_{\eta_1} + \frac{1}{\Lambda_{SR_i}}\right)}\right).$$

Finally, by carrying out the expectation over $\lambda_{\max}$, we have

$$\Phi_1^C = E_\lambda\left[T_1\right] = F_1\left(\Psi_{SR_i}\left(\alpha_{\eta_1}\right)\left[\Psi_{\max}\left(\alpha_{\eta_1} - \frac{1}{\Lambda_{SR_i}}\right) - \Psi_{\max}\left(\alpha_{\eta_1} - \frac{1}{\Lambda_{SR_i}} - \frac{1}{\Lambda_{SD}}\right)\right]\right). \tag{B-9}$$

On the other hand, T_2 is given by

$$T_2 = P\left(\lambda_{SD} < \lambda_{\max}\right)\left[1 - \beta\left(\lambda_{SR_{sel}}\right)\right]\beta\left(\lambda_{R_{sel}D} + \lambda_{SD}\right) \tag{B-10}$$

Inserting $\beta(.)$ in (B-10) and taking expectation of the resulting expression with respect to $\lambda_{SR_{sel}}$, we have

$$E_{\lambda_{SR_{sel}}}\left[T_2\right] = F_2\left(\Psi_{SD}\left(\alpha_{\eta_1}\right)\left[1 - e^{-\frac{\lambda_{\max}}{\Lambda_{SD}}}\right]\left[1 - \Psi_{SR_i}\left(\alpha_{\eta_2}\right)e^{-\frac{\lambda_{\max}}{\Lambda_{SR_i}}}\right]e^{-\lambda_{\max}\alpha_{\eta_1}}\right).$$

Averaging over $\lambda_{\max}$ finally yields

$$\begin{aligned}\Phi_2^C &= E_\lambda\left[T_2\right] \\ &= F_1\left(\Psi_{SD}\left(\alpha_{\eta_1}\right)\left[\Psi_{\max}\left(\alpha_{\eta_1}\right) - \Psi_{\max}\left(\alpha_{\eta_1} - \frac{1}{\Lambda_{SD}}\right)\right]\right) \\ &\quad - F_2\left(\Psi_{SD}\left(\alpha_{\eta_1}\right)\Psi_{SR_i}\left(\alpha_{\eta_2}\right)\left[\Psi_{\max}\left(\alpha_{\eta_1} - \frac{1}{\Lambda_{SR_i}}\right) - \Psi_{\max}\left(\alpha_{\eta_1} - \frac{1}{\Lambda_{SR_i}} - \frac{1}{\Lambda_{SD}}\right)\right]\right)\end{aligned} . \tag{B-11}$$

Bibliography

[1] S. Y. Hui and K. H. Yeung, "Challenges in the Migration to 4G Mobile Systems," *IEEE Commun. Mag.*, vol. 41, pp. 54 - 59, December 2003.

[2] T. S. Rappaport, *Wireless Communications: Principles and Practice*, Prentice Hall PTR, 2000.

[3] W. C. Jakes, *Microwave Mobile Communications*, New York: Wiley, 1974.

[4] G. J. Foschini. "Layered space-time architecture for wireless communication in a fading environment when using multiple antennas," *Bell Labs Technical Journal*, vol. 1, no. 2, pp. 41-59, September 1996.

[5] V. Tarokh, N. Seshadri, A. Calderbank, "Space-time codes for high data rate wireless communication: Performance criterion and code construction", *IEEE Trans. Inf. Theory*, vol. 44, no. 2, pp. 744-765, March 1998.

[6] S. A. Alamouti, "A simple transmit diversity technique for wireless communication," *IEEE J. Sel. Areas Commun.*, vol. 16, no. 8, pp. 15-1458, October 1998.

[7] V. Tarokh, H. Jafarkhani, and A. R. Calderbank. "Space-time block codes from orthogonal designs," *IEEE Trans. Inf. Theory*, vol. 45, no. 5, pp. 1456-1467, July 1999.

[8] T. M. Cover and A. A. El Gamal, "Capacity theorems for the relay channel," *IEEE Trans. Inf. Theory*, vol. 25, no. 5, pp. 572-584, September 1979.

[9] A. Sendonaris, E. Erkip and B. Aazhang, "User cooperation diversity Part I: System description", *IEEE Trans. Commun.*, vol. 51, no. 11, pp. 1927-1938, November 2003.

[10] A. Sendonaris, E. Erkip and B. Aazhang, "User cooperation diversity Part II: Implementation aspects and performance analysis," *IEEE Trans. Commun.*, vol. 51, no. 11, pp. 1939-1948, November 2003.

[11] J. N. Laneman and G. W. Wornell, "Distributed space-time-coded protocols for exploiting cooperative diversity in wireless networks", *IEEE Trans. Inf. Theory*, vol. 49, no. 10, pp. 2415-2425, October 2003.

[12] J. N. Laneman, D. N. C. Tse, and G. W. Wornell, "Cooperative Diversity in Wireless Networks: Efficient Protocols and Outage Behavior," *IEEE Trans. Inf. Theory*, vol. 50, no. 12, pp. 3062-3080, December 2004.

[13] A. Nosratinia, T. Hunter, and A. Hedayat, "Cooperative communication in wireless networks," *IEEE Commun. Mag.*, vol. 42, no. 10, pp. 74-80, October 2004.

[14] R. U. Nabar, H. Bölcskei, and F. W. Kneubühler, "Fading relay channels: Performance limits and space-time signal design", *IEEE J. Sel. Areas Commun.*, vol. 22, no. 6, pp. 1099-1109, August 2004.

[15] K. Azarian, H. E. Gamal, P. Schniter, "On the achievable diversity multilexing tradeoff in half-duplex cooperative channels," *IEEE Trans. Inf. Theory*, vol. 51, pp. 4152-4172, December 2005.

[16] A. Host-Madsen and J. Zhang, "Capacity Bounds and Power allocation in Wireless Relay Channel," *IEEE Trans. Inf. Theory*, vol. 51, no. 6, pp. 2020-2040, June 2005.

[17] N. Ahmed and B. Aazhang, "Outage minimization with limited feedback for the fading relay channel," *IEEE Trans. Commun.*, vol. 54, no. 4, pp. 659-669 April 2006.

[18] Z. Jingmei, Z. Qi, Sh. Chunju, W. Ying, Z. Ping, Z. Zhang, "Adaptive Optimal Transmit Power Allocation for Two-hop Non-regenerative Wireless Relaying System," in Proc. of *IEEE VTC'04*-Spring, 2004.

[19] Z. Jingmei, Sh. Chunju, W. Ying, Z. Ping, "Optimal Power Allocation for Multiple-Input-Multiple-Output Relaying System," in Proc. of *IEEE VTC'04*-Fall, 2004.

[20] Z. Jingmei, Sh. Chunju, W. Ying, Z. Ping, ""Performance of a Two-hop Cellular System with Different Power Allocation Schemes," in Proc. of *IEEE VTC'04*-Fall, 2004.

[21] M. O. Hasna and M.-S. Alouini, "Optimal power allocation for relayed transmissions over Raleigh-fading channels," *IEEE Trans. Wireless Commun.*, vol. 3, no. 6, pp. 1999–2004, November 2004.

[22] Y. Jing and B. Hassibi, "Distributed space-time codes in wireless relay networks," in Proc. of *IEEE Sensor Array and Multichannel Signal Processing Workshop*, pp. 249-253, July 2004.

[23] Y. Jing and B. Hassibi, "Distributed space-time coding in wireless relay networks," *IEEE Trans. Wireless Commun.*, vol. 5, no. 12, pp. 3524-3536, December 2006.

[24] X. Deng, and A. M. Haimovich, "Power Allocation for Cooperative Relaying in Wireless Networks," *IEEE Commun. Lett.*, vol. 9, no. 11, pp. 994-996, November 2005.

[25] M. M. Fareed and M. Uysal, "Optimum Power Allocation for Fading Relay Channels," in Proc. of *IEEE VTC'07-Fall*, Baltimore, Maryland, USA, September 2007.

[26] M. M. Fareed and M. Uysal, "BER-Optimized Power Allocation for Fading Relay Channels," *IEEE Trans. Wireless Commun.*, vol.7, no. 6, p. 2350-2359, June 2008.

[27] M. Uysal and M. M. Fareed, "Cooperative Diversity Systems for Wireless Communication," Chapter in *Handbook on Information and Coding Theory*, I. Woungang, S. Misra and S. C. Misra (Eds.), World Scientific, to be published in 2009.

[28] T. Wang, A. Cano, G. B. Giannakis, and N. Laneman, "High-Performance Cooperative Demodulation with Decode-and-Forward Relays," *IEEE Trans. Comm.*, vol. 55, no. 7, pp. 1427-1438, July 2007.

[29] A. Bletsas, A. Khisti, D. P. Reed, and A. Lippman, "A simple cooperative diversity method based on network path selection," *IEEE J. Select. Areas Commun.*, vol. 24, no. 9, pp. 659-672, March 2006.

[30] E. Beres and R. S. Adve, "Selection cooperation in multi-source networks," *IEEE Trans. Wireless Commun.*, vol. 7, no. 1., pp. 118-127, January 2008.

[31] A. Ibrahim, A. Sadek, W. Su, and K.J.R. Liu, "Relay Selection in Multi-Node Cooperative Communications: When to Cooperate and Whom to Cooperate with?" in Proc. of *IEEE GlobeCom 2006*.

[32] M. M. Fareed and M. Uysal, "A Novel Relay Selection Method for Decode-and-Forward Relaying," in Proc. of *Canadian Conference on Electrical and Computer Engineering (CCECE'08)*, May 2008.

[33] M. M. Fareed and M. Uysal, "On Decode-and-Forward Cooperative Networks with Relay Selection," to appear in *IEEE Transactions on Wireless Communications*.

[34] S. Barbarossa and G. Scutari, "Distributed space-time coding for regenerative relay networks," *IEEE Trans. Wireless Commun.*, vol. 4, no. 5, pp. 2387-2399, September 2005.

[35] H. Mheidat, M. Uysal, and N. Al-Dhahir, "Equalization Techniques for Distributed Space-Time Block Codes with Amplify-and-Forward Relaying," *IEEE Trans. Signal Process.*, vol. 55, no. 5, part 1, p. 1839-1852, May 2007.

[36] K.G. Seddik and K.J.R. Liu, "Distributed Space-Frequency Coding over Broadband Relay Channels," *IEEE Trans. Wireless Commun.*, vol 7, no 11, pp.4748-4759, November 2008.

[37] O-S Shin, A. M. Chan, H. T. Kung, and V. Tarokh "Design of an OFDM Cooperative Space-Time Diversity System," *IEEE Trans. Veh. Technol.*, vol. 56, No. 4, pp. 2203-2215, July 2007.

[38] B. Can, M. Portalski, H. Lebreton, S. Frattasi, and H. Suraweera, "Implementation Issues for OFDM Based Multi-hop Cellular Networks," *IEEE Commun. Mag.,* vol. 45, no. 9, pp. 74-81, September 2007.

[39] K. H. Teo, Z. Tao, and J. Zhang, "The Mobile Broadband WiMAX Standard," *IEEE. Signal Proces. Mag.*, vol. 24, pp. 144-148, September 2007.

[40] L. Guoqing and L. Hui, "Resource Allocation for OFDMA Relay Networks With Fairness Constraints," *IEEE J. Select. Areas Commun.*, vol. 24, no. 11, pp. 2061-2069, November 2006.

[41] T. Ng and W. Yu, "Joint optimization of relay strategies and resource allocation in cooperative cellular networks," *IEEE J. Select. Areas Commun.*, vol. 25, pp. 328-229, February 2007.

[42] M. Pischella and J.-C. Belfiore, "Power control in distributed cooperative OFDMA cellular networks," *IEEE Trans. Wireless Commun.*, vol. 7, pp. 1900-1906, May 2008.

[43] S.-J. Kim, X. Wang, and M. Madihian, "Optimal Resource Allocation in Multi-hop OFDMA Wireless Networks with Cooperative Relay," *IEEE Trans. Wireless Commun.*, vol. 7, no. 5, pp. 1833-1838, May 2008.

[44] J. Lee, H. Wang, W. Seo, and D. Hong, "QoS-guaranteed Transmission Mode Selection for Efficient Resource Utilization in Multi-hop Cellular Networks," *IEEE Trans. Wireless Commun.*, vol. 7, no. 10, pp. 3697-3701, October 2008.

[45] S. Zhang and V. Lau, "Resource Allocation for OFDMA System with Orthogonal Relay using Rateless Code," *IEEE Trans. Wireless Commun.*, vol. 7 no. 11-2, pp. 4534-4540, November 2008.

[46] J.W. Mark and W. Zhuang, *Wireless Communications and Networking*, Prentice Hall, ISBN 0-13-040905-7, 2003.

[47] H. Ochiai, P. Mitran, and V. Tarokh, "Variable Rate Two Phase Collaborative Communication Protocols for Wireless Networks," *IEEE Trans. Inf. Theory*, vol. 52, no. 9, pp. 4299-4313, September 2006.

[48] H. Mheidat and M. Uysal "Impact of Receive Diversity on the Performance of Amplify-and-Forward Relaying under APS and IPS Power Constraints," *IEEE Commun. Lett.*, vol. 10, no. 6, p. 468-470, June 2006.

[49] S. Benedetto and E. Biglieri, *Principles of Digital Transmission with Wireless Applications*, Kluwer Academic, NY, 1999.

[50] I. S. Gradshteyn and I. M. Ryzhik, *Table of Integrals, Series and Products*, Academic Press, 5th ed, 1994.

[51] K. Azarian, H. E. Gamal, and P. Schniter, "On the achievable diversity-multiplexing tradeoff in half duplex cooperative channels," *IEEE Trans. Inf. Theory*, vol. 51, no. 12, pp. 4152-4172, December 2005.

[52] J.-C. Belfiore, G. Rekaya, and E. Viterbo, "The Golden code: A 2×2 full-rate space-time code with non-vanishing determinants," *IEEE Trans. Inf. Theory*, vol. 51, no. 4, pp. 1432–1436, April 2005.

[53] M. K. Simon and M. S. Alouini, *Digital Communication over Fading Channel: A Unified Approach to Performance Analysis*, Wiley, New York, 2000.

[54] http://www.mathworks.com/access/helpdesk/help/toolbox/optim/ug/fmincon.html

[55] P.E. Gill, W. Murray, and M.H. Wright, *Practical Optimization*, London, Academic Press, 1981.

[56] W. A. Pearlman and G. H. Senge, "Optimal Quantization of the Rayleigh Probability Distribution," *IEEE Trans. Commun.*, vol. 27, no. 1, pp. 101–112, January 1979.

[57] Z. Liu, Y. Xin and G. B. Giannakis, "Linear constellation precoding for OFDM with maximum multipath diversity and coding gains", *IEEE Trans. Signal Processing*, vol. 51, no. 3, pp. 416-427, March 2004.

[58] B. Rankov and A. Wittneben, "Spectral efficient signaling for halfduplex relay channels," in Proc. of *Asilomar Conference on Signals, Systems and Computers*, October 2005.

[59] B. Rankov and A. Wittneben, "Achievable rate regions for the two-way relay channel," in Proc. of *IEEE ISIT*, July 2006.

[60] Y. Han, S. H. Ting, C. Ho, and W. H. Chin, "High Rate Two-Way Amplify-and-Forward Half-Duplex Relaying with OSTBC," in Proc. of *IEEE VTC*, Spring 2008.

[61] T. Unger and A. Klein, "Maximum Sum Rate for Non-regenerative Two-way Relaying in Systems of Different Complexities," in Proc. of *19th IEEE PIMRC*, Cannes, France, September 2008.

[62] T. Cui, T. Ho, and J. Kliewer, "Memoryless Relay Strategies for Two-Way Relay Channels: Performance Analysis and Optimization," in Proc. of *ICC*, May 2008.

[63] M. M. Fareed, S. Rehman, and M. Uysal, "Performance Analysis of Multi-Relay Two-Way Cooperative Communication System over Rayleigh Fading Channels,", submitted to *IEEE Pacific Rim Conference on Communications, Computers and Signal Processing*, Victoria, BC, Canada, August 2009.

[64] Y. Li and X.-G. Xia, "A family of distributed space-time trellis codes with asynchronous cooperative diversity," *IEEE Trans. Commun.*, vol.55, pp. 790–800, April 2007.

[65] F. Oggier and B. Hassibi. "A Coding Strategy for Wireless Networks with no Channel Information," in Proc. of *Allerton Conference*, 2006.

[66] T. Kiran and B. S. Rajan, "Partially-coherent distributed space-time codes with differential encoder and decoder," *IEEE J. Sel. Areas Commun.*, vol. 25, no. 2, pp. 426-433, February 2007.

[67] M. Z. Win and J. H. Winters, "Analysis of Hybrid Selection/Maxirnal-Ratio Combining of Diversity Branches with Unequal SNR in Rayleigh Fading", in Proc. of *49th Annual VTC*, vol. 1, Houston, TX, U.S.A., pp. 215-220, May 1999.